

UNITED STATES
DEPARTMENT OF THE INTERIOR
GEOLOGICAL SURVEY

MISCELLANEOUS HYDROLOGIC AND GEOLOGIC OBSERVATIONS
ON THE INNER BEAUFORT SEA SHELF, ALASKA



OPEN-FILE REPORT 77-477

**This report is preliminary and has not
been edited or reviewed for conformity
with Geological Survey standards and
nomenclature**

*Menlo Park, California
April 1977*

Miscellaneous hydrologic and geologic observations on the
inner Beaufort Sea Shelf, Alaska

P. Barnes

E. Reimnitz

D. Drake

L. Toimil

United States
Department of the Interior
Geological Survey
Open File Report 77-477
April, 1977

This report is preliminary and has not been edited
or reviewed for conformity with Geological Survey
standards and nomenclature.

Any use of trade names or trade marks in this
publication is for descriptive purposes only and
does not constitute endorsement by the United States
Geological Survey.

CONTENTS

Hydrologic Studies -

- Part A - Some coastal oceanographic observations, Beaufort Sea, Alaska
Barnes, Reimnitz, Smith.
- Part B - Current meter and water level observations in Stefansson Sound,
Summer, 1976 - Barnes, Reimnitz, and McDowell.
- Part C - Suspended matter in nearshore water of the Beaufort Sea - Drake.
- Part D - A herringbone pattern of possible Taylor-Gortler - type
flow origin seen in sonographs - Toimil and Reimnitz.

Geologic Studies -

- Part E - Preliminary rates of ice gouging, 1975 to 1976, Beaufort Sea,
Alaska - Barnes, Reimnitz, and McDowell.
- Part F - Changes in barrier island morphology, 1949 to 1975, Cross
Island, Beaufort Sea, Alaska - Reimnitz, Barnes and Melchior.
- Part G - Reconnaissance study of Kogru River, Harrison Bay, Alaska -
Reimnitz, Maurer, and Toimil.

Miscellaneous hydrologic and geologic observations on the inner Beaufort Sea Shelf, Alaska

P. Barnes, E. Reimnitz, D. Drake, L. Toimil

Introduction

As part of a multidisciplinary program to assess the impact of development on the continental shelves of the United States, we have engaged in studies of the Alaskan Beaufort Sea. Our aim in this research has been to understand the modern geologic processes that are unique to the arctic. In large part, this has meant a study of ice as a geologic agent.

This report includes several studies of a preliminary nature or of limited scope. Available information on arctic shelf processes is so sketchy that we deemed it appropriate to make these observations available even though the need for further consideration may be obvious.

Acknowledgement

This study was supported jointly by the U.S. Geological Survey and by the Bureau of Land Management through interagency agreement with the National Oceanic and Atmospheric Administration, under which a multi-year program responding to needs of petroleum development of the Alaskan continental shelf is managed by the Outer Continental Shelf Environment Assessment Program (OCSEAP) Office.

PART - A

Some Coastal Oceanographic Observations -- Beaufort Sea, Alaska
Peter Barnes, Erk Reimnitz, Greg Smith, U.S. Geological Survey, Menlo Park.

INTRODUCTION

The coastal oceanography of the Beaufort Sea (Fig. 1) is poorly known. Earlier studies have either been very local or of short time span (Kinney, et al., 1972; Wisemann and others, 1973; Walker, 1974). Others have focused on the outer portion of the continental shelf (Hufford, 1974; Mountain, 1974). The studies of the outer shelf and Canada Basin have documented a generally westward movement of water on the outer shelf during the open water season (Coachman and Aagaard, 1974; Mountain, 1974). But this westerly drift is often complicated by an easterly intrusion of Bering Sea water in the upper 50 m along the shelf break (Mountain, 1974; Hufford, 1973).

Inshore studies indicate that the open water circulation is closely correlated with wind speed and direction (Dygas, 1974; Wisemann and others, 1973) but is generally westerly under a dominance of easterly winds. Coastal and river sediment plumes on Landsat imagery show a dominance of westerly displacements for all of the north coast of Alaska (Barnes & Reimnitz, 1974). Winter circulation is virtually unknown for the inner shelf, although limited data from late spring and early summer show a weak sub-ice westerly drift parallel to the coast (USGS unpublished data).

The seasonal formation of about two meters of ice occurring from September through May, has a profound effect on the inshore temperature and salinity structure. During freezing approximately 80-85% of the solutes are excluded, thereby increasing the salinity and density of the subjacent waters. This effect is most noticeable in shallow waters, especially in isolated and semi-isolated bays and lagoons, where winter salinities are usually above 35 ‰

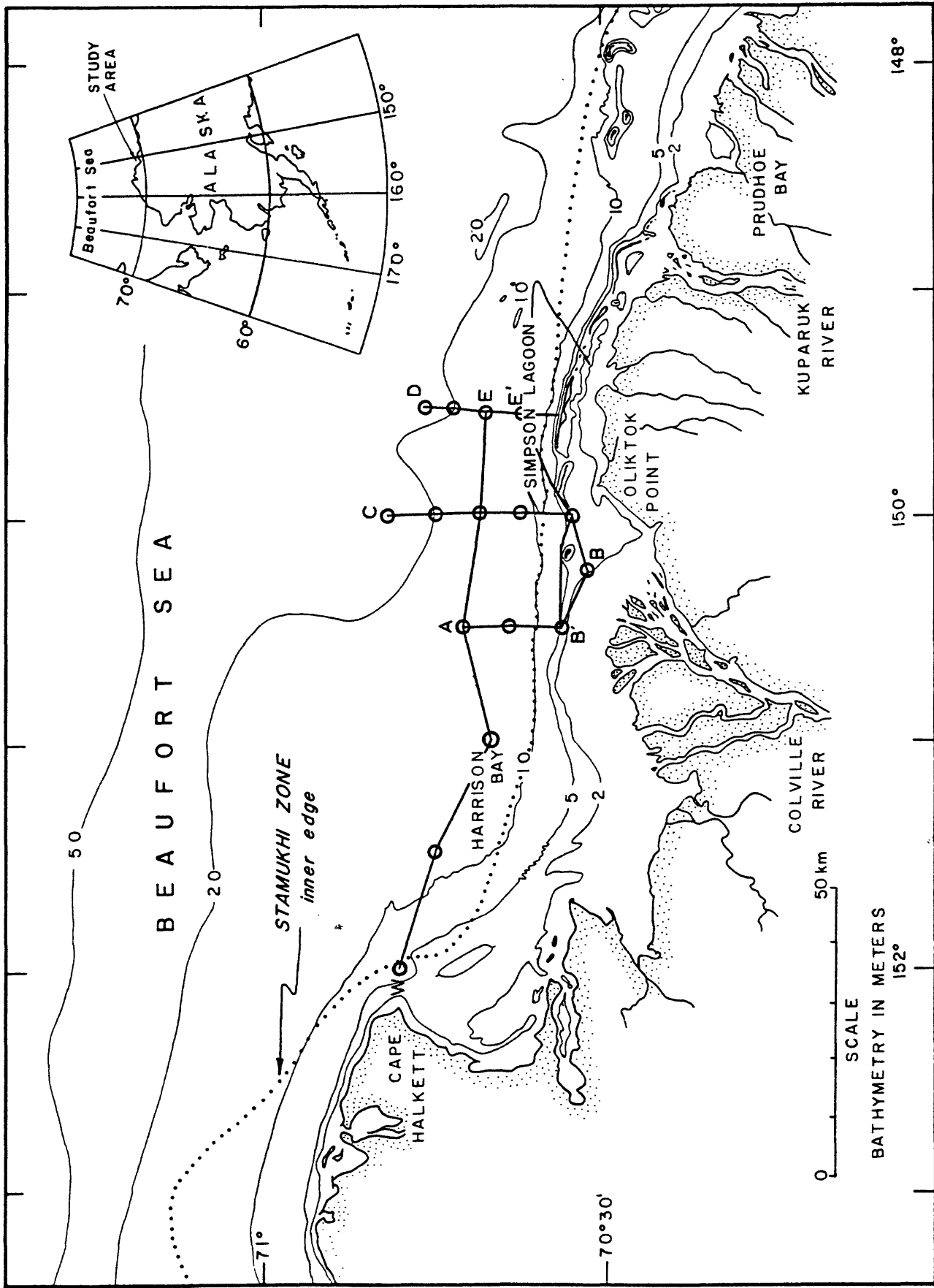


Figure 1. Location map showing areas discussed in the text. In Harrison Bay bottom fast ice extends out to the two meter isobath, floating fast ice extends from the two meter isobath to the first set of grounded ice ridges which mark the inner edge of the stamukhi zone. Tracklines show location of the four profiles for Figures 3 & 5.

and can commonly rise above 50 ‰ (Schell, 1974). The low tidal range of 10-15 cm allows for only minimal volume changes for flushing and mixing the hypersaline waters with the open ocean.

The ice zonation and character on the inner shelf area has been described in detail by Reimnitz and others (1976). Briefly, inshore of the 2 m isobath ice rests on the bottom at the end of the season of ice growth (Fig. 1). Seaward from this bottom-fast ice zone is a zone of floating fast ice up to two meters thick with inclusions of remnants of older ice. Between the 10 and 20 m isobath, interaction of the moving polar pack and the fast ice form the highly deformed ridges of the stamukhi zone. Many ice keels in this zone are in contact with the bottom and may form a partial barrier to the onshore--offshore circulation of water.

In spring, river flow is initiated before the melting and breakup of the fast ice. This fresh water flows over a bottom-fast ice and drains through strudel in the floating fast ice, forming a fresh water layer (Walker, 1974, Reimnitz and others, 1974). As melting proceeds along delta fronts much of the fresh water influx is impounded on the surface by the receding ice front. The bulk of the fresh water input from rivers occurs during this time, prior to the period of open water mixing conditions later in the summer season.

During our geological studies of the inner Beaufort Sea shelf, we have routinely observed temperature, salinity, water turbidity and occasional surface currents. Coverage in two climatically different years, 1972 and 1975, was sufficient in the Harrison Bay area to allow a comparison study. Herein we report the results of these data and speculate on the factors controlling the seasonal and yearly differences in the hydrologic regime of an ice-covered shelf.

Water Characteristics

Three primary sources of surface water on the shelf of the Beaufort Sea during the open water season from mid-July to mid-September can be identified by their temperature, salinity, and turbidity characteristics: river water, sea-ice melt water and oceanic shelf water (Barnes & Reimnitz, 1973; Hufford and Bowman, 1974).

From June to early September river water is distinguishable as warmer water ($1-11^{\circ}\text{C}$) of low to brackish salinity ($0-10\text{‰}$) with significant quantities of suspended sediment and lower transmissivity values ($<15\alpha$ light attenuation coefficient). The initial river floods supply the bulk of the annual water and sediment discharge (Arnborg & Walker, 1962). This occurs in late May and early June, prior to the melting and breakup of the sea ice. The ultimate fate of the water and sediments supplied to the shelf at this time are presently unknown. In part, the initial flood mixes with the highly saline brine remaining from sea ice freezing in the coastal lagoons and lower sections of the deltas (Schell, 1974; Walker, 1974). Subsequent river flow also mixes in part with the sea ice melt waters immediately adjacent to the delta front and in part with the sub-ice shelf waters.

As the sea ice recedes, a second identifiable water type develops from ice melt offshore. This water is of moderate salinity ($5-15\text{‰}$) cold ($0-2^{\circ}\text{C}$), has little suspended material, and therefore is characterized by the high light transmissivities (Barnes, 1974; Hufford et al., 1974). The melt water abundance and dispersion is strongly dependent on seasonal ice distribution and wind regime. Winds act to destroy the density stratification in the surface waters, obliterating the characteristics of this water type. In 1975 an abundance of ice close inshore, aided by restricted wind mixing, resulted in greater amounts of surficial ice melt water than in 1972.

Hufford and others (1974) report mixing processes form a summer surface layer which is stable due to higher surface temperatures and lower salinity thereby decreasing the water density. This stable layer tends to be maintained due to the low wind velocities (rarely over 20 knots) which characterize the open water season.

The third water type, Arctic Surface Water (Hufford and others, 1974), acts as the background influence on the other local water types. Arctic Surface Water of the inner shelf is cold (-1 to 3°C) with salinities of 27-30 ‰, depending on the degree of mixing with river effluent and ice melt waters.

Below the summer surface layer a cold (-1.1 to -1.5°C), saline (30.1-32.2 ‰) layer 5 - 10 m thick is commonly found at depths of 15 to 40 m, east of Prudhoe Bay (Hufford and others, 1974). As winter cooling and convection is more intense than summer heating and mixing, this cold water is presumed to be the remnant of the winter convective processes. A body of water with similar temperature and salinity characteristics occurs in shallow (< 10 m) water of Harrison Bay (this Report).

Methods

Surface temperature and salinity observations were made with a conductivity cell modified for negative temperatures encountered in Arctic use. Measurements of water clarity were obtained routinely from a 10 cm pathlength transmissometer during underway geophysical studies in 1971, 1972, 1973 and 1975. Temperatures are believed to be accurate to $\pm 0.5^{\circ}\text{C}$ salinities to ± 0.5 ‰, and transmissivities to $\pm 2\%$. Early data were obtained from the R/V LOON and R/V NATCHIK, the 1975 data from the R/V KARLUK. Repetitive coverage of the inner shelf in the vicinity of Oliktok Point during 1972 and 1975 by these three vessels was sufficiently dense for us to make a multiyear comparison of the water structure in this area. Landsat imagery is used to correlate our water data with surface water character elsewhere on the inner shelf during the open water period of 1972.

DATA AND RESULTS

Temperature

Temperatures observed in surface waters of Harrison Bay during 1972 are several degrees warmer than those observed in 1975 (Fig.2). 1972 values range from below 0°C off Oliktok Point to over 8° in Simpson Lagoon. With the exception of low temperatures off Oliktok Point, values generally decrease in an offshore direction.

An examination of temperatures and their time of observation suggests a daily fluctuation of surface water temperatures on the order of several degrees. At an anchor station 45 km north of Colville Delta, in 20 m of water, Hufford and others (1974) recorded a temperature variation of 2.3°C during a 32-hour period. Such daily variations are superimposed on variations related to advective and convective processes.

Vertical temperature profiles taken in August and September, 1972 (Fig.3) show a 2 - 6 m thick surface layer of 0.5 to 2.5°C water in central and western Harrison Bay and off the islands to the east of Oliktok Point. Cold surface water found in the region northwest of Oliktok Point (Fig.2A) extends to the bottom or into Harrison Bay (Fig.3D) and eastward outside the islands (Figs.3B & C).

Salinity

The patterns formed by surface salinity variations are more distinctive than temperature patterns. The range of salinity values observed in 1972 is much greater than in 1975 (Fig. 4). In July 1972, values range from less than 8‰ off the Kuparuk River to over 25‰ nearshore west of Oliktok Point, and off central Harrison Bay (Fig. 4A). Later in the same year surface salinity values were generally higher (Fig. 4B). At this time lowest surface salinities (below 20‰) were observed off the Colville and Kuparuk Rivers, and on the central shelf in the northeastern part of the study area. Again the highest

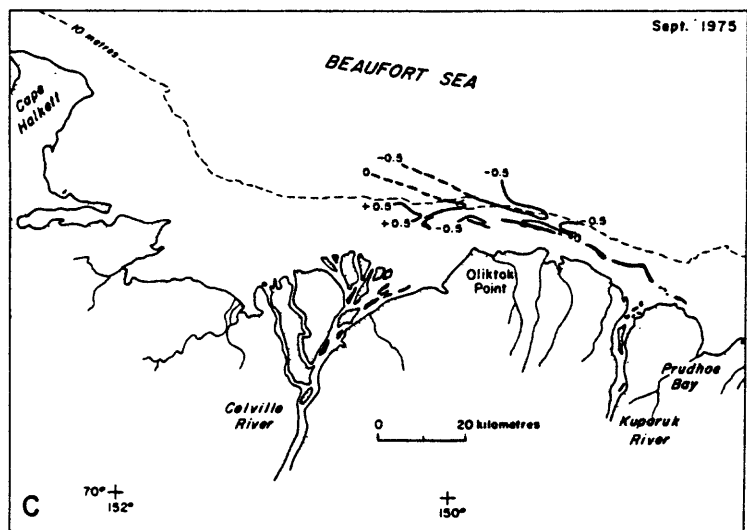
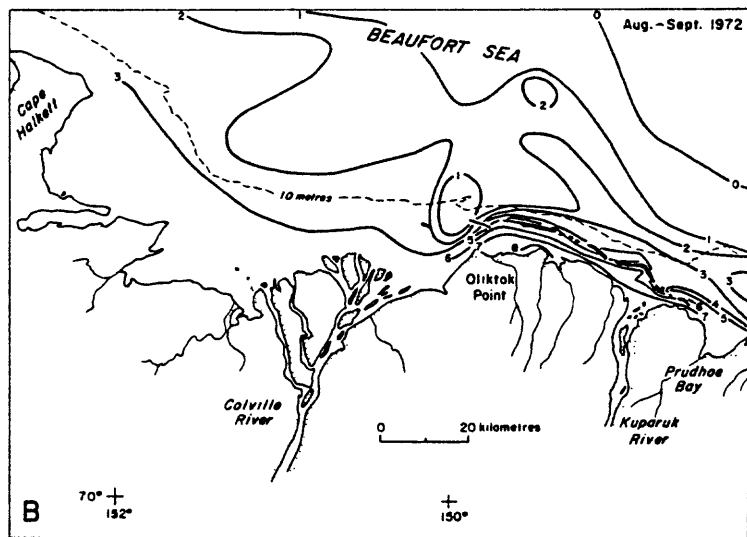
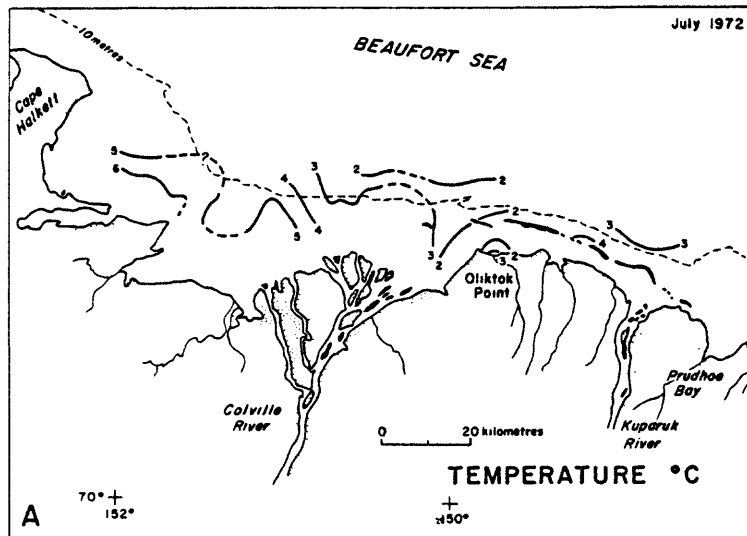


Figure 2. Distribution of surface temperature values during early summer, 1972 (A); late summer, 1972 (B); and late summer 1975 (C). Contour interval; 1972 - 1°C; 1975 - 0.5°C.

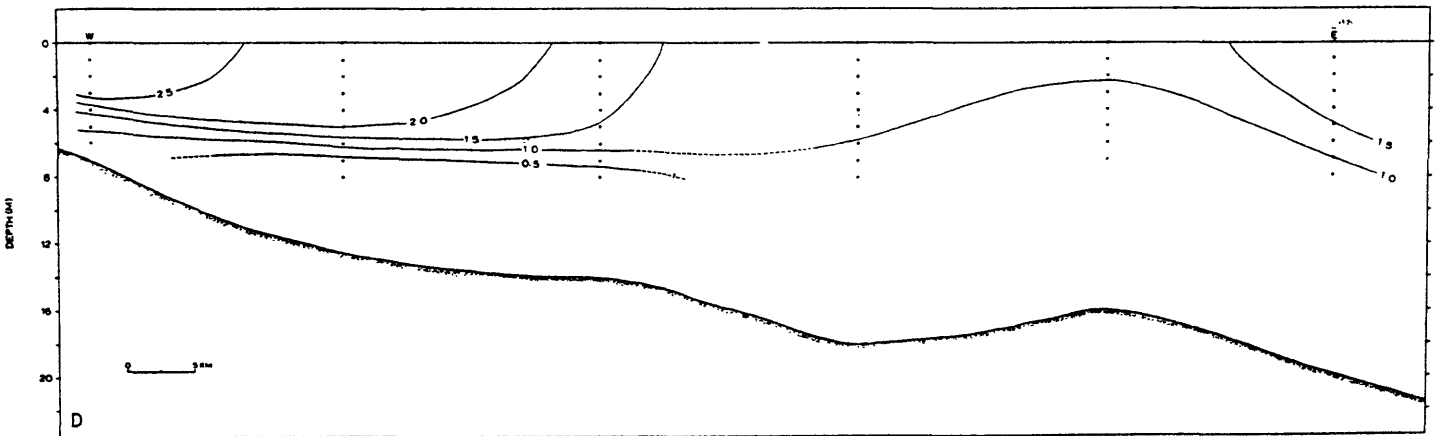
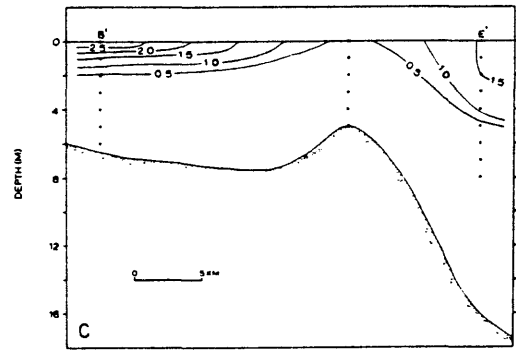
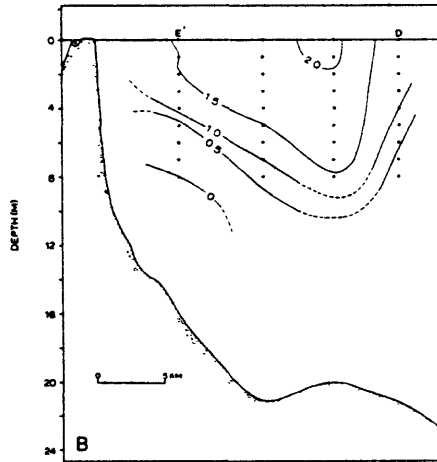
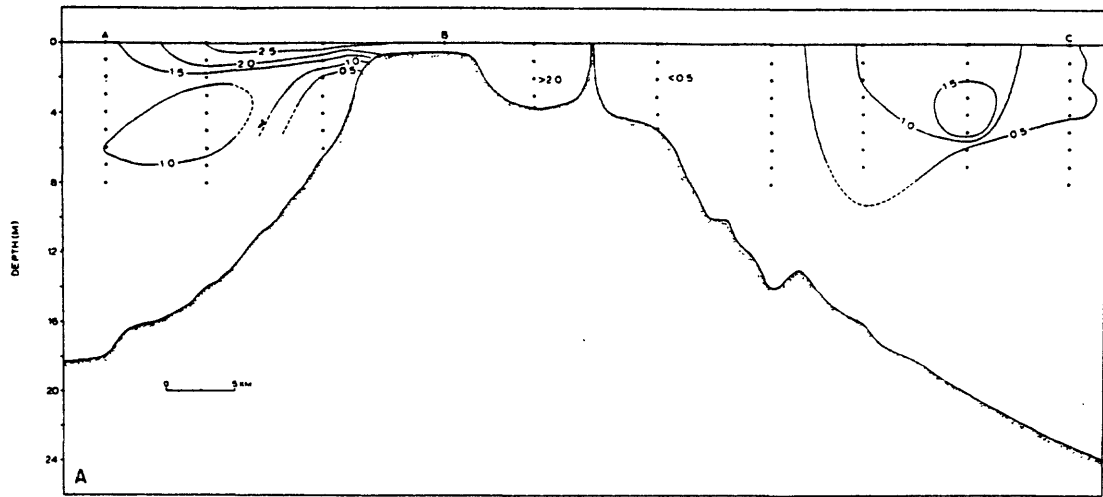


Figure 3. Vertical distribution of temperature in the Harrison Bay area in late August and early September, 1972. Location of the four profiles is shown in Figure 1. Contoured at 0.5°C interval. Surface values are contoured in Figure 2B.

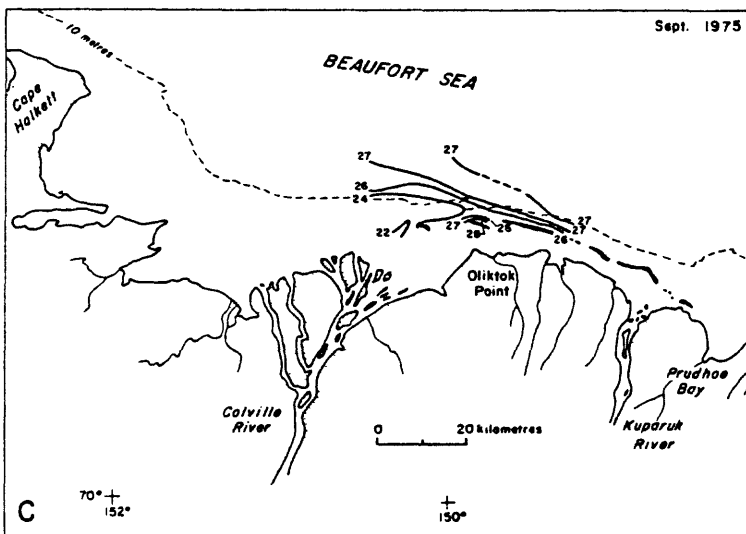
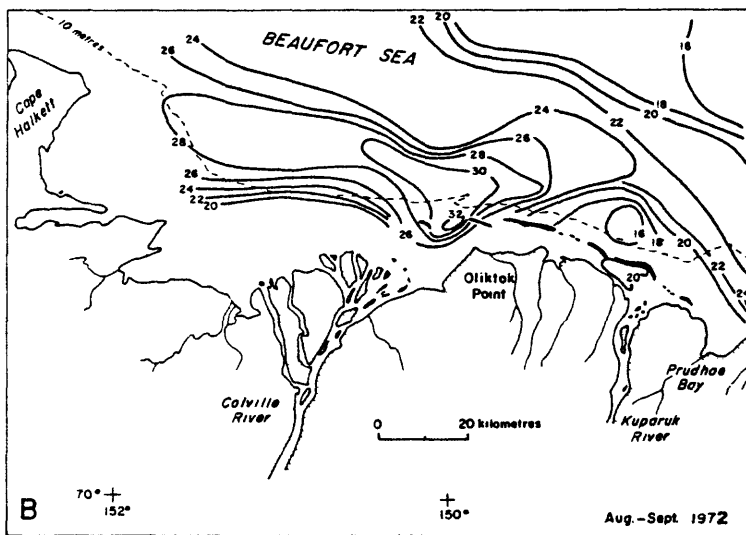
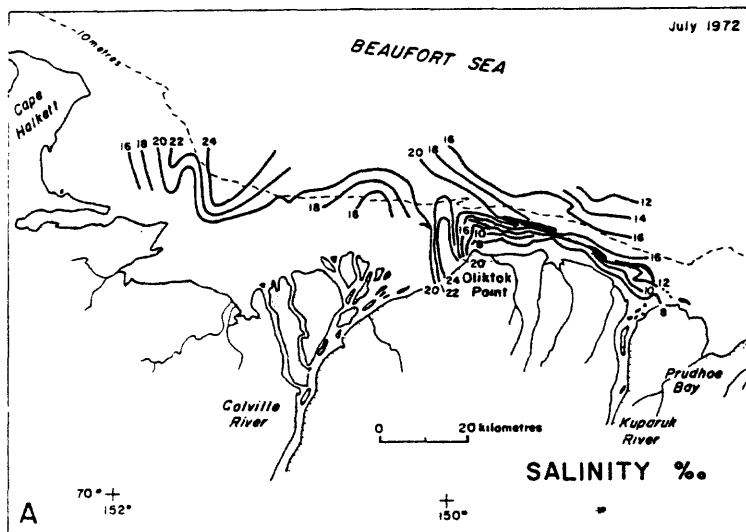


Figure 4. Surface distribution of salinity values during early summer, 1972 (A); late summer, 1972 (B); and late summer 1975 (C). Contour interval $2^{\circ}/\text{oo}$. Note the occurrence of high salinity surface water off Oliktok during all three surveys - $24^{\circ}/\text{oo}$ water in July, 1972; $32^{\circ}/\text{oo}$ water in August and September, 1972; and $28^{\circ}/\text{oo}$ water in September, 1975.

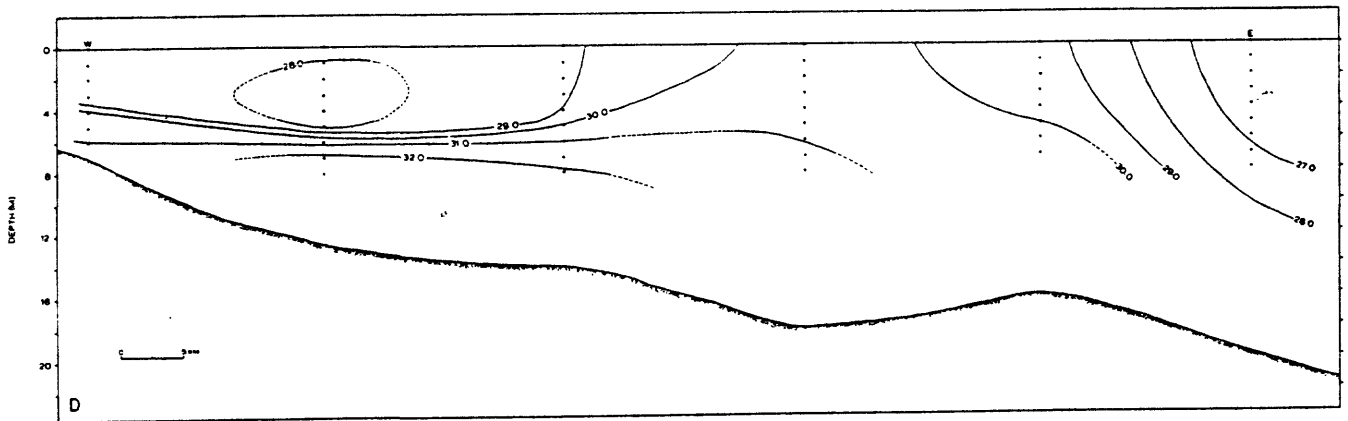
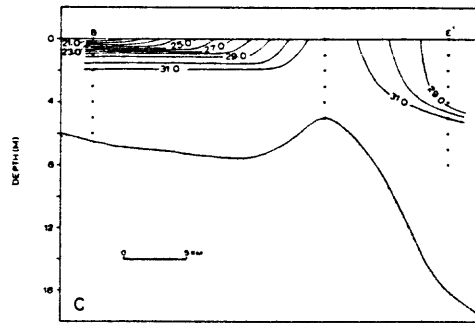
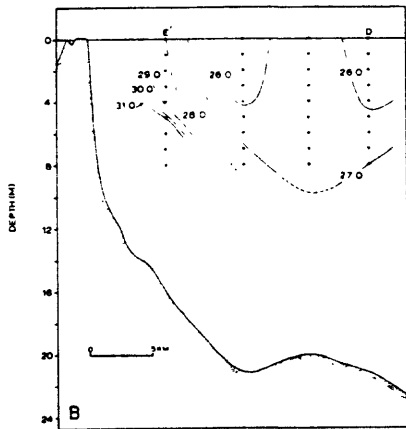
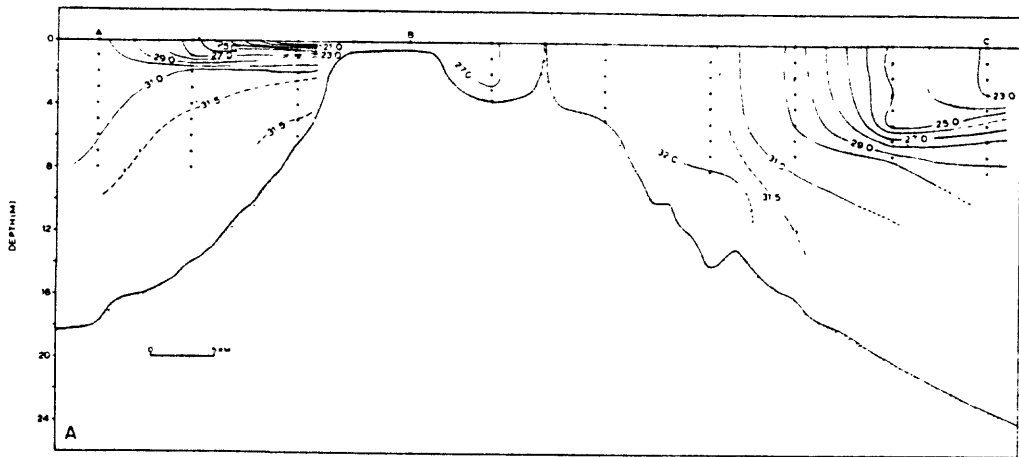


Figure 5. Vertical distribution of salinity in Harrison Bay during late August and early September, 1972. Location of the four profiles is shown in Figure 1. Contour interval 1/‰. Surface values are shown in Figure 4B.

salinities (greater than 32 ‰) were observed off Oliktok Point. In 1975 the area of high salinity is displaced eastward along the outside of the islands by the fresher waters of Harrison Bay (Fig. 4C) when compared to either of the 1972 data sets (Figs. 4 A&B). During this year the surface salinity gradient is less pronounced than in earlier surveys.

Vertical profiles of salinity which complement the August -September 1972 surface distribution (Fig. 4B) show a thin (2-m surface layer of low salinity water off the central Colville Delta (Figs. 5 A & C). Elsewhere the salinity surface layer is thicker (4-6 m). The underlying layer of high salinity water is best developed in central Harrison Bay (Fig. 5 D) west of its surface expression off Oliktok Point (Fig. 4 B). It appears to be less developed offshore (Figs. 5 A & B) and to the east (Fig. 5 D).

Transmissivity

Patterns of water clarity measured as light transmission (transmissivity) show a gradual seaward decrease in surface water turbidity (Fig.6). In July, 1972, (Fig.6A) coastal waters were most turbid in Simpson Lagoon and off the Kuparuk River. A zone of clearer water extended from the coast near Oliktok Point to the northwest. A Landsat 1 image taken on 25 July, 1972, during the period of shipboard observations, also shows this area of less turbid water (Fig.7). A band of turbid water can be traced close inshore along the mainland coast from the Kuparuk River to Oliktok Point and across the front of the Colville Delta to Cape Halkett. Darker, less turbid offshore waters extend to the coast just south of Oliktok Point. Winds during this period were from the east-northeast.

Later in the same year there is a similar seaward decrease in turbidity, but the gradient is much less pronounced (Fig.6B). Furthermore, the surface waters are generally more turbid than during the July observations with the comparable transmissivity contours located further offshore. The tongue of clear water extending landward to Oliktok observed in the July surface data

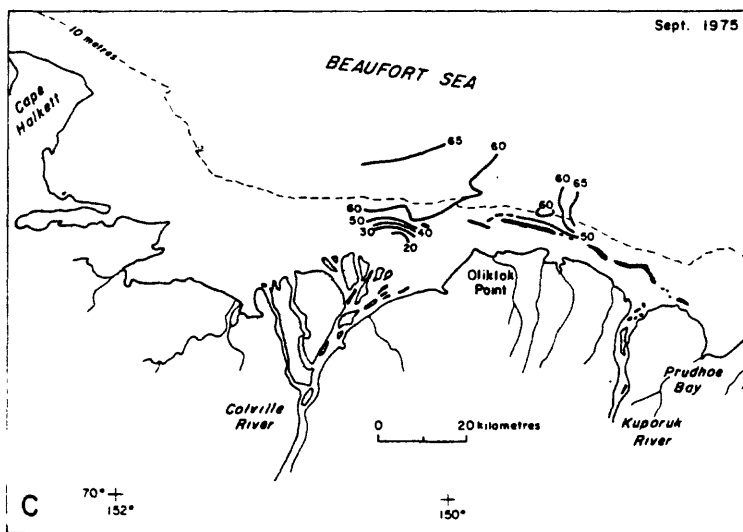
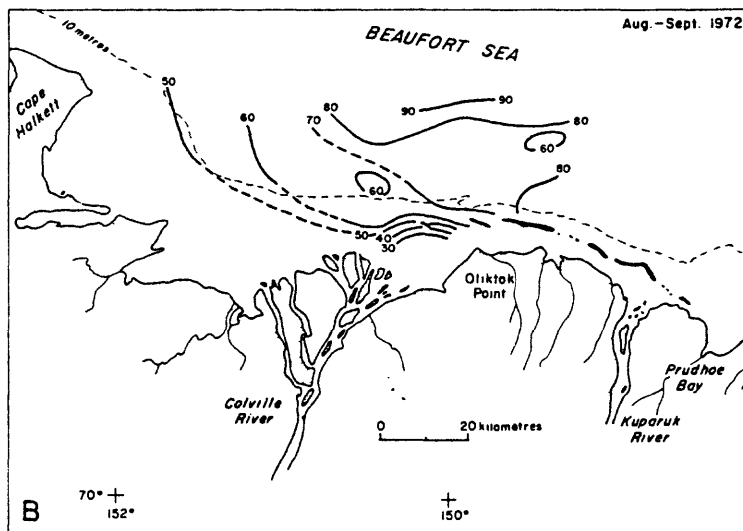
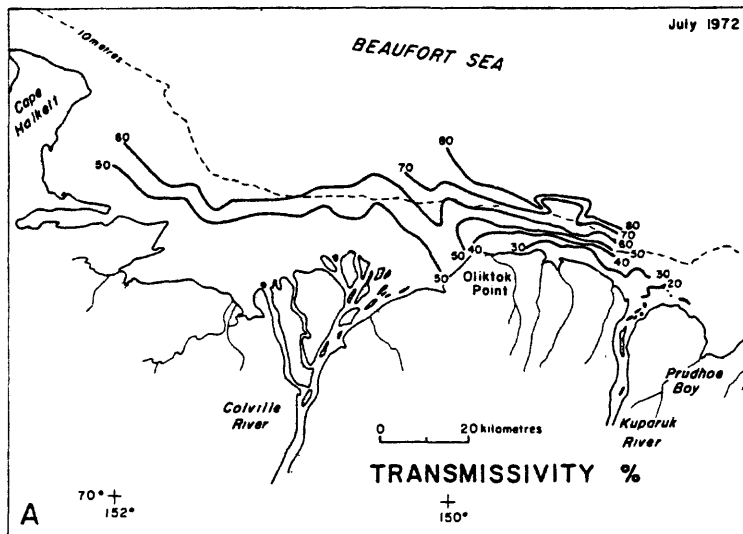


Figure 6. Surface distribution of water clarity expressed as percent transmissivity. Early summer, 1972, (A); late summer, 1972 (B); and late summer, 1975 (C). Contour interval 10%.

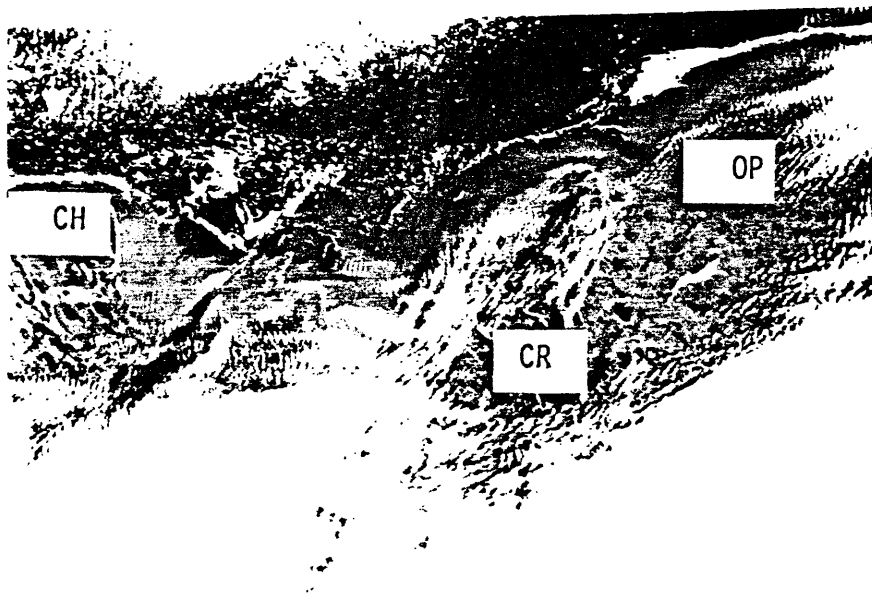


Figure 7. LANDSAT image of Harrison Bay area, Beaufort Sea. Image taken 25 July, 1972, during the period of observations which are shown in Figures 2A, 4A, and 6A. Note the displacement of Colville River (CR) plume to the west toward Cape Halkett (CH) and the tongue of clear water extending almost to the coast at Oliktok Point (OP).

(Fig. 6A and satellite image Fig. 7) is not present. On the contrary, the waters are most turbid in this area. Winds during late August and early September were generally strong from the east and during the first week in September a storm occurred with strong northeasterly wind and an unusually large 8-10 sec swell. Aerial observations during this storm indicated considerable resuspended material was present inside of about the 5 m contour. This storm is probably the major cause of the turbidity pattern of Figure 6.

During September of 1975, inshore waters were generally more turbid than in either period of observation in 1972 (Fig. 6C). In addition to the coastal and river-supplied turbid waters there appears to be a zone of turbid water extending northeastward from Oliktok Point. Winds during the 1975 study were dominated by westerlies.

DISCUSSION AND CONCLUSIONS

A comparison of surface water characteristics indicates that the three periods of observation were distinctly different. Yet more saline, colder water was consistently present northwest of Oliktok Point throughout all of the periods of observation.

The July 1972 (Figs. 2A, 4A and 6A) data with lowest salinities and generally transmissivities appear to reflect the influence of fresh, warm and turbid Colville River water from the melting of the fast ice. These data also show a decrease in surface salinities toward the pack ice edge, a source of melt water.

The August-September 1972 (Figs. 2B, 4B and 6B) distribution of variables is apparently dominated by oceanic influences. The river flow is lower at this time of the summer and pack ice melting is reduced due to lower temperatures. The summertime coastal salinities are therefore at their highest as mixing

processes have had an extensive period in which to act.

During both 1972 observation periods the flow of surface water appears to be westerly, with the less saline, turbid plumes of the Colville displaced to the west of the delta front. This conclusion is supported by Landsat imagery (Fig. 7) and by the dominance of easterly winds during the 1972 open water season, which kept the pack-ice well offshore in this area during much of the summer (Hufford, 1974) and encouraged westerly surface drift.

In 1975 the dominance of westerly winds kept sea ice close onshore and apparently resulted in easterly surface flow for the coastal water off Oliktok (Figs. 2C, 4C and 6C). At the end of the open water season in the average year, oceanic mixing is well advanced. However, in 1975, large amounts of pack ice in shallow water may have restricted spreading of river waters resulting in low salinities observed in September.

The relation of wind to the distribution of surface water character has been noted by others. Hufford and Bowman (1974) in an aerial radiation thermometer survey of Harrison Bay in August, 1973, show a surface thermal pattern, which they relate to westerly wind during the time of their survey. Two significant findings were noted: the lack of a major river plume off the Colville and a cold water zone extending from northwest Harrison Bay toward the delta of the Colville. They relate the cold water intrusion ($1-3^{\circ}\text{C}$), paralleling the 5 m depth contour, to surface waters. The boundary between warm inshore waters and colder offshore waters was also marked by a color change from brown to green. During the survey, the warmer waters were confined to inner Harrison Bay and to the vicinity of Oliktok Point by the westerly winds. Thus, it appears that the general distribution of summer surface water character in Harrison Bay is primarily wind controlled with ice as a secondary influence.

It is apparent from the above discussion that the surface patterns are derived primarily from the influence of river input, ice melt and mixing with shelf waters. However, the source of the recurring colder and relatively more saline waters in the vicinity of Oliktok Point in 1972 and 1975, and for the cold (saline?) water in 1973 (Hufford and Bowman 1974) is not obvious. For the year in which we have vertical profiles (1972), the data shows the water seen at the surface occurs as a bottom layer along the islands to the east and also in central Harrison Bay. Water of similar character (temperatures below 0.5°C and salinities of about 32 ‰ can only be found 60-70 km seaward at 70 m depth beyond the shelf break (Hufford and others, 1974). At the time of our survey these two similar water types were not connected. Although we can not rule out the possibility of a slug of water being a remnant from an upwelling episode (Hufford, 1974), these cold saline waters may well represent a remnant slug of the previous winter's convective cooling.

The winter freezing of 2 m of ice, coupled with the exclusion of solutes under conditions of reduced winter circulation, has a significant effect on the inner shelf temperature and salinity regime. The winter convective cooling is more intense than the summer heating of the near surface waters. The characteristics of winter water may be preserved throughout the summer (Zubov, 1943).

We attempted to test this hypothesis by calculating the salinity increase of the sub-ice water in Harrison Bay resulting from brine exclusion during the formation of ice (Neshyba and Badan-Dangon, 1974). Because of some unknowns, and in order to simplify the calculations we are assuming a closed system. Arbitrarily we have chosen the area between a line due north from Cape Halkett and one north from Oliktok Point out to the 10-m and

20-m isobath for our calculations. Assuming no advection across the above boundaries, an 80% exclusion of solutes during 2 meters of ice growth (Schell, 1974) and initial fall surface salinities of 20 and 30 ‰, the waters within these boundaries would increase in salinity as follows:

Fall Surface salinity	Spring Salinity of sub-ice water between 2 and 10 m isobath	Spring salinity of sub-ice water between 2 and 20 m isobath
20 ‰	46.7 ‰	34.3 ‰
30 ‰	55.0 ‰	36.4 ‰

Clearly enough cold saline water is generated to account for the volume observed in 1972, and could have been a partial remnant of the previous winter's convective cooling and brine exclusion from the winter ice cover.

The stagnation of this water mass in Harrison Bay may be aided by the stamukhi zone ice boundary which forms generally along the 20 m isobath (Reimnitz and others in press) and undoubtedly forms a partial barrier to offshore advection during the winter. In some years the stamukhi ice barrier may remain in place for much of the summer season, further isolating the inshore waters.

With dominant easterly winds during the 1972 summer season, it is apparent that the surface water in Harrison Bay moved offshore to the northwest and was replaced by cold, high-salinity subsurface water remaining from the winter. This type of upwelling should be expected to occur rather commonly as the summer winds are commonly from the east.

REFERENCES CITED

- Barnes, P.W. and Reimnitz, E., 1974, Sedimentary Processes on Arctic shelves off Northern Alaska: in: The Coast and shelf of the Beaufort Sea, J.C. Reed and J.E. Sater eds., Arctic Inst. of North America, Arlington, Virginia, p. 27-42.
- Coachman, L.K., and K. Aagaard, 1974, Physical oceanography of Arctic and subarctic seas, Chap. 1, p 1-72 in: Marine Geology and Oceanography of the Arctic Seas, Y. Herman, ed., Springer Verlag, New York.
- Dygas, J.A., 1974, A study of wind, waves and currents in Simpson Lagoon, in: Environmental Studies of an Arctic Estuarine System; V. Alexander, ed., University of Alaska, Inst. of Marine Science, Report R74-1.
- Hufford, G.L., 1973, Warm water advection in the southern Beaufort Sea, August-September, 1971, Jour. Geophys., Resch., 78: 2702-2707.
- Hufford, G.L., 1974, On apparent upwelling in the southern Beaufort Sea, Jour. Geophys. Resch., 79: 1305-1306.
- Hufford, G.L., Fortier, S.H., Wolfe, D.E.; Doster, J.G., and Noble, D.L., Physical oceanography of the western Beaufort Sea, in: Websec 71-72, An ecological survey in the Beaufort Sea, U.S. Coast Guard, Oceanographic Report No. 373-64.
- Hufford, G.L., and Bowman, R.D., 1974, Airborne temperature survey in Harrison Bay, Arctic, 27: 69-70.
- Mountain, D.G., 1974, Preliminary analysis of Beaufort shelf circulation in summer, in: The Coast and shelf of the Beaufort Sea, J.C. Reed and J.E. Sater eds., Arctic Inst. of North America, Arlington, Virginia, p. 27-42.
- Neshyba, S., and Badan-Dangon, A., 1974; On ocean current induced by a prograding ice pack, Geophysical Research Letters VI, p. 351-354.
- Reimnitz, Erk, Toimil, L.J., and Barnes, P.W., Arctic continental shelf processes and morphology related to sea ice zonation, Beaufort Sea, Alaska: AIDJEX Bull. (Arctic Ice Dynamics Joint Experiment, University of Washington) 36 p., 20 illus. (in press).

Schell, D.M., 1974, Seasonal variation in the nutrient chemistry and conservative constituents in coastal Alaskan Beaufort Sea waters, in: Environmental studies of an arctic estuarine system; V. Alexander ed., University of Alaska, Inst. of Marine Science, report R74-1, p. 217-282.

Wiseman, W.J., Coleman, J.M., A. Gregory, Hsu, S.A., Short, A.D., Suhayada, J.N., Walters, D.D. Jr., and Wright, L.D., 1973, Alaskan Arctic coastal processes and morphology; Coastal Studies Institute, Louisiana State University, Tech. Rept. No. 149.

Zubov, N.N., 1943, Arctic sea ice, translated by the Naval Oceanographic Office and the Am. Meteorological Soc., 1963, Published by Naval Electronics Laboratory, San Diego, California, 491 pp.

PART - B

Current meter and water level observations in Stefansson Sound, Summer, 1976.

Peter Barnes, Erk Reimnitz, and David McDowell

As part of the program to determine the rate and direction of sediment movement, an Aanderaa RCM-4 Current meter and an Aanderaa water level gauge were moored along with a Montadero nephelometer-transmissometer in 5.5 meters of water in central Stefansson Sound, northeast of Prudhoe Bay, Alaska in late July, 1976 (Fig. 1). The water level gauge was resting on the bottom and the current meter sensors were located about 1 m above the sea floor. The instrument array, in excellent condition, was recovered in late September of the same year for a record length of 52 days. The current meter and tide gauge data tapes were interpreted at both the NOAA Pacific Marine Environmental Laboratory in Seattle and at the Environmental Protection Agency Corvallis office. The nephelometer-transmissometer data tape has yet to be decoded.

OBSERVATIONS -

Just prior to mooring this meter, a Bendix Q-15 vector-averaging current meter measured currents of 60 cm/s at $-085^{\circ}T$ 1.5 m below the surface. Bottom currents were 40 cm/s ($110^{\circ}T$) at 0.5 m off the sea floor. Initial Aanderaa current meter readings were 25 cm/s at $-075^{\circ}T$. The water character, similar to the current regime, is very different at the surface and near the bottom. Surface temperatures were about $5^{\circ}C$ and salinities about 11 ‰, while the initial temperature values from the current meter near the bottom were $0.5^{\circ}C$ and 24 ‰. Continuous surface weather observations from Deadhorse, Alaska (Prudhoe Bay) were used for barometric pressure, windspeed and direction data in interpreting the current and water level records.

SEA LEVEL -

Graphical methods were used to determine if a correlation exists between sea level and barometric pressure. Water pressure as measured by the gauge includes both effects of atmospheric pressure and water density. These factors have to be considered before true sea level differences can be compared. A non-tidal water pressure curve was obtained from the mid-points of the semi-diurnal tidal ranges. Water density was determined from temperature and salinity values measured by the current meter. These values were used to approximate the temperature and salinity character of the entire water column. As noted above there could be significant differences between the surface and near bottom waters. Sigma-t values were taken from Hydrographic Office Special Publication No. 68. The pressure factor of water density was omitted as it is insignificant at four meters. True sea level was then calculated using the following equation:

$$H = \frac{P(\text{gauge}) - P(\text{atm})}{\rho g}$$

where H equals sea level₃ in centimeters; P equals pressure in bars and ρ equals density in gms/cm³ and g is the acceleration of gravity.

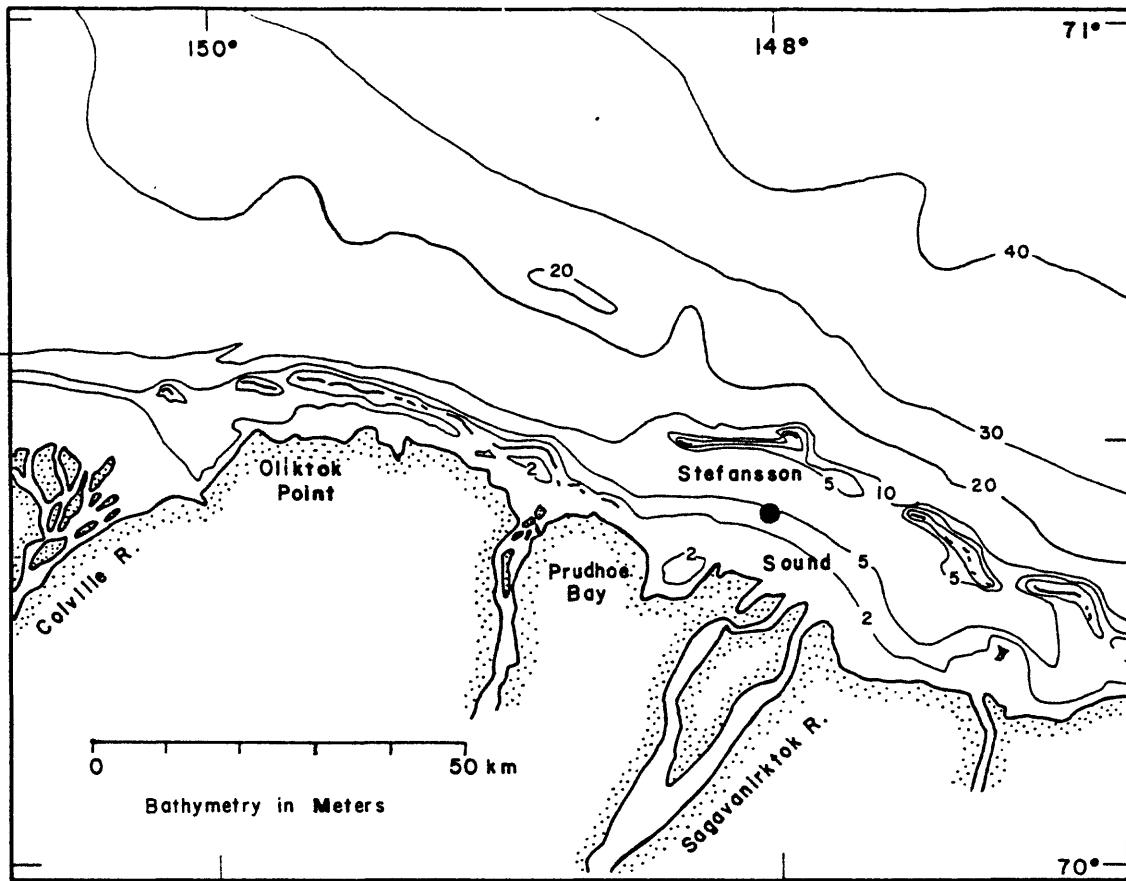


Figure 1. Map showing the location of the current meter mooring of August and September, 1976, in Stefansson Sound.

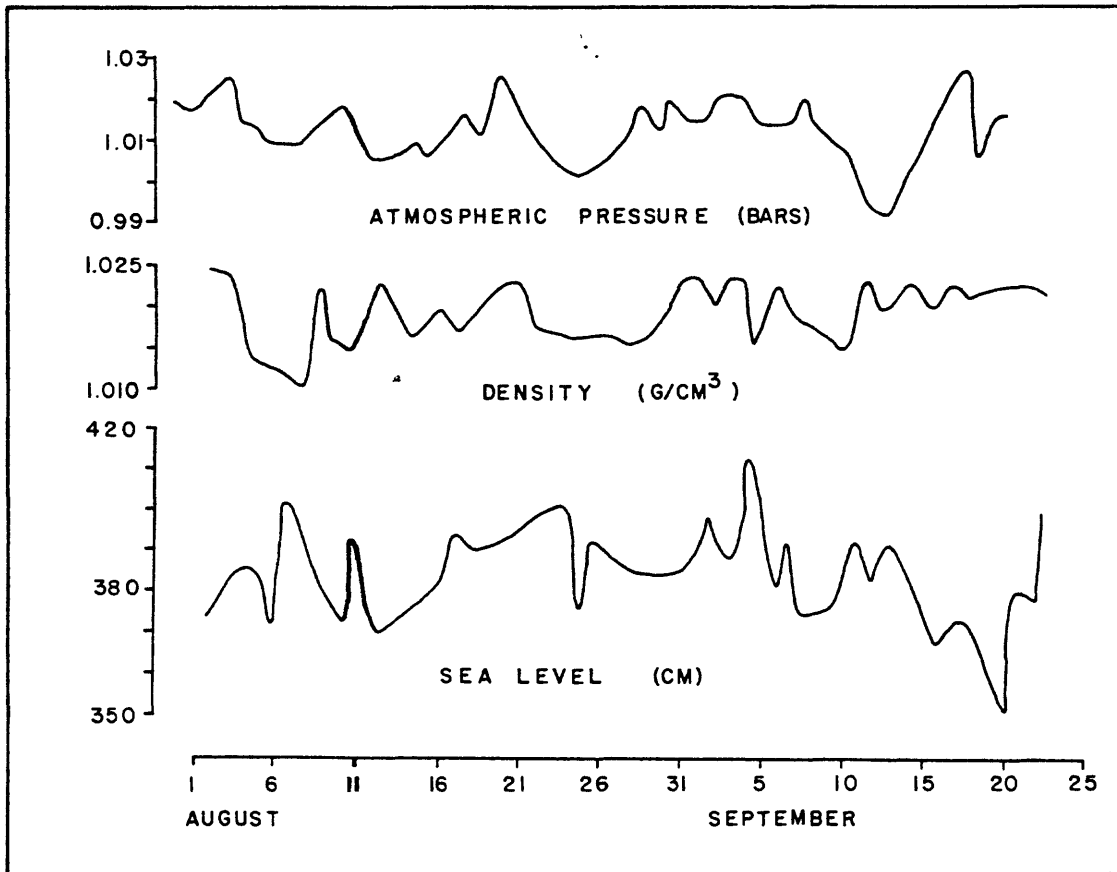


Figure 2. Relationships between atmospheric pressure(Deadhorse airport), water density(current meter sensors), and sea level. Note; $\text{Sigma-t} = (\text{density} - 1) \times 10^3$.

The observed density, and atmospheric pressure are compared to the computed sea level data in Figure 2. Density which is directly related to temperature and salinity, tends to increase from August (about 16 sigma-t unit) to September (about 23 sigma-t units). This is probably partly due to the decreasing air temperatures toward the end of summer, and partly to increasing salinity from mixing processes which have masked the early summer fresh water input from river flooding and ice melt. There does not appear to be a strong relationship between density and sea level.

Atmospheric pressure and sea level show a very similar trend. The atmospheric highs and sea level highs correspond well between about 15 August and 22 September, although the sea level maxima occur one to several days after the atmospheric pressure peaks. The matching of sea level highs with high atmospheric pressures would seem to be the inverse of what one might expect to observe. Apparently wind forces associated with atmospheric pressure changes are more influential on sea level than pressure itself.

Currents

The progressive vector diagram for currents at this site (Fig. 3) shows an overall transport of water 200 plus km to the northwest, the direction of the western entrance to Stefansson Sound (Fig. 1). There are notable secondary excursions to the northeast. As one might expect most of the water motion at this location is essentially parallel to the coast, and to the bathymetric contours. Peak velocities on the order of 53 cm/s were recorded (sufficient to resuspend and transport coarse sand) and the mean velocity was about 13 cm/s. A correlation exists between the progressive vector diagram and sea level, or atmospheric pressure. When these latter two factors are rising it appears that the net water transport is to the east, while falling sea levels generally correspond to westerly transport (Figures 2 & 3). Comparing winds to atmospheric pressure, we find that in general westerly water transport can be correlated with northeasterly winds and lowered sea levels. Weak or westerly winds correspond to easterly water transport and higher water level. Of course any native familiar with the area can tell you this same story about currents, sea level and wind relationships but, here is the scientific proof.

The correspondence between temperature and salinity at the current meter site is straightforward (Figure 4). Bottom water temperature values ranged from a minimum of -0.9°C to 7.5°C , averaging 1.73°C while salinities varied from a low of 12.8 ‰ to 30.6 ‰, averaging 24.4 ‰. Both the minima and maxima of salinity and temperature occurred at the start of the record in early August. Throughout the record there is good correlation between temperature and salinity with high values of salinity being associated with low temperatures and conversely, low salinities with warmer waters. The record suggests a general cooling of the bottom waters starting around the first of September.

DISCUSSION

An inter-relationship between the surface winds at the Deadhorse airport and the movement and character of water at the current meter is apparently complex. At first glance it would appear that prevailing northeasterly

STATION*STEFANSSON
PROJECT*USGS

LATITUDE*70 23.95 N
LONGITUDE*148 01.40W
DEPTH* 5.50 METERS

METER*17562

DEPTH*4.5 METERS

MEAN PRESSURE* 0.00 METERS

RECORD LENGTH* 52.58 DAYS

NET DRIFT* 3.75 CM/SEC, 330° T

MEAN SPEED* 12.78 CM/SEC

U-VARIANCE* 195.3

V-VARIANCE* 43.0

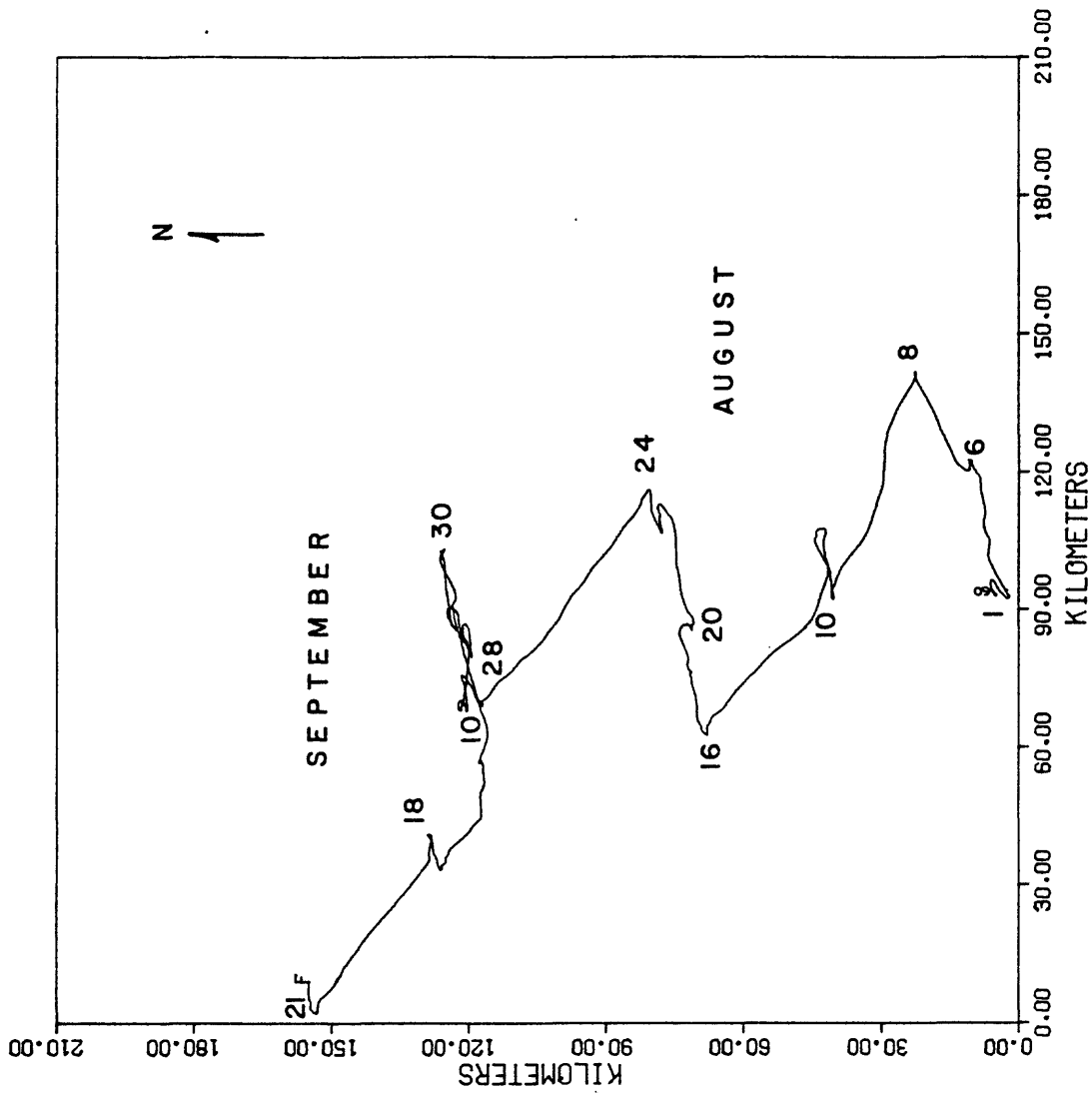


Figure 3. Summary characteristics and progressive vector diagram.

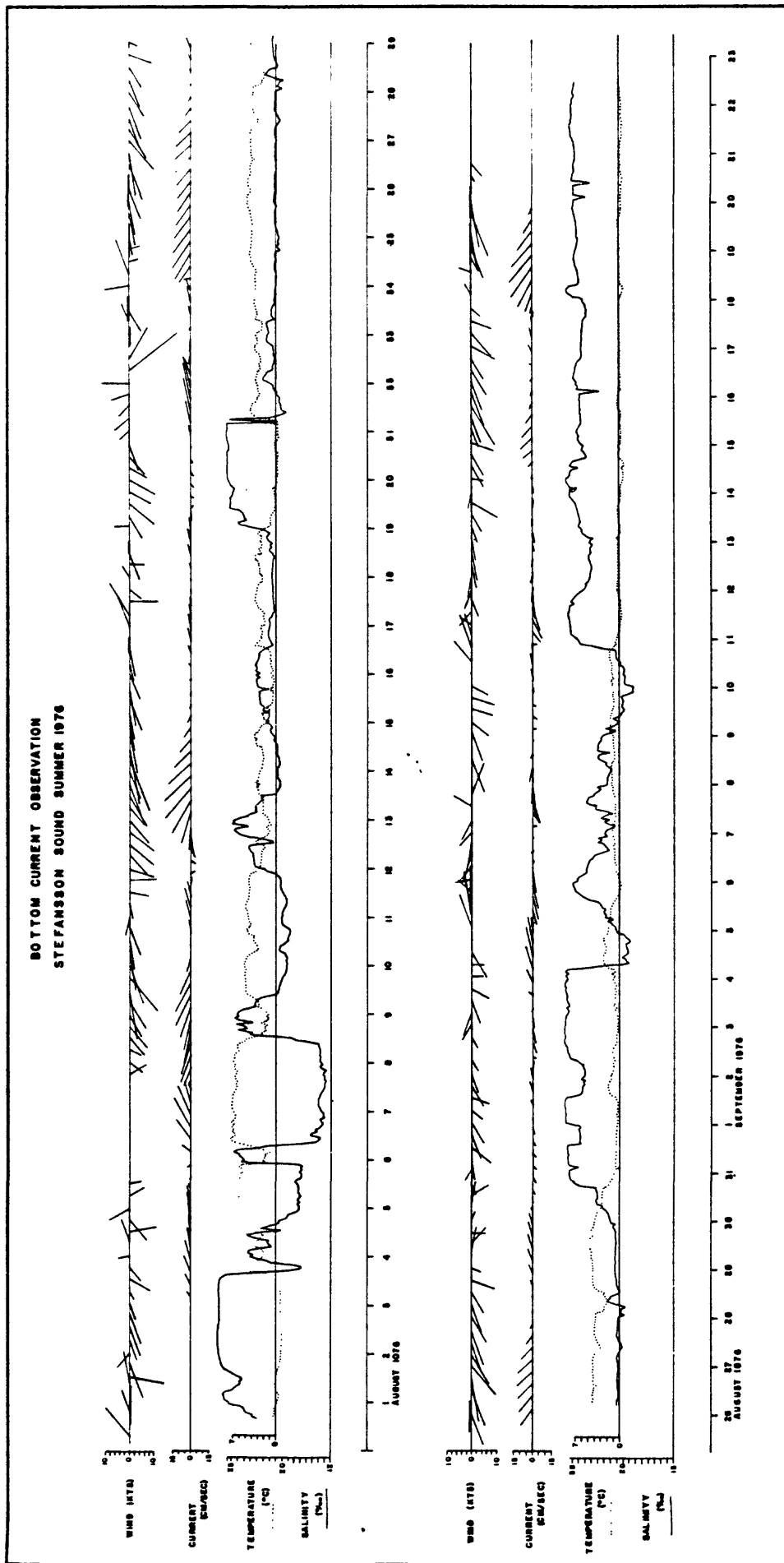


Figure 4. Plot of wind and current as direction of motion, and temperature and salinity versus time at the current meter site in Stefansson Sound.

winds are associated with northwesterly currents (Figure 4), demonstrating the classical influence of Coriolis force and Eckman spiral. Upon close examination, this relationship does not always hold true. Furthermore, it is apparent that during periods of weak, variable, or westerly winds, the currents flow to the east. We interpret this to suggest that under such conditions near bottom currents were trying to flow eastward, perhaps under geostrophic pressures, but were periodically reversed due to the influence of surficial wind stress from the northeast. In any event it is apparent that the response of current to wind stress occurs very rapidly.

Temperature and salinity changes are also associated with the alterations in the flow regime. Easterly currents are usually associated with warmer less saline waters while westerly's are coupled with colder more saline water. This relationship can best be explained, in our opinion, by a model in which warm, fresh surface water overlies more saline and colder near-bottom water (Figure 5). When the water moves in a westerly direction the surface water spreads out offshore due to the influence of Coriolis forces, and the near-bottom sensors see upwelling of cold saline water that enters the sound through the passes in the island chain to the northeast. During periods of easterly flow the surface layer tends to be piled up against the coast and if it is sufficiently thickened the warmer less saline water is seen at the current meter sensors.

In summary the following conclusions can be drawn from the records taken in Stefansson Sound during the open water season of 1976:

1. Sea level parallels changes in barometric pressure, but lags slightly behind.
2. Rising sea levels are associated with easterly currents and lowering levels with westerly currents as expected for Ekman transport induced by these winds.
3. Currents are essentially parallel to the isobaths, with a slight offshore component and a net drift to the northwest in the summer of 1976.
4. Warmer and less saline waters occur in the bottom water during periods of easterly flow, which is accompanied by rising sea levels and weak, westerly or offshore winds.
5. Westerly flow is associated with strong northeasterly winds, lowered sea levels, low temperatures and high salinities.
6. Current velocities are commonly sufficient to erode and transport medium to fine sands.
7. Currents respond quickly to changes in the wind regime.

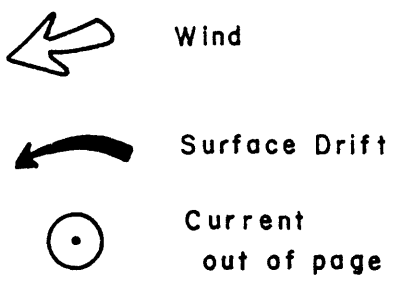
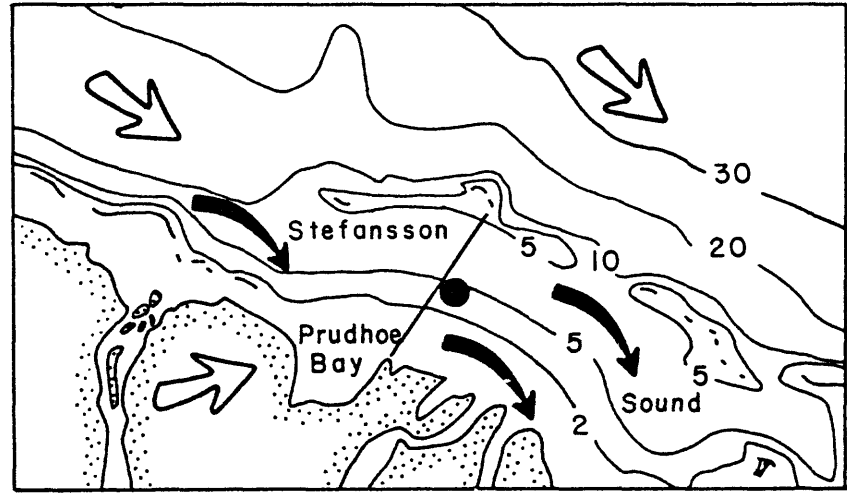
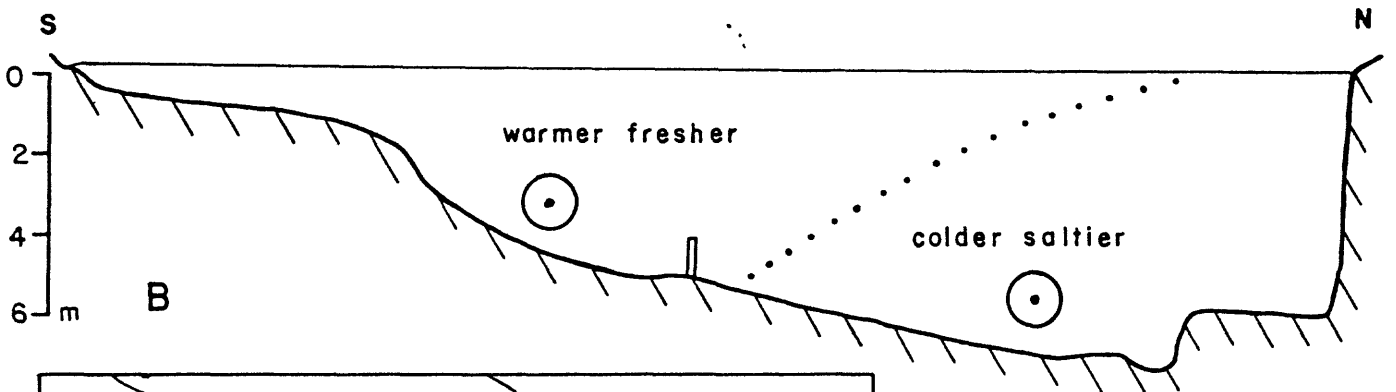
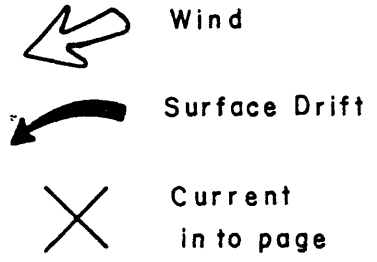
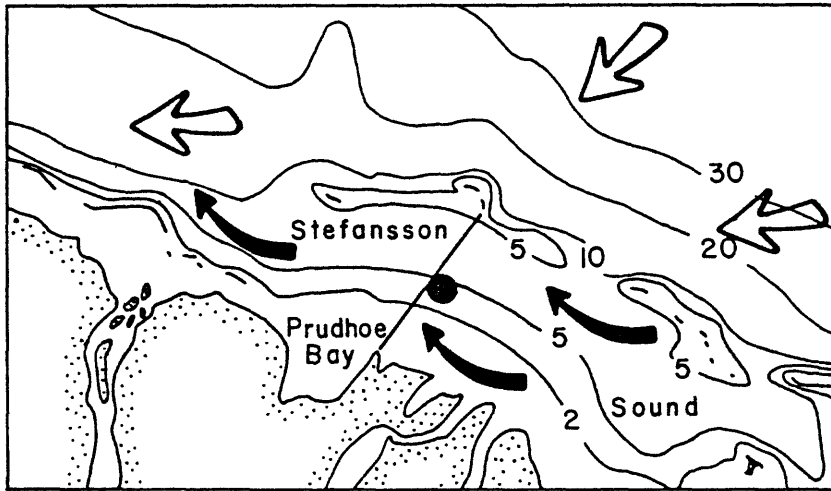
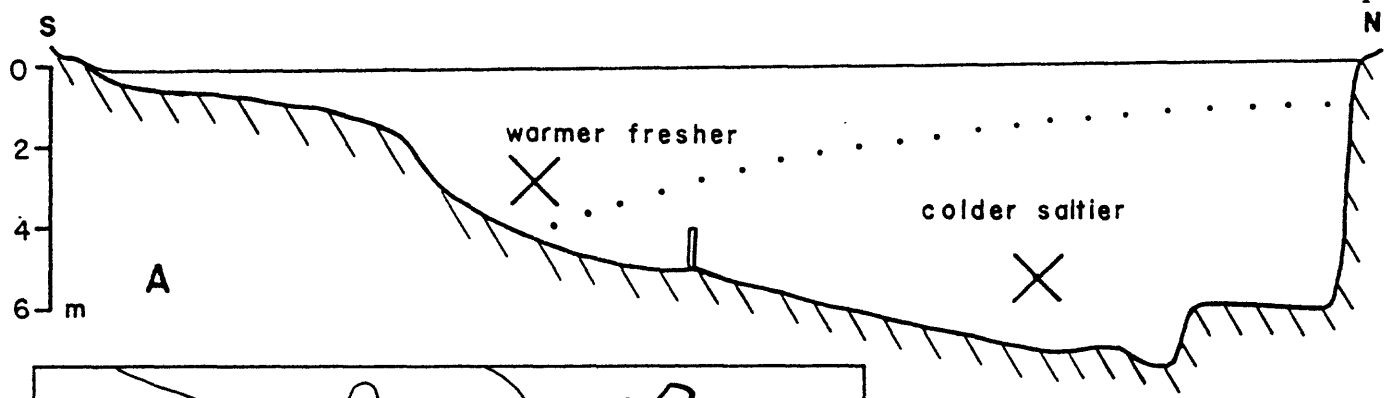


Figure 5. Wildly speculative model of wind, current and water regime in Stefansson Sound used to explain the variances in the record.

PART - C

Suspended Matter in Nearshore Waters of the Beaufort Sea, 1976

David E. Drake, U.S. Geological Survey

I. Summary

The objectives that were emphasized during this year were:

1. determination of the concentrations and composition of suspended matter during the ice-covered winter season near Prudhoe Bay and the Colville Delta.
2. examination of the temporal variability in near bottom currents and suspended matter at selected nearshore sites.
3. determination of the distribution of suspended matter during the summer period between the Canning River and Cape Halkett.

Useful results were obtained on objectives 1 and 3. Unfortunately, the rigors of the environment and equipment malfunctions combined to prevent us from accomplishing objective 2.

Suspended matter concentrations below the ice in March 1976 ranged from 130 $\mu\text{g}/\text{l}$ to 1200 $\mu\text{g}/\text{l}$ (mean value, 340 $\mu\text{g}/\text{l}$) on two transects; one off Prudhoe Bay and one off the eastern part of the Colville Delta. Concentrations of total suspended matter (TSM) were similarly low on both of these transects; however, the particles off Prudhoe Bay were predominantly organic (combustible or noncombustible parts of plankton) whereas the suspensions near the Colville Delta contained substantially more fine-grained (clay) inorganic grains. Sub-ice water currents are generally sluggish and, combined with the low suspended matter values, indicate that shelf sediment transport is minimal in the winter. Nevertheless, the compositional differences between the samples on the two transects show that some resuspension and entrainment of Colville sediment occurs even under a complete ice cover.

During summer 1976 suspended matter concentrations increased markedly along the entire coastal area but especially near the Colville River. Owing to direct application of wind stress, the summer flow field is significantly more active, and therefore, sediment transport is proportionately more important.

Characteristics of the suspended matter within 50 km of the coast in the summer suggest the following conclusions:

1. the sediment discharge of the Colville River far overshadows the discharges of the smaller north slope rivers. In fact, by late August and September suspended matter concentrations exceeding 5 mg/l are generally restricted to Harrison Bay and areas near the Colville Delta.
2. the great bulk of the suspended matter transport in surface waters occurs within 5-15 km of the shore.

3. wind-driven transports (both direct flow of surface water and indirectly-forced upwelling) appear to be the major mechanism controlling the fate of suspended clay and silt.

4. consequently, the movement of water and suspended matter is highly variable over the inner shelf. Nevertheless, data which bear on the pathways followed by surface suspended matter suggest a net transport to the west within 20 km of the coast between Prudhoe Bay and Cape Halkett.

II. Introduction

Significant increases in concentrations of trace metals and hydrocarbons in the environment are a likely result of petroleum development. Both natural and artificial levels of these materials tend to be higher in fine-grained sediments. Therefore, it is important to understand the fate of fine-grained sediments which are introduced by rivers, coastal and sea floor erosion.

The problem involves two major aspects. First, the "fairweather" regime during both winter and summer seasons must be evaluated and, secondly, the transport rates which occur during storms must be determined. In particular, for the Beaufort Sea shelf influxes of new sediment occur during well-defined, short periods in June and July. Ice-free conditions prevail from July to September and one would expect that during this period the transport of suspended matter would be of relatively greatest importance. From late September through June, ice cover over the inner shelf is essentially complete and this factor should substantially reduce the sediment transport rate (by preventing wave resuspension and wind-driven currents). However, the magnitude of this seasonal effect has never been directly investigated and this was one of the specific objectives of the first year of this research.

III. Current State of Knowledge

Principally through the efforts of Barnes and Reimnitz (1974) and Naidu and Mowatt (1974) the distribution of surficial sediments on the Beaufort Sea shelf between Cape Simpson and Barter Island is reasonably well known. Basically the distribution is characterized by nearshore and outer shelf bands of silty sand (and locally gravel) separated by a mid-shelf zone of mud (mean diameter, 0.016 mm). The distribution of clay minerals presented by Naidu and Mowatt (1974) bears on the fate of river-borne materials and will be discussed later in this report.

Research on the physical oceanography of the area has increased substantially in the past several years. However, the difficulties encountered in these investigations make additions to our understanding come slowly (Mountain, 1974). Pieces of information have been collected at various times and places but coordinated research programs which will eventually lead to a coherent synthesis are just beginning. Moored current meter measurements of suitable duration are critical to understanding any shallow water circulation system; this type of data is severely limited for the Beaufort Sea shelf (see other sections of R.U. report). The available data (Barnes and Reimnitz) show that

inner shelf currents near the Sagovanirktok Delta respond quickly to the prevailing local winds. Easterly winds which tend to predominate during July and August (Mountain, 1974) drive surface waters westward and offshore inducing a near bottom onshore flow. Shifts to northwesterly winds rapidly reverse this system by piling surface water up on the coast and possibly causing downwelling in the subsurface.

Current measurements below winter ice cover (Barnes and Reimnitz, this report) reveal sluggish flow with very little net directionality. Removal of ice cover allows wind driven currents and a substantial increase in flow velocities.

Suspended matter samples were collected by P. Barnes in 1971 and 1972 aboard the USCGS GLACIER and NATCHIK (Barnes, 1974). This is the only sampling directed toward the suspended matter transport problem that has been attempted prior to the present research.

IV. Data Collection

Water samples for suspended particulate matter determination were collected in March of 1976 at eleven ice hole stations on two transects (figure 3). The samples were recovered using 5 liter Van Dorn bottles lowered on a polypropylene line. Water was immediately transferred to plastic bottles and vacuum filtration using preweighed 0.4 μm Nuclepore filters was accomplished in the evening at the shore station in Deadhorse. In addition, a Martek beam transmissometer (1 m path) was used to obtain a profile of water clarity to the bottom at each station; the sensor included a thermistor for temperature determination. The sample filters were stored in plastic petri dishes and shipped to our California laboratory for analysis.

During the summer field season (1976) P. Barnes and E. Reimnitz collected 82 surface water samples (500 ml) between Canning River and Cape Halkett and to ~20 km offshore. Owing to the nature of the USGS KARLUK operations, it was not feasible to process the samples in the field. Therefore, all samples were kept cold and shipped to California for filtration. The water samples were stored in opaque plastic bottles to minimize biologic action. Nevertheless, some changes in the organic components undoubtedly took place but it is likely that the concentrations of noncombustible particles were not markedly changed.

Noncombustible and combustible fractions of the suspended matter were determined by ashing 1/2 of each sample filter for 6 hours at 550°C (Manheim et al., 1970). The remaining 1/2 of each filter was set aside for microscope investigation.

During March 1976 P. Barnes and the author attempted to deploy two bottom moorings for long-term current velocity and light transmission and scattering measurements. One mooring off the Colville Delta was successfully deployed but could not be found when recovery was attempted in July. The second mooring near Reindeer Island was damaged (the light transmissometer) and only one

current meter was satisfactorily placed. Thus, our efforts to obtain time-series data which included optical sensing of water turbidity were unsuccessful.

V. Results

The results of our winter and summer sampling programs illustrate the seasonality of the suspended matter transport system (figures 1 and 3). Total suspended matter (TSM) concentrations in March ranged from 130 $\mu\text{g}/\text{l}$ to 1200 $\mu\text{g}/\text{l}$ with a mean of ~ 340 $\mu\text{g}/\text{l}$. Most of this material was organic in origin and mineral particles represented <20% of the suspended matter off Prudhoe Bay. None of the samples contained grains larger than 16 μm in diameter. For comparison, concentrations of 100-300 $\mu\text{g}/\text{l}$ TSM are generally present on the outer shelf and continental slope in mid-latitude regions (Meade et al., 1975; Drake, 1976). Total suspended matter values were also low off the Colville Delta but the higher ash percentages (fig. 4) here reflect the presence of very fine-grained inorganic grains.

The light transmission profiles (figures 5 and 6) show that the vertical distribution of suspended matter is simple during the ice-covered situation. Stratification is essentially lacking except for a slight but ubiquitous reduction in light transmission near the sea floor. This near-bottom layer implies that processes of fine particle resuspension from the bottom do not cease entirely in the winter. However, the particles in this layer were in all cases very fine silt or clay-sized (<8 μm). These materials could be maintained in suspension by weak currents flowing over locally rough topography.

Following shorefast ice breakup in July, samples were collected seaward of the Sagavanirktok delta and in Harrison Bay (figures 1 and 2). These early summer surface water samples reveal the following:

1. samples immediately seaward of the Sag delta contained surprisingly low concentrations of noncombustible mineral particles (600-1040 $\mu\text{g}/\text{l}$);
2. similarly, TSM concentrations in Prudhoe Bay were less than 5 mg/l except within 1 to 2 km of the shore;
3. TSM concentrations and the content of terrigenous materials were significantly higher off the Colville River and in the central, nearshore section of Harrison Bay. These high concentrations (>10 mg/l) decreased dramatically at distances of 10-15 km offshore;
4. although the major tributary of the Colville River is on the northeast (Walker, 1974) the TSM values there and seaward of Oliktok Point were relatively low and also richer in plankton.

Following a crew exchange and completion of a vibracoring program, the KARLUK began a second regional sampling pattern (September 2-16). From September 2 to September 11 samples were collected east of 150°W and the samples in Harrison Bay were collected between September 11-16. Freeze-up was in process by mid-September. Figures 3 and 4 show the results of this sampling. The following aspects of the suspended matter distribution are noteworthy:

*the value of 1200 $\mu\text{g}/\text{l}$ may have been somehow contaminated because this particle concentration should result in a much lower light transmission than was measured at this site.

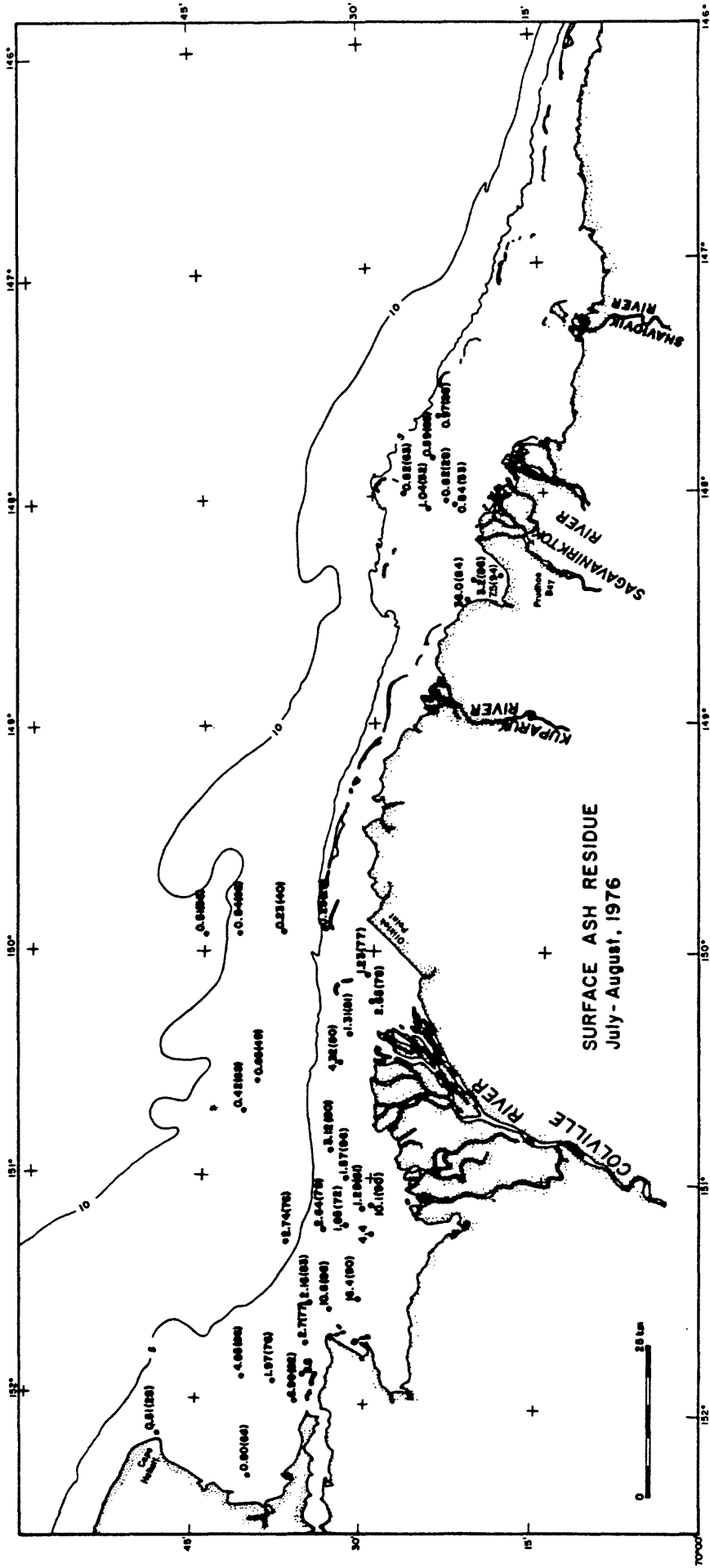
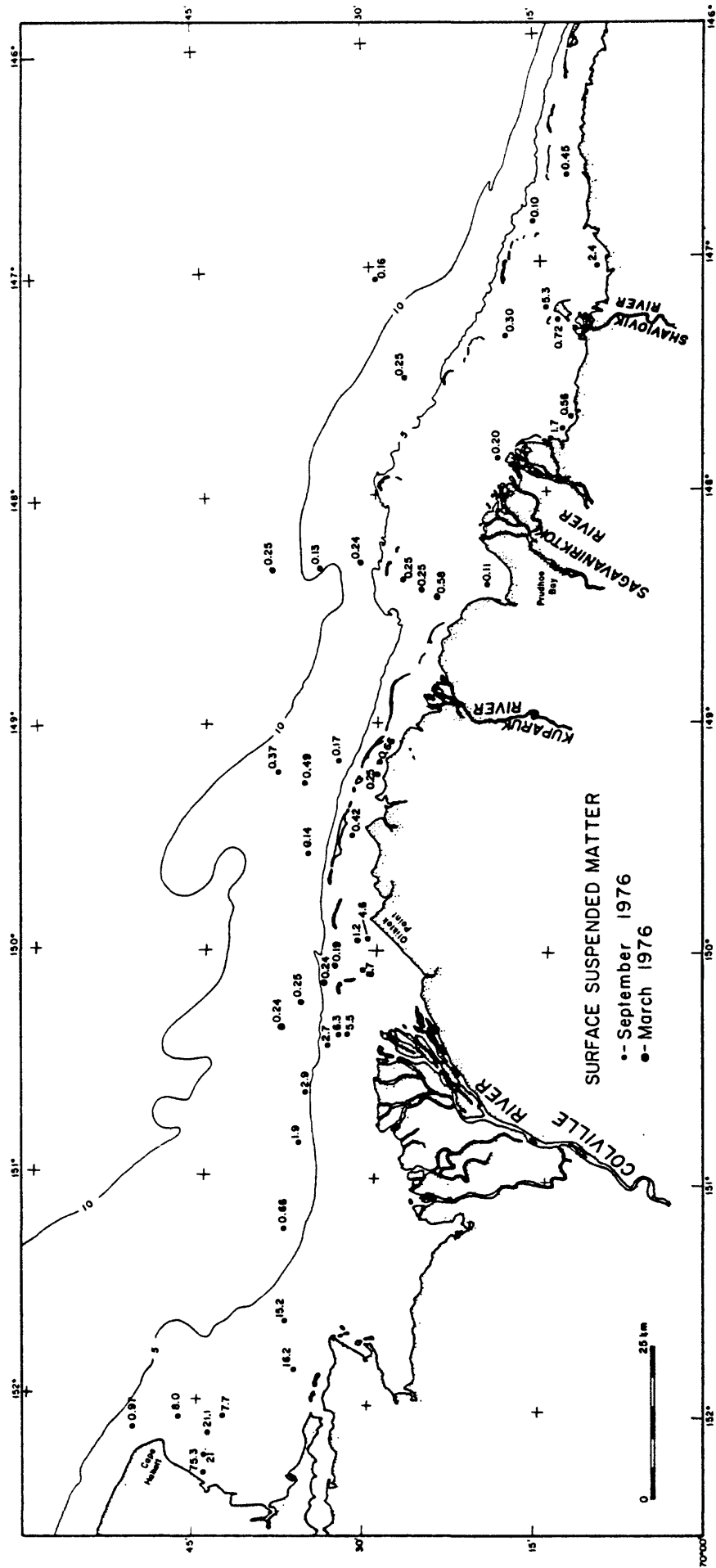


Figure 2. Noncombustible matter and ash residue percentages (shown in parenthesis) for surface water suspended matter, July - August 1976.



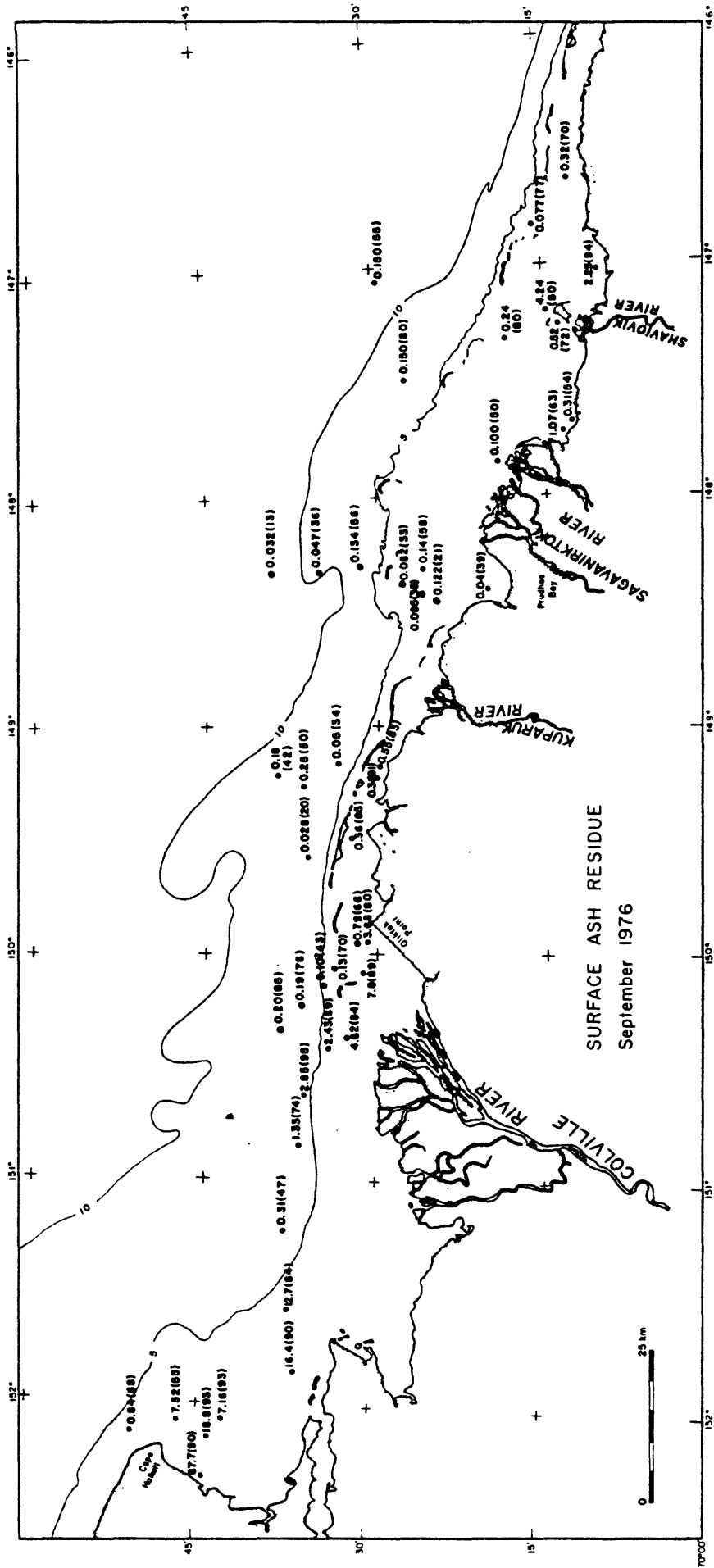


Figure 4. Noncombustible matter and ash residue percentages (shown in parenthesis) for surface water suspended matter in March 1976 (stations marked by X's) and September 1976.

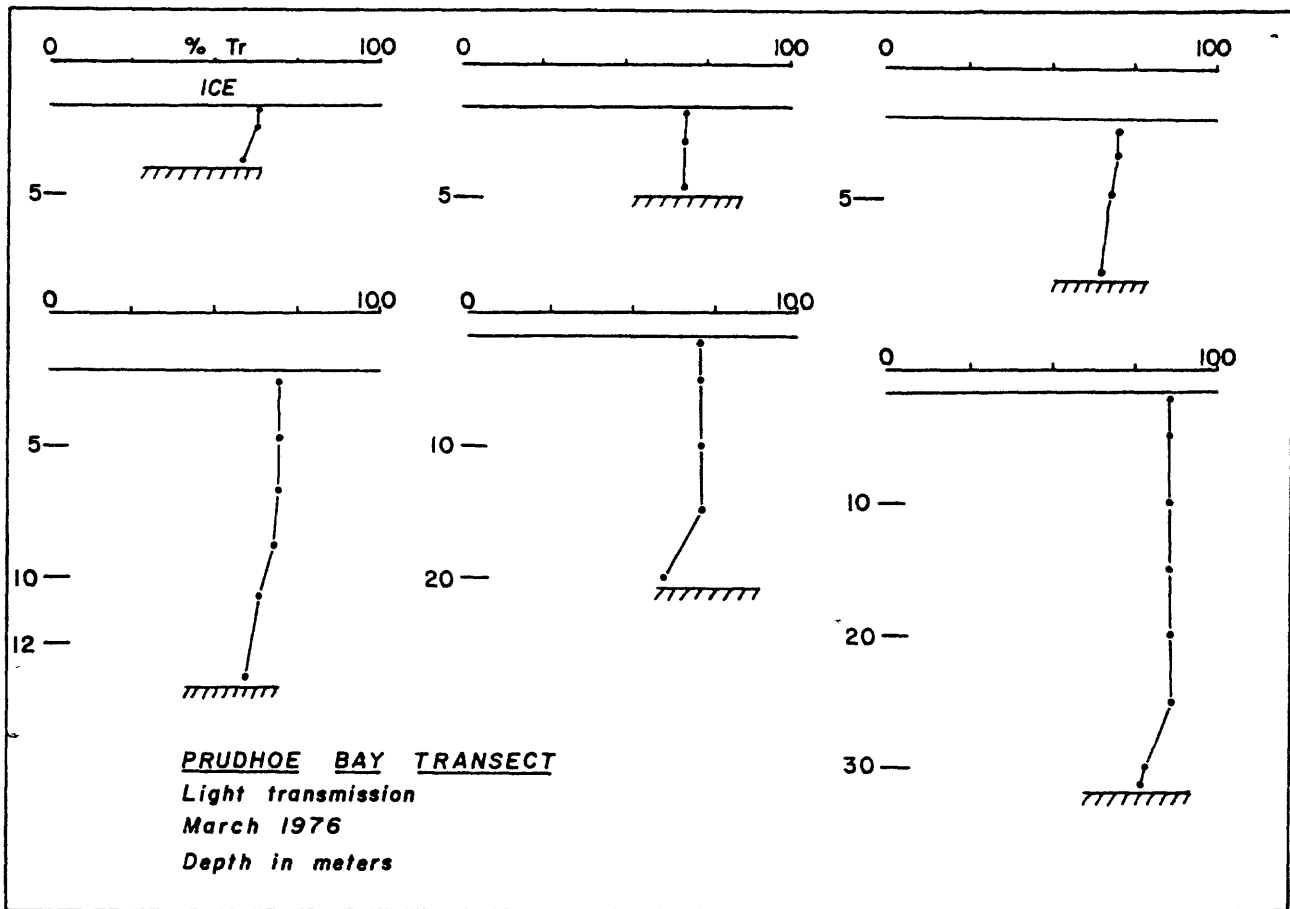


Figure 5. Light transmission (%) and temperature ($^{\circ}\text{C}$) profiles below the ice in March 1976. The stations are numbered according to increasing distance offshore from Prudhoe Bay (see Fig. 3 for locations).

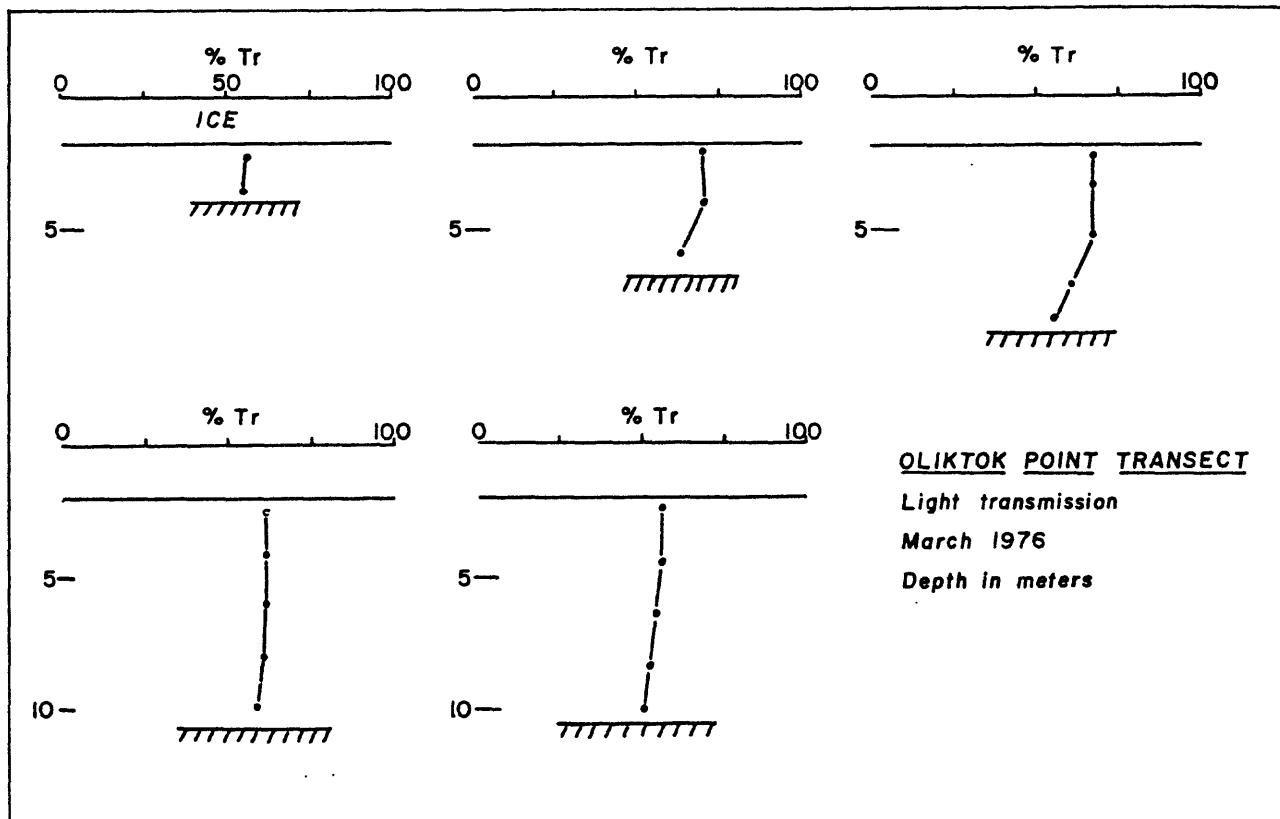


Figure 6. Light transmission (%) and temperature ($^{\circ}\text{C}$) profiles below the ice in March 1976 off the Colville Delta. See Fig. 3 for locations.

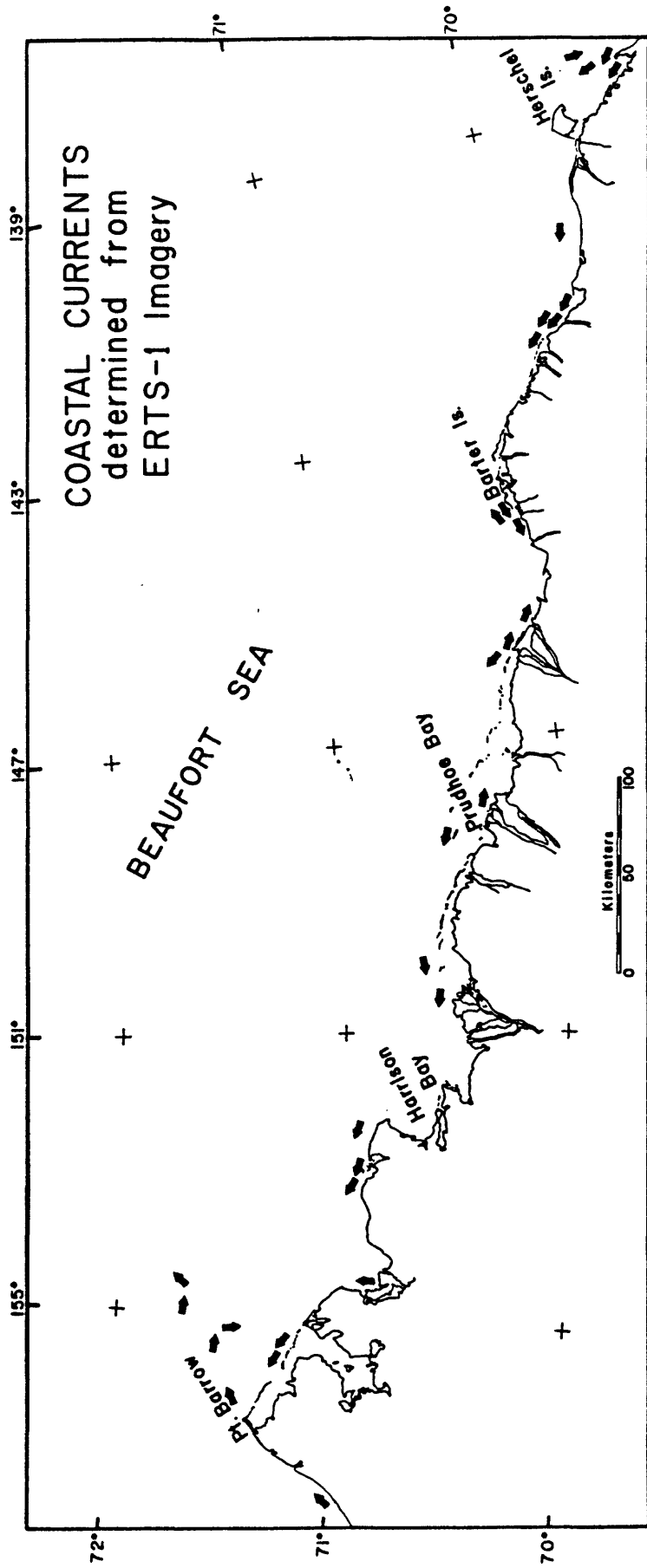


Figure 7. Nearshore transport based on analysis of ERTS-1 imagery for 1972 and 1973 (Barnes and Reimnitz, 1974).

comparatively minor effect on suspended matter concentrations (figures 3 and 4). By September, flow from these small streams has little influence on nearshore TSM distributions (figure 3). In fact, the September TSM concentrations east of Oliktok Point are not substantially greater than those present below the winter ice in March (figure 3), although the late summer particulate matter contains more noncombustible grains (higher ash residues).

The low suspended matter concentrations below the ice in March 1976 combined with current meter data that reveals very sluggish sub-ice water flow (<1 cm/s; Barnes and Reimnitz, this report) show that the winter sediment transport regime is relatively significant. This conclusion is, of course, based on "fairweather" data. Meteorological tides associated with low pressure systems could produce important sediment transport during the winter. However, Mountain (1974) points out that the ice cover will tend to reduce the impact of storms. We need data with which to evaluate higher energy events (in both winter and summer), but at this point it appears that the great majority of sediment transport occurs in the summer.

Naidu and Mowatt (1974) presented mineralogical evidence which implies that mud deposits at water depths of 20-40 m northeast of Prudhoe Bay were supplied by the Colville River. The location of this material more than 100 km east of its suggested source contradicts the arguments for westward sediment transport discussed above. The problem is that this deposit is completely disconnected from materials of similar clay mineralogy in Harrison Bay. One would expect some evidence for a connection if the deposits were the result of a transport system operating at the present time. Nevertheless, we cannot present new data bearing on this anomalous sediment distribution and it represents an interesting possibility for research.

VII. Conclusions

The first full year of research on suspended matter transport on the Beaufort Sea shelf leads to the following preliminary conclusions:

1. The transport of sediment during the winter season of ice cover is a small fraction of the transport which occurs in the summer (June through September).
2. The Colville River sediment discharge far overshadows the discharges of all the smaller rivers. By late summer the discharges from the small streams has a negligible impact on nearshore suspended matter concentrations.
3. There is no evidence for transport of Colville River suspended matter eastward around Oliktok Point. Easterly winds and possible upwelling near Oliktok appear to prevent eastward sediment transport.
4. Westward migration of suspended matter occurs throughout the summer in the nearshore portion of Harrison Bay.

VIII. References

- Barnes, P. W., and Reimnitz, E., 1974. Sedimentary processes on arctic shelves off the northern coast of Alaska. In Reed, J. C. and Sater, J. E. (eds.), The Coast and Shelf of the Beaufort Sea, Arctic Institute of North America, Arlington, Virginia, pp. 439-476.
- Barnes, P. W., 1974. Preliminary results of marine geologic studies off the northern coast of Alaska. U.S. Coast Guard, Oceanographic Report Series, 373-64.
- Drake, D. E., 1976. Suspended sediment transport and mud deposition on continental shelves. In Stanley, D. J. and Swift, D. J. P. (eds.), Marine Sediment Transport and Environmental Management, John Wiley and Sons, Inc., New York, pp. 127-158.
- Hufford, G. L., 1974. An apparent upwelling in the southern Beaufort Sea. Jour. Geophysical Res., 9: 1305-1306.
- Manheim, F. T., Meade, R. H., and Bond, G. C., 1970. Suspended matter in surface waters of the Atlantic continental margin from Cape Cod to the Florida Keys, Science, 167: 371-376.
- Meade, R. H., Sachs, P. L., Manheim, F. T., Hathaway, J. C., and Spencer, D. W., 1975. Sources of suspended matter in waters of the Middle Atlantic Bight, J. Sediment. Petrology, 45: 171-188.
- Mountain, D. G., 1974. Preliminary analysis of Beaufort Shelf circulation in summer. In Reed, J. C. and Sater, J. E. (eds.), The Coast and Shelf of the Beaufort Sea, Arctic Institute of North America, Arlington, Virginia, pp. 27-42.
- Naidu, A. S., and Mowatt, T. C., 1974. Clay mineralogy and geochemistry of continental shelf sediments of the Beaufort Sea. In Reed, J. C. and Sater, J. E. (eds.), The Coast and Shelf of the Beaufort Sea, Arctic Institute of North America, Arlington, Virginia, pp. 493-510.
- Short, A. D., Coleman, J. M., and Wright, L. D., 1974. Beach dynamics and nearshore morphology of the Beaufort Sea coast, Alaska. In Reed, J. C. and Sater, J. E. (eds.), The Coast and Shelf of the Beaufort Sea, Arctic Institute of North America, Arlington, Virginia, pp. 477-488.
- Wiseman, Wm. J., Jr., Suhayda, J. N., Hsu, S. A., and Walters, C. D., Jr., 1974. Characteristics of nearshore oceanographic environment of arctic Alaska. In Reed, J. C. and Sater, J. E. (eds.), The Coast and Shelf of the Beaufort Sea, Arctic Institute of North America, Arlington, Virginia, pp. 49-64.
- Walker, H. J., 1974. The Colville River and the Beaufort Sea: some interactions. In Reed, J. C. and Sater, J. E. (eds.), The Coast and Shelf of the Beaufort Sea, Arctic Institute of North America, Arlington, Virginia, pp. 513-539.

A Herringbone Pattern of Possible
Taylor-Görtler-type Flow Origin seen in Sonographs

by

Lawrence J. Toimil and Erk Reimnitz, U.S. Geological Survey
345 Middlefield Road, Menlo Park, California 94025

ABSTRACT

The potential usefulness of sidescan sonar in detailed studies of helical flow phenomena is indicated by records obtained within a shallow arctic lagoon. The records obtained in 2 m water depths reveal a herringbone pattern of current-aligned linear reflectors with branching diagonals. Major longitudinal reflectors have no detectable relief (<20 cm), are spaced 10-30 m apart and are believed to represent current-aligned, helical cell boundaries recorded in the silty fine sand of the lagoon floor. The pattern suggests a three-dimensional flow regime of the Taylor-Görtler type.

INTRODUCTION

Three-dimensional flow of the Taylor-Görtler type has been described by Allen (1968) as consisting of an array of pairs of oppositely rotating helical spiral vortices, whose axes lie parallel to the direction of primary (net) flow. Depositional bedforms ascribed to such flow have been observed in subaerial, intertidal, estuarine, and abyssal environments and have been used to depict flow characteristics otherwise not easily detected. A large-scale herringbone pattern with characteristics similar to bedforms ascribed to Taylor-Görtler flow, was found in sonographs obtained in the shallow eastern part of Leffingwell Lagoon, named in honor of E. de K. Leffingwell, a pioneer geologist who studied the northeastern part of arctic Alaska. The lagoon is located 90 km east of Prudhoe Bay and is partially separated from the Beaufort Sea by Flaxman Island (Fig. 1). The lagoon extends westward for a distance of 52 km.

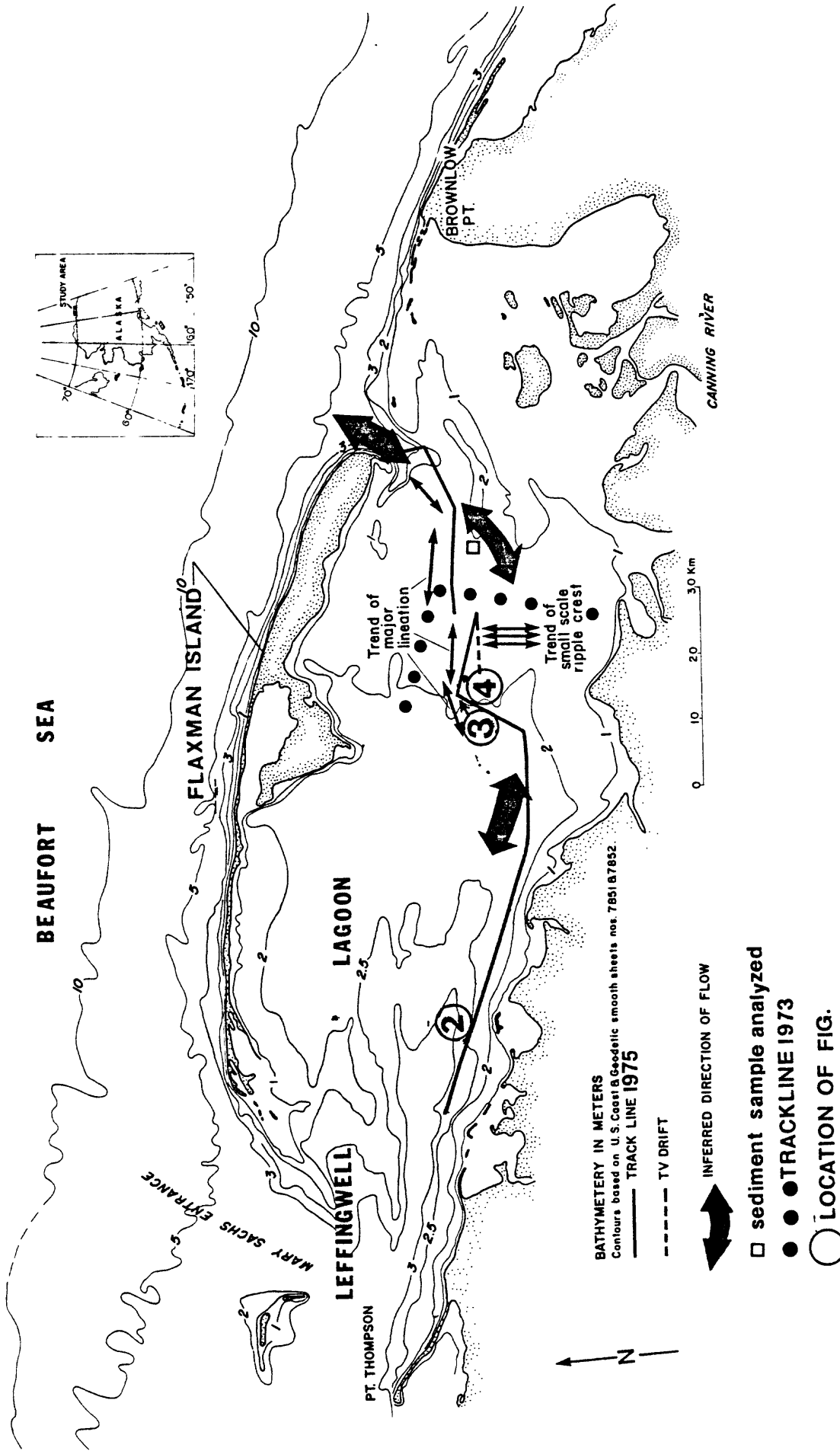


Figure 1. Chart of eastern Leffingwell Lagoon showing track lines, inferred trend of primary flow, and representative orientations of major lineations and small-scale ripple crest.

REGIONAL SETTING

Flaxman Island is a remnant of the inundated coastal plain and is marked by tundra-capped bluffs up to 7 m high. Both the island and the mainland shore are retreating by erosion (Lewellen, 1970) except for the very east end of the lagoon, where a small distributary of the Canning River is discharging and building extensive shoals (Fig. 1). A major inlet east of Flaxman Island connects the lagoon and the open sea. The only analyzed sediment sample, collected in the eastern part of the lagoon (Figure 1), consists of silty fine sand (mean dia. 0.125 mm).

Ice plays a dominant role in the lagoon environment. It starts forming in late September, attains a maximum thickness of 2 m by April-May, and breaks up in late June. The ice canopy rises and falls throughout the winter. These fluctuations are related to small astronomical tides (<0.5 m) and to more significant meteorological events. During westerly summer storms these fluctuations can exceed +3 m (Reimnitz et al., 1972a) and, with easterly winds, reach -1 m. Such fluctuations cause cracking of the ice and periodic adfreezing of sediments to the underside of the ice landward of the 2-m depth contour, as described by Barnes and Reimnitz (1974). Barnes and Reimnitz (1974) also suggested that constriction of flow during the late stages of ice growth results in intensified currents landward of the 2-m isobath, possibly resulting in winnowing and transport of sediments to beyond the 2-m depth contour.

ERTS-1 satellite imagery of June 12, 1973 indicates that the Canning River flooded the lagoon ice as far west as the central part of Flaxman Island. This arctic phenomenon and associated processes and results at other locations along the coast have been described by Reimnitz and Bruder (1972b), Reimnitz et al., (1974), Walker (1974), Barnes and Reimnitz (1974) and Reimnitz and Barnes (1974). The flooding proceeds to its maximum extent within about 2

days. Initially, the floodwaters depress the floating part of the ice canopy seaward of the 2-m depth contour rapidly displacing large volumes of water below. The character of under-ice flow during these events is unknown. The river water subsequently drains at holes and cracks, i.e. strudel (Reimnitz and Bruder, 1972b), and flows seaward under the floating ice. During this period the cross section for flow is greatly reduced by the presence of ice in the shallow lagoon.

Starting about mid-July, the lagoon is free of ice and its sediments are subject to reworking by wind-generated waves and currents. Fetch is limited for all but westerly winds, which generally result in a raised sea level. Eight days prior to our survey of September 5, 1975, westerly winds of more than 20 m/sec were recorded at Barter Island, located 42 km east of the study area (N.O.A.A. Climatological Data, v. 61, no. 7). Winds remained westerly for the next six days with average speeds less than 6 m/sec. Light northerly winds were recorded during the survey.

METHODS

Side-scan sonar and precision fathometer records were obtained concurrently along the track lines shown in Figure 1. The survey was carried out aboard the U.S. Geological Survey's R/V KARLUK. The side-scan sonar transmits short bursts of high frequency (105 kHz) sound in fan-shaped beams on each side of the survey track. The return echoes, when processed and graphically recorded, produce an acoustic picture (sonograph) of the seabed, detailing morphology and spatial distributions not delineated by fathometers (Belderson et al., 1972). In the sonographs the distance parallel to the ship track (length) is dependent on ship speed and rate of paper advance. Across the record (width) the scale is fixed for a given scan angle. In the records shown (Figs. 2, 3 and 4) the width scale is exaggerated relative to the length scale by a factor of 2.0 and necessitates the use of correction tables when obtaining measurements directly from the recordings.

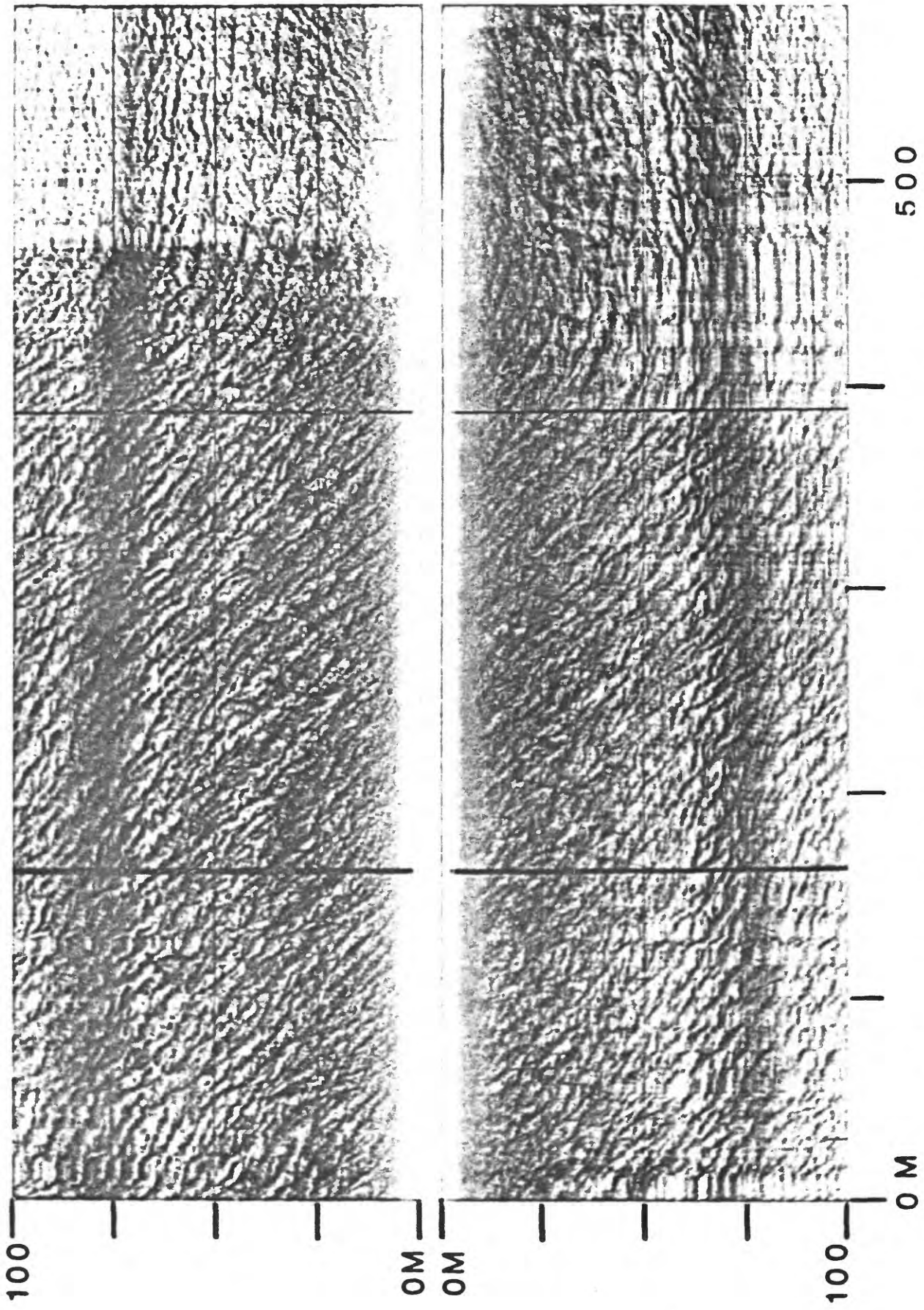


Figure 2. Side-scan sonar record obtained oblique to trend of major lineations circled number 2 in Fig. 1). The dark bands paralleling the ship's track near the outer margin of each channel of the sonographs presented are reflections from the ship's wake. Individual reflectors may be traced through a 70° course change marked by the vertical line on the right.

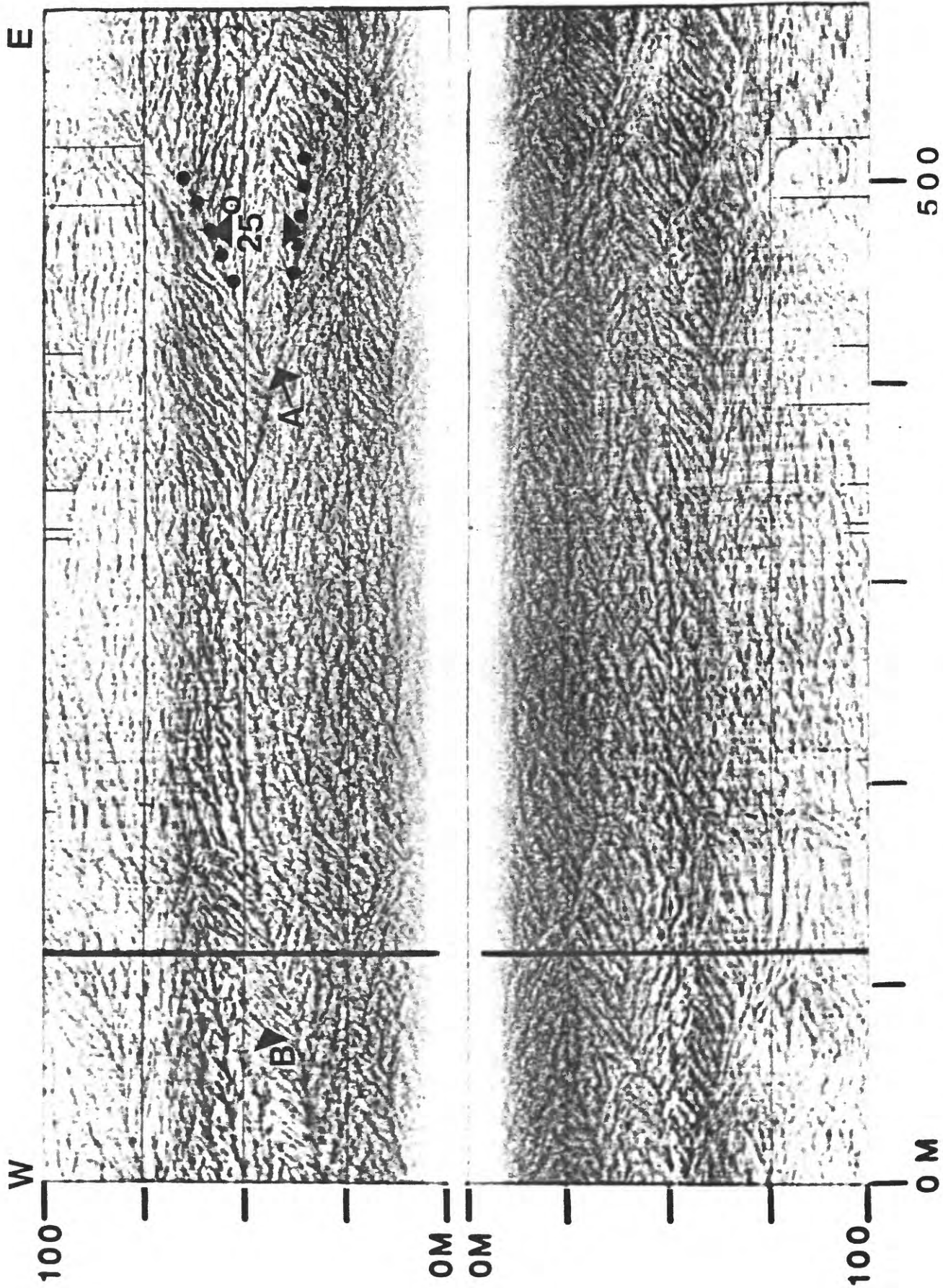


Figure 3. Side-scan sonar record taken on a course nearly parallel to trend of major lineations (marked A in the Figure) revealing herringbone pattern and tuning fork junctions. The line segment over which the record was obtained is shown in Figure 1 by the circled number 3. Minor lineations are indicated by the arrow marked B.

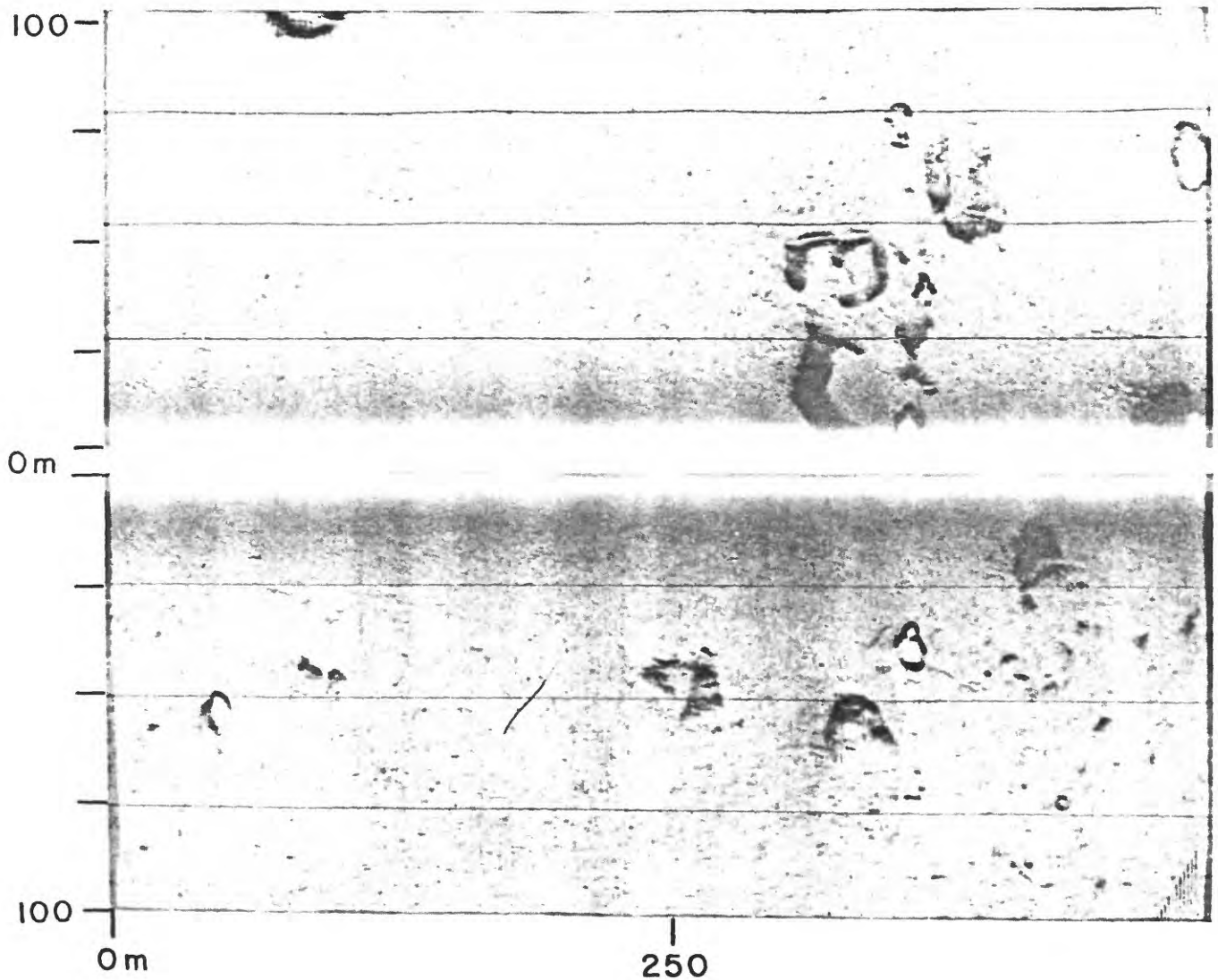


Figure 4. Side-scan sonar record obtained along the western portion of the survey track in water depth between 2.5 and 3 m. (circled number 4 in Figure 1). The dark circles seen scattered about the sea bed are strudel scour depressions (after Reimnitz and Bruder, 1972b) formed during spring river breakup.

The fathometer employed an 8° cone-angle, 200-kHz transducer capable of resolving bottom relief of about 20 cm. Direct observations of the seabed were made by underwater television and recorded with a video tape recorder. Navigation during the survey was based on radar ranges and considered accurate to within 200 m.

DESCRIPTION OF RESULTS

Along the western half of the track in water depths between 2 and 3 m, a flat bottom marked only occasionally by strudel scour depressions was observed (Fig. 2). But, upon approaching the 2 m isobath in the eastern part of the lagoon (Fig. 1), alternating light and dark, irregular, roughly parallel bands were observed on the sonographs (Figs. 3 and 4). The dark lineations represent zones where sea floor reflections are strong relative to those from the intervening bottom. The lineations lie approximately parallel to 085°T and change to 050°T near the eastern inlet of the lagoon (Fig. 1). No detectable relief was associated with the lineations on either the side-scan sonar or fathometer records. The vertical line across the right side of Figure 3 marks the 70° course change shown in Figure 1 just east of the 2 m isobath. During the turn, individual lineations can be followed into a more complex pattern recorded along a course more nearly parallel to their dominant trend (Fig. 4). Viewed from this course, the spacing of bands is slightly expanded relative to that of the oblique crossing because the scale (width) is exaggerated. In this orientation one can clearly discern that minor discontinuous reflectors (marked by the letter 'B' in Fig. 4), spaced 1 to 3 m apart, branch off from the major more continuous longitudinal reflectors (marked by the letter 'A' in Fig. 4) at angles between 20° and 40° , forming a herringbone pattern. The major longitudinal reflectors are spaced 10 to 30 m apart, and commonly bifurcate, forming 25° angles (approximately) opening to the east.

By lowering a television camera while the vessel drifted in this area (Fig. 1), we saw symmetric sand ripples, too small to show on the sonographs. The ripple crests trend north-south, with wavelengths of 6 to 8 cm and heights of 1 to 2 cm. The ripples were considerably disturbed by bioturbation and contained some organic debris in the troughs. A suspension layer, perhaps 0.5 cm thick, locally covered the sea floor. Bottom sediment collected during these observations and examined with a hand lens, consisted of silty fine sand. Figure 1 illustrates representative orientations of the small-scale ripple crests along the track surveyed with television.

DISCUSSION AND CONCLUSIONS

Comparing the sonographs with the television images and with the fathograms, we find that the herringbone pattern has no detectable (<20 cm) relief. Newton and Stefanon (1975) have shown that subtle differences in sediment grain sizes (between muddy and washed sand) with no associated relief were clearly defined in sonographs obtained with a side-scan sonar system identical to that used in our survey. Because of the high quality of the records obtained along the western portion of the survey track, which show the ability of the sonar system to perform well even across shallow depths; and the stationary orientation of the linear reflectors with respect to differing ships' headings (Fig. 2), we believe the herringbone pattern observed to be real. We suggest two possible causes for the dark reflectors seen: (1) similar to the washed sands described by Newton and Stefanon (1975) they represent coarse fractions winnowed from the fine-silty sand covering the lagoon floor. (Winnowed zones may not have been observed with the television camera because they were partly masked by suspended matter, and also because the resolution of the camera was insufficient to detect subtle changes in grain sizes.); or (2) the result of linear bedforms of positive relief which are below the 20-cm resolution of our fathometer.

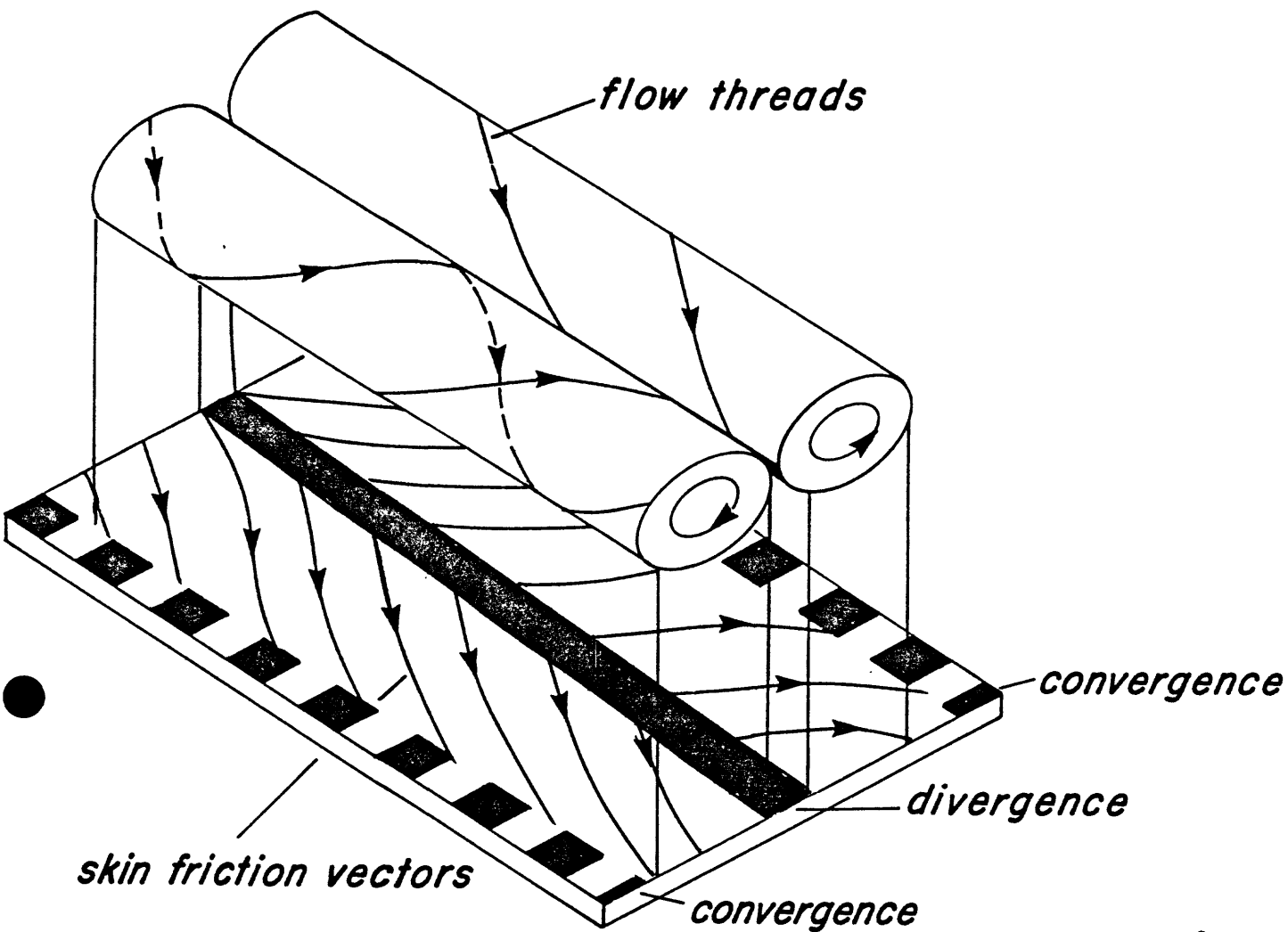


Figure 5. Vortices of Taylor-Görtler type flow and skin friction vectors associated with such flow, modified from Allen (1968). Regions of helical cell convergence and divergence are indicated respectively by broken and solid bands.

The direction of primary flow in the study area (Fig. 1), inferred from the configuration of the lagoon and the location of the tidal inlet and river input, is nearly parallel to representative orientations of the major lineations.

Current-aligned bedform patterns similar to those seen in our sonographs have been attributed to secondary Taylor-Görtler type flow (Karcz, 1967; Houbolt, 1968; Hanna, 1969; and Hollister et al., 1974). Secondary flow of this type has been described by Karcz (1967) as "flow which has been split into a series of longitudinal vortex tubes with an alternating sense of rotation. The individual flow filaments advance helically, and the kinematic picture of the flow is that of a system of arrays of spiral flow threads" (Fig. 5). Bedforms resulting from such flow characteristically exhibit current parallel lineations that commonly bifurcate in the up-current direction, forming junctions the shape of a tuning fork (Folk, 1971) similar to those seen in our sonographs (Fig. 3). It has also been shown that the major longitudinal bedforms frequently have superimposed small-scale ripples trending transverse to the direction of primary flow (van Straaten, 1951; Karcz, 1967). In some cases, secondary current produced bedforms branch obliquely from major longitudinal features in herringbone patterns, as observed by Hollister et al. (1974) and Folk (1971). These secondary bedforms apparently lie transverse to the skin-friction lines of the flow system, as illustrated by Allen (1968) and shown in Figure 5. The characteristic bedform patterns attributed to three-dimensional helical flow regimes discussed above are strikingly similar to those seen in our sonographs.

Using the pattern from Figure 3 as a base, two helical flow patterns may be constructed. The first assumes that (1) the major longitudinal lineations represent erosional zones corresponding to flow divergence at the sea floor; (2) the minor diagonal lineations lie transverse to the skin-friction lines of

a secondary flow system (Fig. 5); and (3) the "tuning fork" junctions open upcurrent. Such an interpretation is shown in Figure 6a. Assumption (2) above implies that the minor diagonal lineations are associated with some relief, which we did not detect. The second flow pattern illustrated in Figure 6b assumes: (1) that the major longitudinal lineations represent linear bedforms of positive relief corresponding to flow convergence at the sea floor; (2) that the minor diagonal lineations represent winnowed zones parallel to the skin-fraction lines of the secondary flow system and result from a tertiary flow regime. (Such a tertiary regime would imply a more complex flow pattern than that discussed here); and (3) that as in the first model the tuning fork junctions open upcurrent. Although the interpretation of the minor diagonal lineations remains questionable, we believe it is reasonable to assume that Taylor-Görtler type flow is responsible for the formation of the pattern observed in our study. The factors producing the flow itself are still unanswered. One possibility is that significant centrifugal instability to develop such flow may result from streamline curvature of lagoonward flow along the concave surface of the tidal inlet. It may also be significant that the pattern is only apparent in areas shallower than 2.5 m where the constriction and intensification of flow by an ice cover can be expected.

Sonographs obtained in 1973 (along the trackline shown in Fig. 1) indicate a similar pattern in the same area and depths, which implies a permanence of recurrence of the pattern. One of the alternative routes for a proposed gas line to Canada crosses the study area. Under-ice processes, which are poorly understood in the shallow lagoons of the Arctic, may significantly redistribute sediments. This possibility underlines the need for detailed studies in this environment. We believe that the spatial distributions resolvable using side-scan sonar will prove useful in these studies and future studies of bedforms and sediment distribution patterns of helical flow origin.

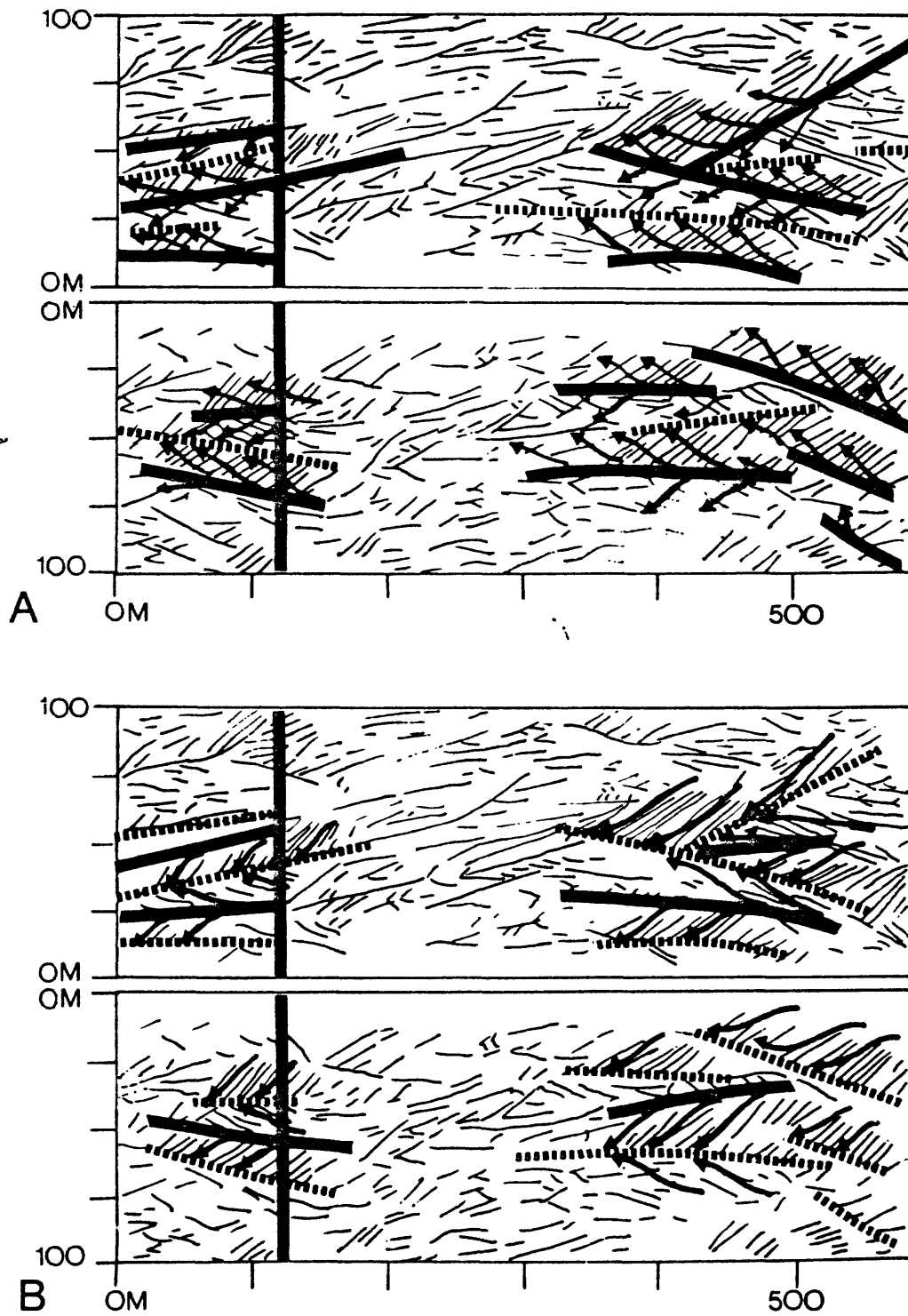


Figure 6. a and b. Line drawings of major and minor lineations seen in Figure 3 showing two differing interpretations of secondary flow vector fields. Respective zones of implied helical cell divergence (solid black bands) and convergence (broken black bands) are patterned after Figure 5.

ACKNOWLEDGMENTS

We wish to thank A. Sallenger who was very helpful in formulating our thoughts for this report and R. Hunter and H. E. Clifton of the U.S. Geological Survey for reviewing the manuscript.

REFERENCES CITED

- Allen, J.R.L., 1968, The nature and origin of bedform hierarchies, sedimentology; Elsevier Publishing Company, Amsterdam, The Netherlands (10) 1968, pp. 161-182.
- Barnes, P.W., and Reimnitz, Erk, 1974, Sedimentary processes on Arctic Shelves off the northern coast of Alaska; in The Coast and Shelf of the Beaufort Sea. Proceedings of the Arctic Institute of North American Symposium on Beaufort Sea Coast and Shelf Research, Arlington, Va., Arctic Institute of North America.
- Belderson, R.H., Kenyon, N.Y., Stride, A.H., and Stubbs, A.R., 1972, Sonographs of the sea floor: A Picture Atlas, Elsevier Publishing Company, Amsterdam, The Netherlands.
- Folk, R.L., 1971, Genesis of Longitudinal and Oghurd Dunes Elucidated by Rolling upon Grease, Geol. Soc. of America Bulletin, v. 82, pp. 3461-3468.
- Hannä, S.R., 1969, The formation of longitudinal sand dunes by large helical eddies in the atmosphere: Jour. Applied Meteorology, v. 8, pp. 874-883.
- Houbolt, J.J.H.C., 1968, Recent sediments of the southern bight of the North Sea; Geologie en Mijnbouw, v. 47, pp. 245-273.
- Hollister, D.C., Flood, R.D., Johnson, D.A., Lonsdale, P., and Southard, J.B., 1974, Abyssal furrows and hyperbolic echo traces on the Bahama Outer Ridge, Geology, v. 2, no. 8, pp. 395-400.
- Karcz, Iaakov, 1967, Harrow marks, current aligned sedimentary structures, Jour. Geol., v. 76, pp. 113-121.
- Lewellen, R.I., 1970, Permafrost erosion along the Beaufort Sea Coast, Private Publication, Geography and Geology Dept., University of Denver, Denver, Colorado, 25 p.
- Newton, R.S., and Stefanon, A., 1975, Application of sidescan sonar in Marine Biology, Marine Biology by Apringer-Verlag, 1975, v. 31, pp. 287-291.
- Reimnitz, E., Barnes, P., Forgatsch, T., and Rodeick, C., 1972a, Influence of grounding ice on the Arctic shelf of Alaska, Marine Geology, 13, pp. 323-334.
- Reimnitz, E., and Bruder, K.F., 1972b, River discharge into an ice-covered ocean and related sediment dispersal, Beaufort Sea, Coast of Alaska: Geol. Soc. America Bull., v. 83, no. 3, pp. 861-866.
- Reimnitz, E., Rodeick, C.A., and Wolf, S.C., 1974, Strudel Scour: A unique Arctic marine geologic phenomenon, Jour. of Sed. Petro., v. 44, no. 2, pp. 409-420.
- Reimnitz, E., and Barnes, P.W., 1974, Sea ice as a geologic agent on the Beaufort Sea shelf of Alaska, in The coast and shelf of the Beaufort Sea. Proceedings of the Arctic Institute of North American Symposium on Beaufort Sea Coast and Shelf Research, Arlington, Va., Arctic Institute of North America, pp. 301-353.

von Straaten, L.M.J.V., 1951, Longitudinal ripple marks in mud and sand, Jour
of Sedimentary Petrology, v. 21, no. 1., pp. 47-54.

Walker, H.J., 1974, The Colville River and the Beaufort Sea: some interactions;
in The coast and shelf of the Beaufort Sea, Proceedings of the Arctic
Institute of North American Symposium on Beaufort Sea Coast and Shelf
Research. Arlington, VA., Arctic Institute of North America,
pp. 513-540.

PART - E

Rates of Ice Gouging, 1975 to 1976, Beaufort Sea, Alaska

P. Barnes, D. McDowell, E. Reimnitz

INTRODUCTION

Sea ice on the continental shelves of arctic Alaska impinges on the sea bottom at varying intervals of space and time. Knowledge of the recurrence interval at which ice is likely to interact with the sea floor, or the rate of ice gouging, is important from several standpoints. Using gouge recurrence and depths, the rates of sediment reworking can be estimated, and the effect on benthic communities evaluated. Furthermore it is of utmost importance in the planning and design of offshore installations, such as pipelines and subsea well heads, to know the rate and depth to which ice is likely to penetrate into the sea floor.

In the area of this study (Fig. 1) sea ice zonation falls into three general categories (Reimnitz and others, 1976): 1) a bottom fast ice zone inside the two meter isobath, where ice at the end of the season of ice growth rests on the sea floor; 2) the zone of floating fast ice, with varying quantities of thicker, older ice, seaward of the bottom fast ice; and 3) at the seaward edge of the floating fast ice, a zone of grounded ice ridges forming the stamukhi zone. The two fast ice zones remain essentially stable during the winter. The stamukhi zone, commonly occurring in 15-20 m depths, marks the boundary between the stable fast ice and the moving polar pack, and is an area of shear and pressure ridge formation and ridge grounding during the winter. During the summer open water season, drifting ice of various drafts is commonly present at all water depths on the inner shelf. Solidly grounded stamukhi may remain grounded throughout one or several seasons of melting.

The area of this study (Fig. 1) is located north of Oliktok Point in water depths of 6 to 12 m, the zone of floating fast ice (Reimnitz and others, 1976). In some years an early winter shear line crossing the test area (Fig. 1) develops in the vicinity of the 10 m isobath in Harrison Bay. The sea floor in the study area slopes steeply offshore from the islands to depths of about 7 m, then more gradually seaward. Test line 1 runs northwest from Thetis Island and test line 2 heads just about due north from Spy Island.

METHODS

In 1973, 1975 and 1976 a side-scan sonar and fathometer were used on carefully navigated test lines to repeatedly examine the same area of sea floor in each of the three years (Fig. 1). A comparison of gouging on testline 1 between 1973 and 1975 has already been reported on (Reimnitz and others, 1977). Sonographs from the side-scan sonar were the key data to define the presence of new gouge features from one year to the next. The 1973 and 1975 records cover a 125 m swath on each side of the ship's track while the 1976 survey flubbed and covered only 100 m on either side. Depending on sea state, bottom reflectivity, and system tuning the sonographs produced by the side-scan can resolve features less than 10 cm high.

Navigation along the test lines was accomplished by ranging on landmarks onshore and by a precision range-range navigation system which reads to the

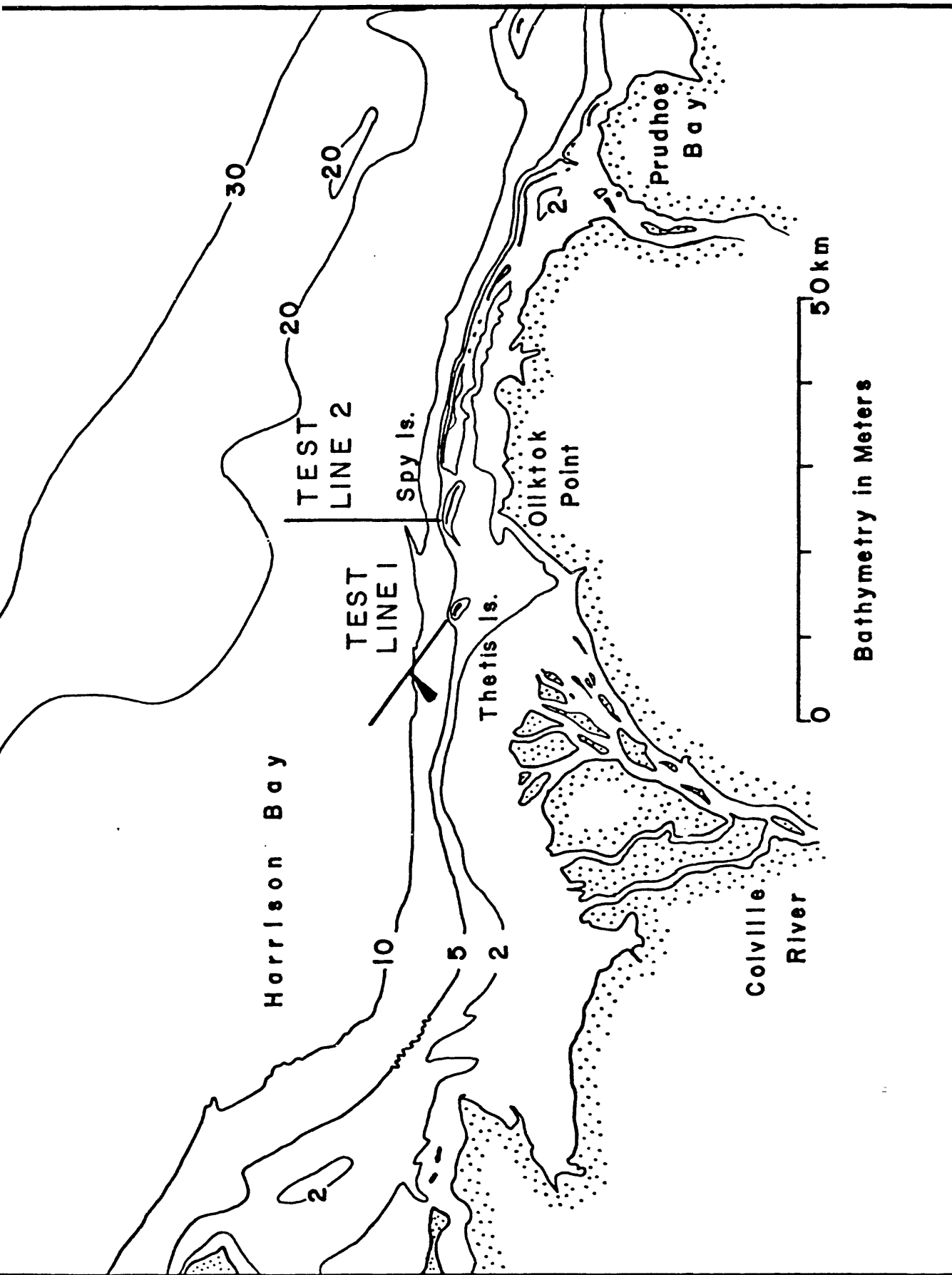


Figure 1. Location map of the study area indicating the location of test lines 1 and 2. The arrow indicates the location of the sonographs and fathograms of Fig. 4.

nearest meter and is accurate to ± 3 m. With these techniques the test lines were re-surveyed within 50 m from year to year and obtained overlapping sonographs of the sea floor except in areas of detours to avoid ice. The fathometer used in this survey utilized an 8° cone in 1975 and a narrow beam 4° cone in 1976 and was capable of resolving bottom relief of less than 15 cm.

RESULTS AND DISCUSSION

The analysis of ice gouge character along the two test lines was divided into two parts. First the summary character of ice gouging of 1/2 km line segments were tabulated from the 1975 records. Secondly, the new gouge features formed between 1975 and 1976 were examined using both the 1975 and 1976 records. Only the data from test line 1 have been completely analyzed at this time.

An idealized gouge cross section is shown in Figure 2 as an aid in clarifying the terminology used in this report. Note that: a) "incision depth" is generally less than true relief; b) the final gouge depression may be narrower than the incision due to slumping; and c) the "extent of disruption" probably often reaches beyond the original incision.

Summary of ice gouge characteristics

The dominant gouge trend, depth profile, density, maximum incision depth, and maximum disruption was determined for 1/2 km segments of the test lines (Fig. 3). We have tried to standardize as many of the admittedly subjective observations (Hnatiuk and Brown, 1977) as noted below, in an effort to make them comparable from one area to another and from year to year.

Gouge trend: Most ice gouge features are linear. The gouge trend is the orientation of the major portion of the linear features within a given segment. As both the boat speed and paper speed are variable, the sonographs exhibit horizontal exaggeration. By removing the exaggeration and computing the true orientation relative to the ship's course, the gouge trends may be determined. A dominant trend was computed for each 1/2 km segment. Occasionally subordinate trends were evident, or the variability and non-linearity of orientation were so pronounced that it was not possible to plot a representative trend.

On test line 1 the dominant trend is clearly east-west, which is essentially parallel to the depth contours in this area (Fig. 1 & 3). The trend is uniform on both the inner and outer parts of the line. The dots circumscribed by circles (Fig. 3) denoting no dominant trend occur on the inner parts of test line 1. On test line 2, (not shown), the lack of preferred orientation was associated with the tops of submerged ridges.

Gouge density: To determine the density of gouges per square kilometer, every linear feature resulting from ice contact with the bottom was counted, including each individual scratch produced by multi-keeled ridges, as we wished to assess the effects of ice on the bottom. As more gouges would be seen when the ship's track is perpendicular to the trend of gouges over a given distance than when the track is parallel to the features, due to limited scan width of the sonar, gouge counts were normalized to represent the number of gouges that could be seen if all gouges were at right angles to the ship's track using the

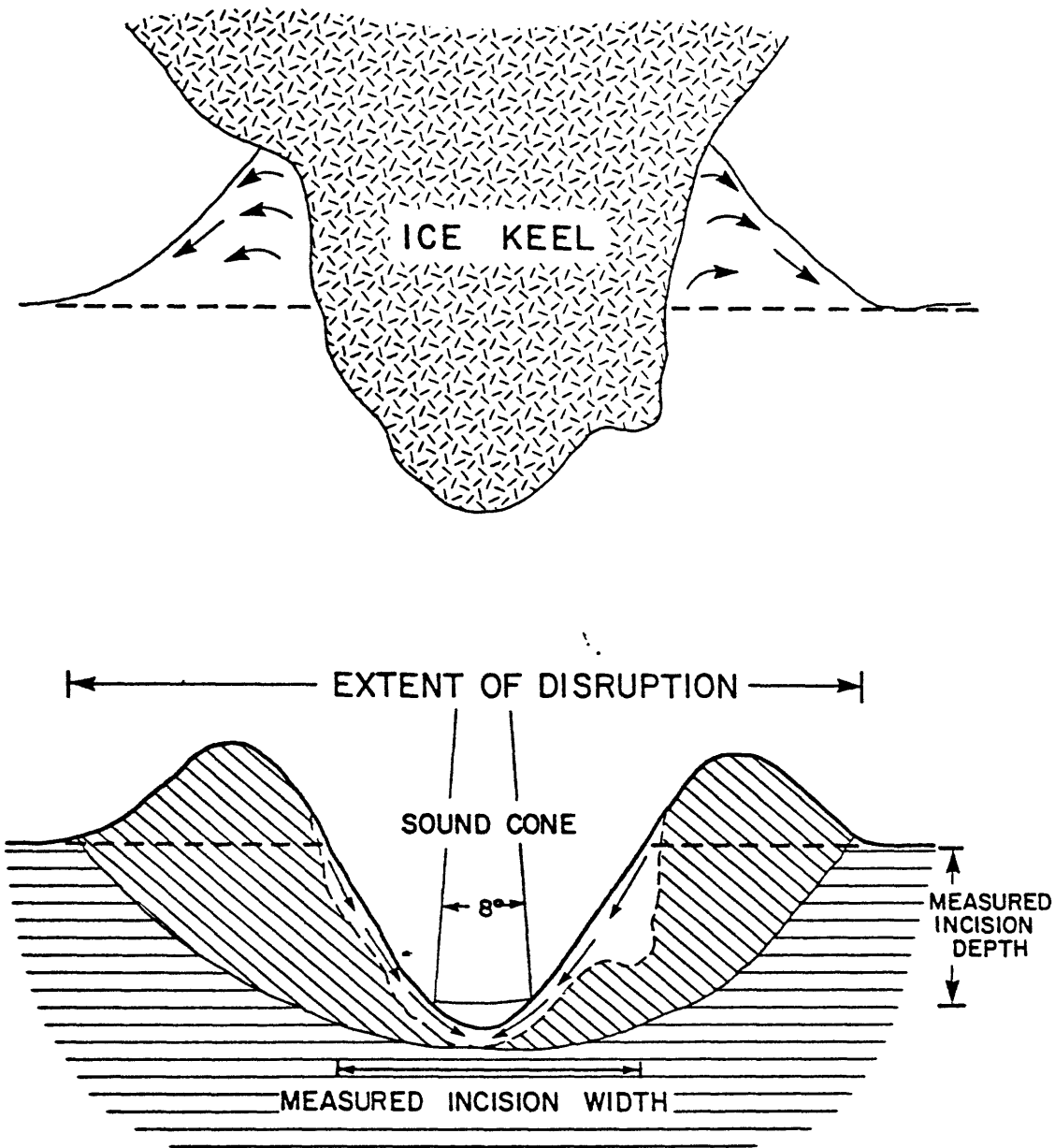


Figure 2. Drawing of an idealized ice gouge cross section explaining gouge terminology. A) Gouge being excavated by ice keel. B) The same gouge after the ice keel has passed by and some slumping of the sides has occurred. (after Reimnitz and others, 1977)

SUMMARY OF ICE GOUGE CHARACTERISTICS TEST LINE I

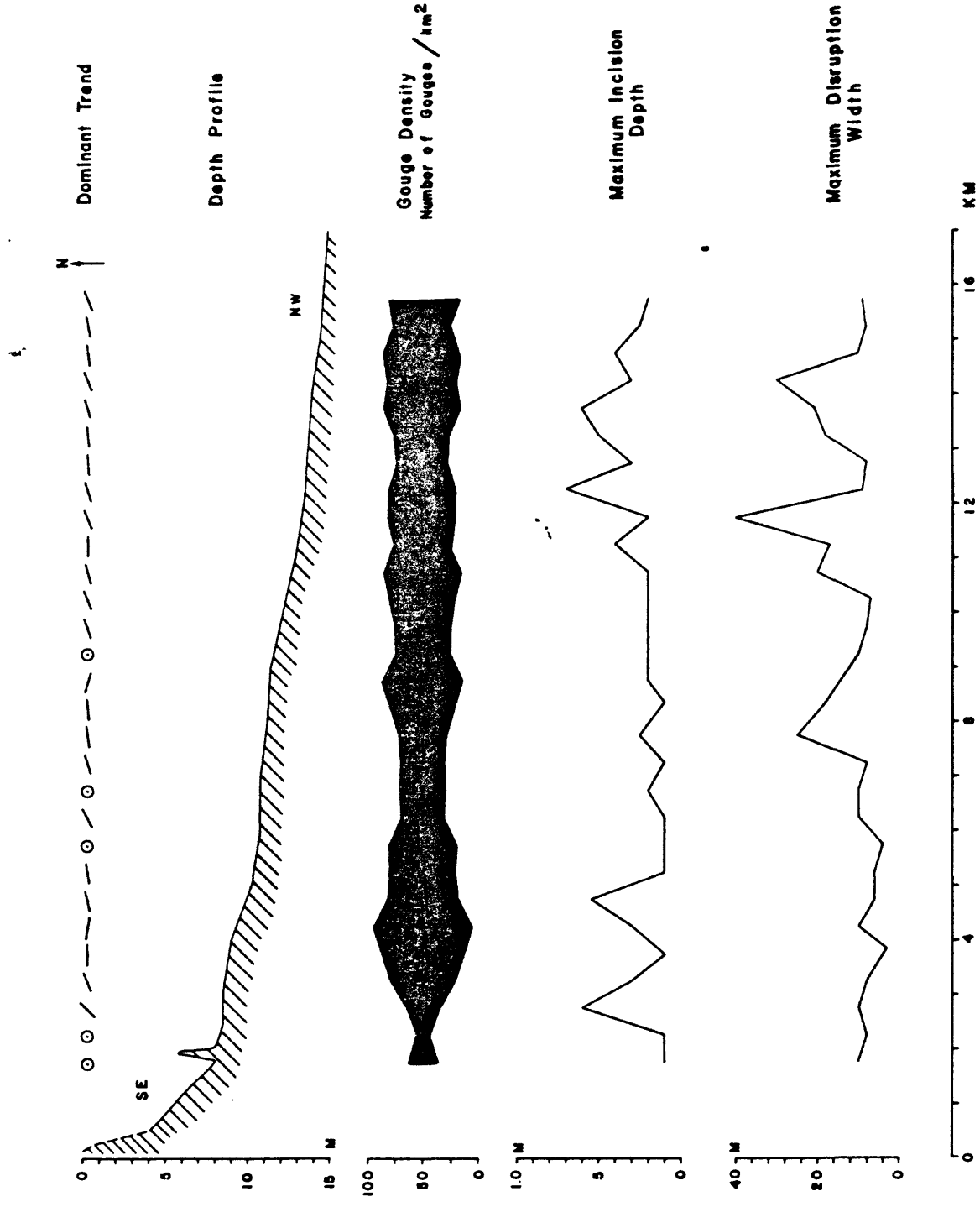


Figure 3. Summary of ice gouge characteristics from the 1975 sonographs of test line 1. Values shown were determined for 1/2 km segments of trackline.

following equation:

$$N = \frac{i}{i \sin \phi + R \cos \phi} (N_{\text{obs}})$$

Where: N = corrected number of gouges in counting interval

N_{obs} = observed gouges in interval

R = recorded width of sonograph - meters

i = counting interval length in meters

ϕ = dominant trend angle of gouges relative to ship's track

(90° = perpendicular to track).

For the 1975 records and a 500 m counting interval this formula reduces to:

$$N = \frac{500}{500 \sin \phi + 250 \cos \phi} (N_{\text{obs}}) \quad \text{or}$$

$$N = \frac{1}{\sin \phi + .5 \cos \phi} (N_{\text{obs}}).$$

Thus a count of 20 gouges in a 1/2 km segment of track, oriented with a dominant trend of 45° to the ship's track, calculates to 18.8 gouges per 1/2 km of track 1/4 km wide.

Assuming that the distribution of gouges immediately adjacent to the zone scanned with the sonar is similar to that on the sonograph, the density of gouges per unit area may be calculated. This is only possible because the gouge count has been normalized for right angles to the ship's track and the assumptions made that all gouges have the same trend, and that they are linear. As the gouges are at right angles by the above formula, the number of gouges calculated for a kilometer segment of trackline should be the same as the number in a kilometer square bisected by that trackline segment. Thus, the above example of 20 gouges in a 1/2 km segment of track can be converted to a gouge density of 37.6 gouges/km as follows: 18.8 gouges per 1/2 km of trackline, which is equivalent to 37.6 gouges per km of track, which is equivalent to 37.6 gouges per km^2 when gouges are at right angles to the track.

On test line 1 the gouge densities correlate with bottom slope: portions with steeper slopes have higher density values (Fig. 3). Densities are highest (88/km) in 9 m of water depth at the upper edge of a steeply sloping segment of the bottom profile. The lowest values are associated with the flat upper surface of a subtle topographic high about 2 km from shore. The overall trend on testline 1 shows a slight increase in gouge densities in the offshore direction.

Incision depth: The depth to which ice penetrated below the sea floor (incision depth) was measured rather than the overall vertical distance from the top of the ridges to the gouge floor (Fig. 2). This incision depth is a true measure of the depth of sediment reworking. The maximum incision depth was determined for each 1/2 km interval from the fathogram.

Maximum incision depths on test line 1 appear to be related to the maximum densities of gouging (Fig. 3). One might conclude that a greater number of ice-bottom interactions increased the chances for the deeper gouges. Intuitively, less incision depth might be expected inshore as the size of the cutting tools decreases due to draft limitations. This would appear not to be the case, at least not within the area and depth ranges examined on test line 1.

Disruption width: Within each track segment the widest gouge disruption created by a single ice event was measured, taking into account the horizontal exaggeration of the sonograph records. The disruption width was measured (Fig. 2) as the incision width could not be accurately determined from the fathograms due to ridge slumping and sedimentation. The largest feature within the scanned bottom did not always cross the trackline and thus often was not recorded on the fathogram.

Maximum disruption widths for the 1/2 km segments on test line 1 tend to increase in an offshore direction (Fig. 3) with a maximum observed width of 40 m. Gouges over about 15 m in disruption width are almost always the result of the action of a multi-pronged ice keel. The wide gouges are not associated with the deepest gouges. In fact, the opposite may be true. Deep gouges commonly are narrow.

New gouges, 1976

By comparing the 1975 and 1976 sonographs of Line 1 for morphologic traits such as intersections of lineations, characteristic angles, and notable debris piles (Reimnitz and others, 1977), area matches could be made (Fig. 4). By careful analysis of the 1976 sonographs, new ice gouge features were identified. Time ticks were used to key the sonar records to the fathograms for depth and width measurements.

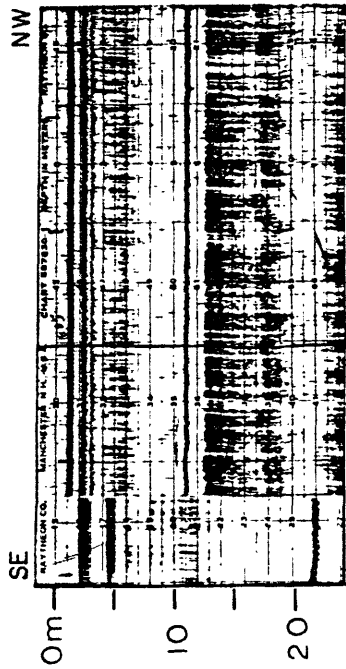
The 1975 Survey was run in the middle of September, shortly before freeze-up, while in 1976, reoccupation of the test line occurred shortly after the sea ice break-up in early August. Thus most of the new gouges seen in the 1976 records most likely occurred during the arctic winter when the area was ice covered.

The actual trend, incision depth, incision width, and disruption width was determined for each of the 39 new gouges, along with observations on their morphologic character (Fig. 5). For comparative purposes gouge densities, maximum incision depths, and maximum disruption widths were determined for the same 1/2 km intervals used for the summary (Fig. 3).

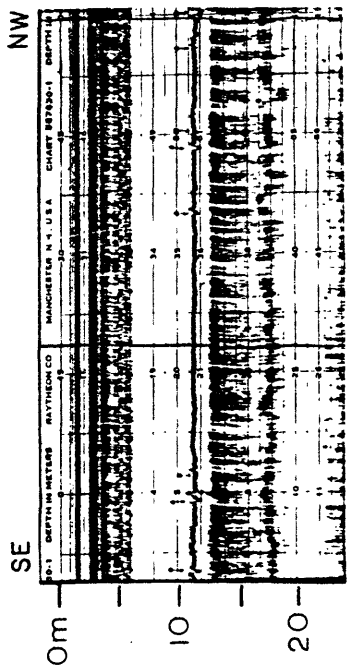
Gouge trend: The dominant northeast-southwest trends of 1976 gouges is clearly different than the dominant trend seen in the 1975 records (Figs. 3 & 5). The change in orientation is evident along the entire length of the survey line. The new gouge trend is more onshore or more in keeping with ice moving into Harrison Bay (Fig. 1). The bulk of the new gouges have the same trend and are very straight (Figs. 4 & 5) suggesting that they may have formed during the same ice event when the ice acted as a single unit.

Gouge density: The densities of new gouges are remarkably evenly distributed over the length of the test line (Fig. 5). The highest number of new gouges occurs near the middle of the test line, in water depths of 11 - 11.5 m.

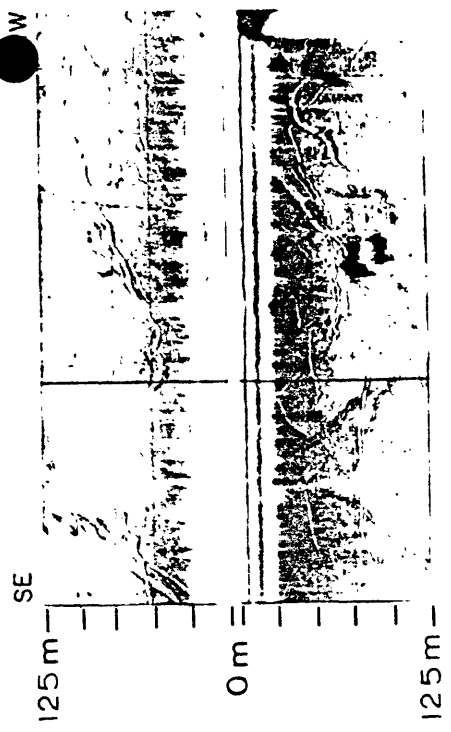
Incision depth: The average depth of incision for all of the new gouges was determined to be 31 cm. Some of the new gouges delineated on the sonographs could not be detected on the fathograms. For these gouges we assumed a depth of 10 cm for our calculations. The maximum new incision was 120 cm deep, deeper than any seen in the 1975 records (Fig. 3). In plotting the maximum incision



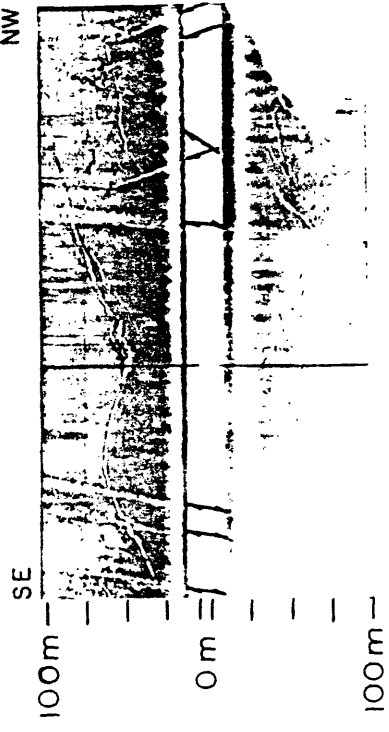
1975



1976



1975



1976

Figure 4. Comparison of 1975 and 1976 sonographs and fathograms, showing the morphology of new gouges formed between September, 1975 and August, 1976. Note the radical change in fathograms from 1975 to 1976. Three gouge events can be distinguished on the sonographs; a) an event forming the series of 5 parallel gouges seen on the left side of the 1976 record, b) a single gouge which weaves across the record toward the upper right hand corner, and c) the set of three parallel gouges that terminate on the sonograph on the upper part of the trace. Location of trackline segment is shown in Figure 1.

NEW GOUGES - 1976
TEST LINE 1

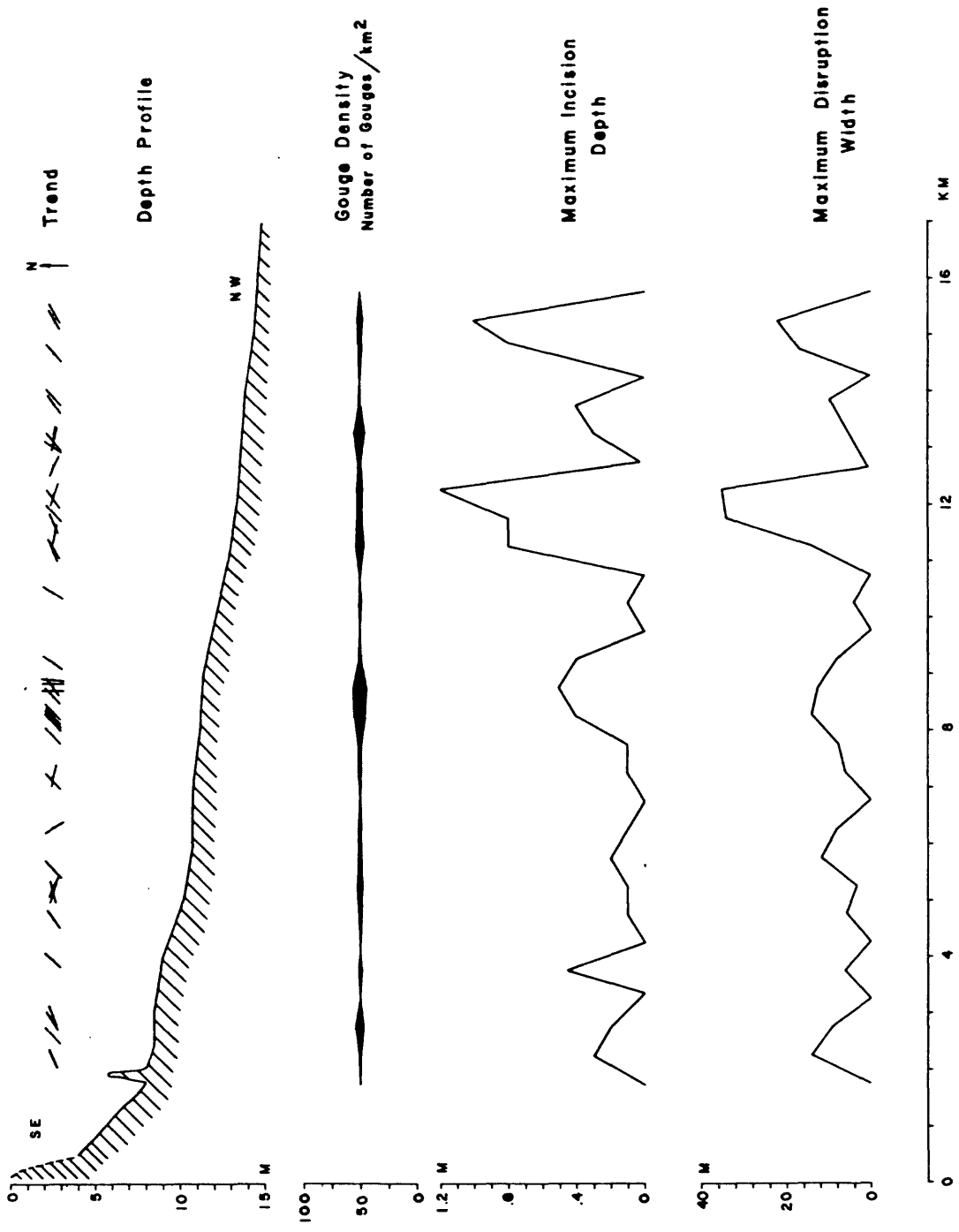


Figure 5. Characteristics of gouges created between 1975 and 1976. Data for test line 1 from sonographs and fathograms. Trend shown is for each new gouge feature. Density, depth, and width values were determined for $\frac{1}{2}$ km segments of the track line.

depth observed in each 1/2 km segment (Fig. 5) it is apparent that the deeper gouges occur further seaward, and they are not restricted to areas of the highest number of gouges. The fact that new gouges are much deeper than old implies that old gouges may have been filled in by sediment redistribution.

Gouge width: Two width parameters were measured for the 1976 gouges. The incision width (Fig. 2) was used in calculating rates of sediment reworking and the disruption width as measured on the fathograms was used in comparing new gouges to the summary gouge characteristics (Figs. 3 & 5). As most gouges were not crossed at right angles, width measurements from the fathogram had to be corrected for the trend of the gouges.

From the 39 new gouges, the maximum incision width observed for a single-pronged ice gouge event was 10.9 m, while the maximum disrupted width was almost 36 m wide from a multi-keeled event. The interval distribution of maximum disruption widths (Fig. 5) shows a strong correlation with the maximum incision widths.

Rate of ice gouging and sediment reworking

Using the data on depth of incision, incision width, length of test line compared, and the time interval between surveys, a rate of ice gouging and sediment reworking may be calculated. The rates thus derived are predicated on the assumption that gouging will proceed in a systematic manner and will not replot the same area until the entire sea floor is reworked. Based on these assumptions the bottom along test line 1 would be reworked to an average depth of 31 cm every 82 years. For the 1973 to 1975 data on the the same test line we reported reworking to 20 cm or more every 50 years (Reimnitz and others, 1977). Data from 44 new gouges on test line 2 (Fig. 1) shows gouging to an average depth of 19 cm and a gouge recurrence rate of 53 years.

As ice interaction with the bottom probably does not occur in a systematic manner, a better approach to the rate problem might be to analyze individual segments of the test line for the amount of gouging occurring in each segment. From such an analysis of the 1973-1975 and 1975-1976 data (Table I), several interesting things appear although the number of new gouges is small in each interval.

The highest rates of gouging and sediment reworking in both periods of observation occur on the innermost and outer parts of the test line, with lower values between 4 and 10 km in water depths of about 10 to 11 m (Table I). Fewer but wider gouges were observed during the two-year interval between 1973 and 1975 (21 gouges) than in the single season from 1975 to 1976 (39 gouges). This may be due to the lower quality of records obtained in 1973 although the rates of gouging are of the same order of magnitude (Reimnitz and others, 1977). The widely differing character of gouging during the two periods suggests that gouging is a very sporadic process and perhaps is strongly dependent on ice and storm conditions of the preceding fall and winter.

Lewis and others (1976), give rates of gouging for the Canadian Beaufort Sea in water depths of 15-20 m. Examination of the Canadian sonographs show gouging of the same character as we observe off Alaska and we would expect similar processes. For two different areas on the Canadian shelf, they show re-plot recurrence rates of about 500 and 50 years on the average, less than our span of interval rates in shallower water (Table 1). This would suggest that the area studied in the Alaskan Beaufort Sea is susceptible to more gouging than in the Canadian area off the MacKenzie delta, or more likely, a difference exists in methods of interpretation.

Table I - ICE GOUGE DATA- NEW GOUGES

	Interval on test line 1							Total/Avg.
	2-4 km	4-6 km	6-8 km	8-10 km	10-12 km	12-14 km	14-16 km	
Water depth-meters	7.6m	9.7	10.5	11.3	12.6	13.1	13.7	-----
Number of gouges/yr								
1973-1975	2	4.5	0	1	.5	1	1.5	21(2 yrs)
1975-1976	5	5	3	10	6	8	3	39
Incision width - m								
1973-1975	17m	79	0	7	45	105	12	263(1 yr)
1975-1976	13m	10	9	40	43	25	24	161
Average incision depth								
in cm								
1973-1975	40 cm	37	0	45	30	45	27	37
1975-1976	35 cm	12	10	31	40	31	80	31
Amount of trackline								
gouged, m/km/yr								
1973-1975	8m	40	0	4	22	53	6	19
1975-1976	6m	5	4	26	21	12	12	12
Rate of reworking -								
yrs - "no reflow"								
1973-1975	119yr	25	-	285	45	19	166	52
1975-1976	157yr	202	230	38	47	81	84	81

In considering the rates of sediment reworking and the amount of bottom disturbed by gouging, our estimates are very conservative. Gouge depths do not include the height of the flanking debris ridges, nor do they include a correction for the cone angle of the fathometer which will give conservative values for narrow deep gouges (Fig. 2). The "extent of disruption" by ice keels often includes a considerable area on one or both sides of the incision (Fig. 2). Measurement of the 1976 gouges on test lines 1 and 2 indicates that widths were 1 1/2 to 3 times wider than the incision widths. If these widths are used to determine rates of reworking, the values we report above would have to be increased by 1/3 to 2/3.

As we reported in earlier work (Reimnitz and Barnes, 1974; Reimnitz and others, 1976) higher rates of ice gouging and ice bottom interaction are related to: steeper bottom slopes, local topographic highs, geographic exposure to drifting ice, and ice zonation. The segments of test lines 1 and 2 reported here are somewhat geographically protected by updrift shoals and are located inside of the major stamukhi zone, within the zone of floating fast ice (Reimnitz and others, 1976). As it is within the stamukhi zone that winter ice deformation is most intense, we would expect rates of gouging to be greater further seaward along the test lines. To date the presence of stamukhi in summer has kept us from obtaining repetitive surveys in this area although one set of data exists for the 1973 and 1976 season in different areas.

REFERENCES

- Reimnitz, Erk, P.W. Barnes, L.J. Toimil, and J. Melchoir: 1977, Ice gouge recurrence and rate of sediment reworking, Beaufort Sea, Alaska, Geology, (in press).
- Reimnitz, Erk, and P.W. Barnes: 1974, Sea ice as a geologic agent on the Beaufort Sea shelf of Alaska; in J. Reed and J. Sater eds., the Coast and Shelf of the Beaufort Sea, Arctic Institute of North America, Arlington, VA. p. 301-351.
- Reimnitz, Erk, P.W. Barnes, and L.J. Toimil: 1976, The development of the stamukhi zone and its relation to arctic processes and morphology, Beaufort Sea, Alaska, Final Report to NASA, NTIS document E77-10043, 44p.
- Lewis, C.F.M., Blasco, S.M., McLaren, P., and B.R. Pelletier: 1976, Ice scour on the Canadian Beaufort Sea continental shelf; Poster discussion, Geol. Assoc. of Canada, Annual Meeting, May, 1976, Edmonton, Alberta, Canada.
- Hnatiuk, J. and K.D. Brown, 1977, Sea bottom scouring in the Canadian Beaufort Sea; in Proceedings of the 1977 Offshore Technology Conference - (Preprint) - 14 p.

Changes in Barrier Island Morphology - 1949 to 1975,
Cross Island, Beaufort Sea, Alaska

by

E. Reimnitz, P.W.Barnes, and J. Melchior

Introduction

Sand and gravel is in high demand on the northslope as construction material. Most of the barrier islands including Cross Island, are composed of sand and gravel. Some of the islands near Prudhoe Bay have already been mined. It is anticipated that others will be soon. For this reason it is important to know the gravel sources that supply the islands with new material, and to know how erosion and deposition change the shapes and locations of the islands.

The location of the stamukhi zone (Reimnitz and others, 1976) off Prudhoe Bay is controlled by Cross Island, located approximately 12 miles north of the Sagavanirktok River delta (Fig. 1). Considering the energy expended by the moving ice field on the island, the action of storm waves, and its location at the downdrift terminus of a barrier island chain, changes in the island might be expected over several decades. An attempt was made to document the changes in the morphology and position of the island using aerial photos, both vertical and oblique, photos from the ground, and published navigational charts. The changes in morphology over the years were measured using characteristic embayment, lake and ridge patterns of the island as the stable bases for alignment of photos and charts. The series of drawings in Figure 2 show how the island appeared on the earliest (1914?) map by Leffingwell (1919) up to the present day. The Leffingwell drawing could not be keyed into the other drawings accurately, because of the lack of identifying features used to match the scales between pictures. It is

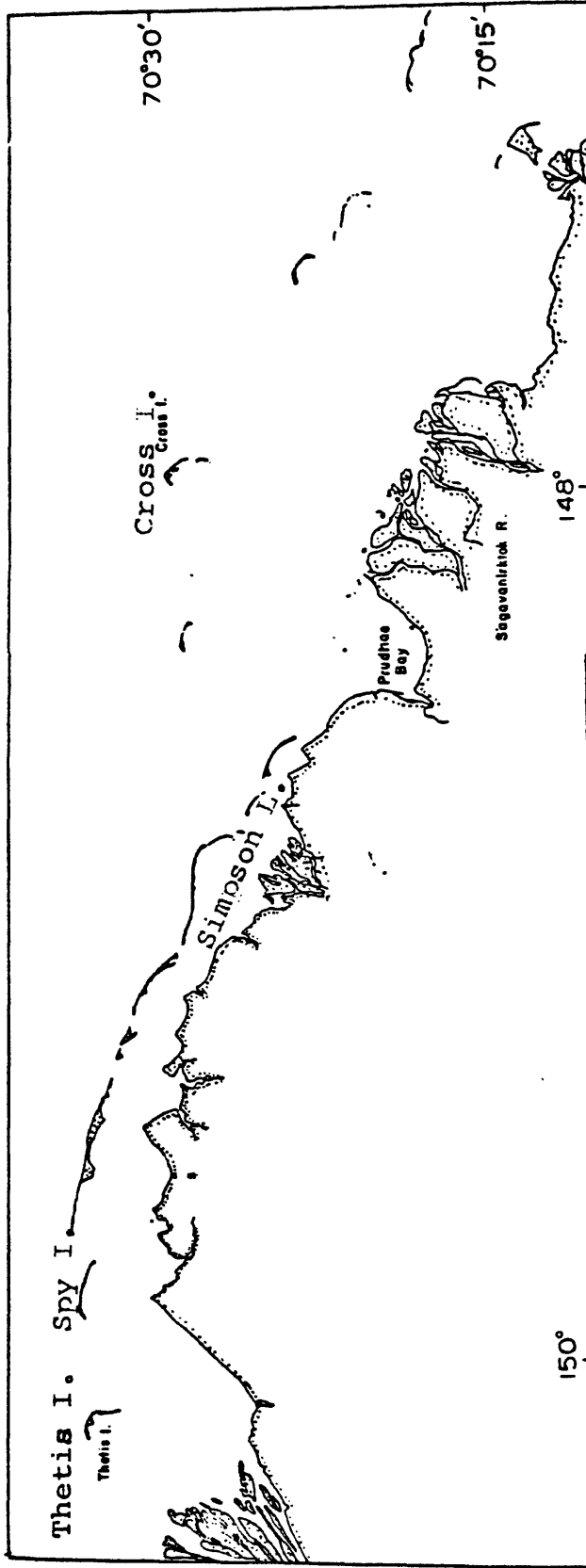


Figure 1. Location map showing Cross Island other locations named in the text. Both Cross and Thetis Islands are at the western ends of long barrier chains.

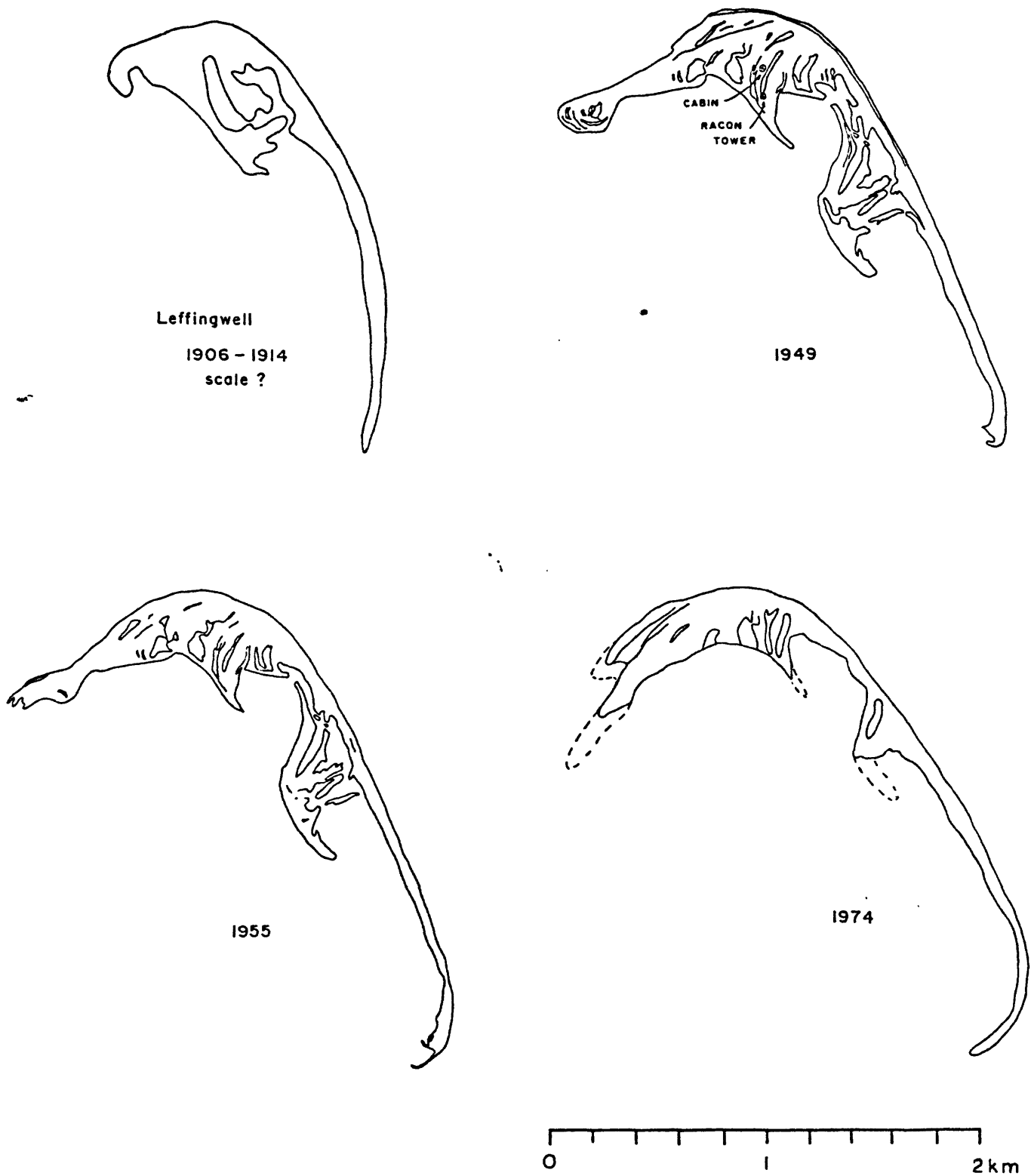


Figure 2. Configuration of Cross Island from 1914 to 1974. From sources mentioned in the text. 1974 outline is dashed where uncertain (See Figure 4).

shown only to give the general impression of the earliest recorded view of the island.

The information gathered for the comparison of the island's shape and position consisted of 1) vertical B&W photo taken in July 1949 from 10,000 feet altitude, 2) vertical B&W photo taken in July 1955 from 25,000 feet altitude, 3) vertical U-2 color photo taken in June 1974 from 65,000 feet altitude, 4) April 1955 edition of NOAA chart #9472 with coastal revisions updated to June 1973, and 5) U.S. Hydrographic Survey Chart #7761 from 1950.

Cross Island as seen on the NOAA chart appears to have been taken from the 1949 photo, and matches nearly perfectly. This chart was used to determine changes in overall position. The Hydrographic Survey chart was only used to study changes in position relative to the mainland, since the island was drawn too crudely to give details of morphologic changes. The 1949, 1955 and 1974 photos were brought to common scale, with all the details of stream, lake and topography that could be unambiguously identified. These patterns remained stable through the years and enabled us to measure the shoreline changes. Close examination of vertical photos, oblique photos taken from the air in August 1970, June 1971, and September 1976 and photos from the top of a 20 m RACON navigation tower on the island in 1973 confirm the stability of these land-locked features. A small wooden cabin approximately 30 years old (Fig. 3) that is located on a high point of the island, was also used as an artificial "benchmark" to confirm positions seen in the photos. The two linear depressions on either side of the cabin, and the lake seen in the far left of the photo can be precisely located on all the photos. In Figure 2, in the 1949 photo, the cabin and RACON tower positions are shown.

The 1974 U-2 photo shows Cross Island surrounded by ice and some snow

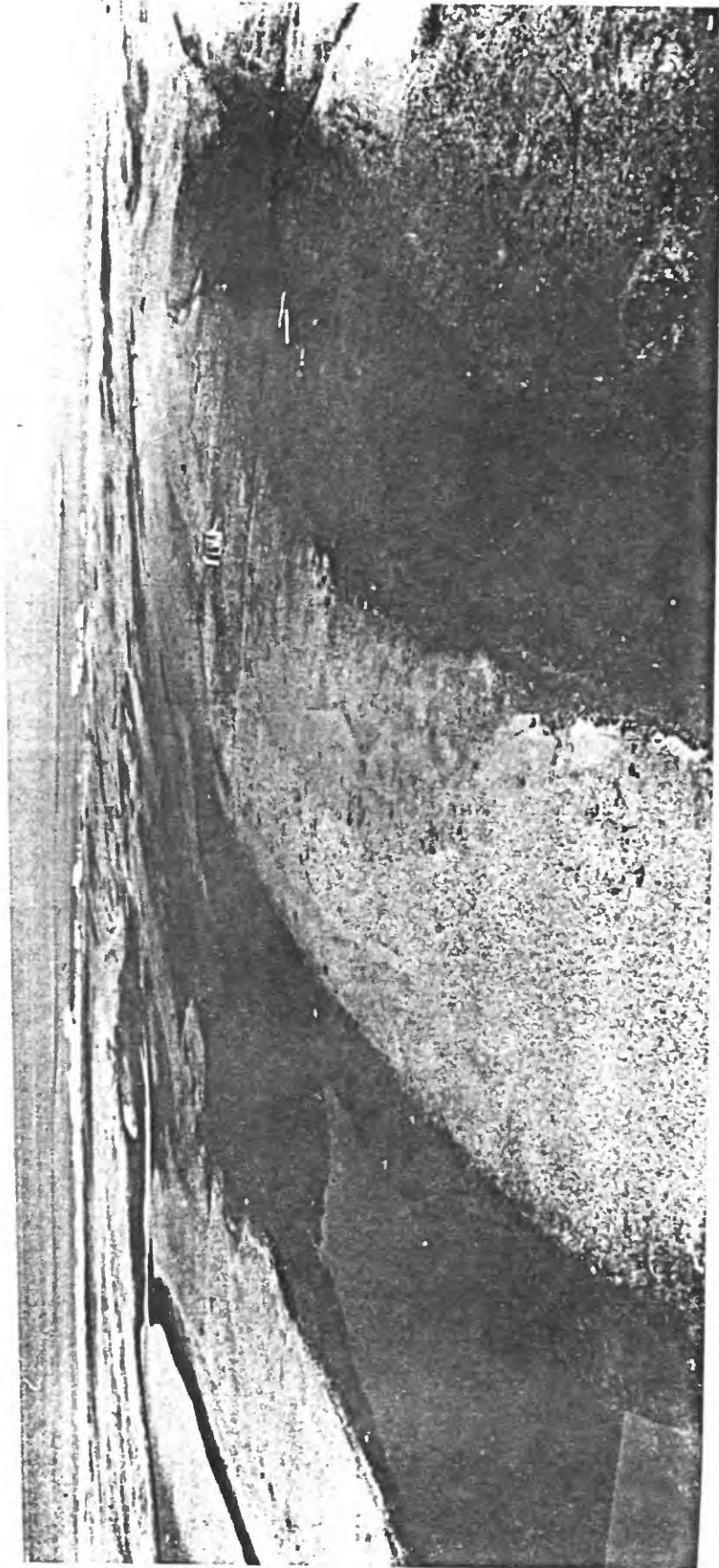


Figure 3. Photo from the top of RACON tower looking north past the cabin on Cross Island (See Figure 2).

cover still present which partially obscures the shoreline. For this reason, the 1974 shore is not as accurately represented as in 1949 and 1955. However, the personal observations by Reimnitz of the shore area during periods of ice cover, and examination of the photos taken from the RACON tower and aircraft which show the width of the island between the north shore and the lagoon during the summer (Fig. 4) indicate that for the north shore the U-2 photo coastline is accurate to within 20 m. The southern (inner) beaches have gentle slopes. With fast ice and snow drifts lapping onto this shore, an accurate determination of the shore was nearly impossible. Dashed lines in Figure 2 indicated where shoreline positions are in doubt and are roughly drawn in from photographic contrast changes seen in the U-2 photo. In fact, the southern shore of the island is probably poorly known planimetrically for 1974 (see Fig. 4).

The attempt to document the large scale movement of the island by comparing its position to mainland based features was not successful because the comparison between the Mercator projections of the NOAA and Hydrographic survey charts and the planimetrically photographed U-2 image was not possible within the accuracy needed. Leffingwell's map of the area was considered too inaccurate to use in a comparison since the method of fixing the island's position must have involved numerous extended surveys far out onto the ice to reach the island, introducing errors fatal to the accuracy desired for a comparison.

Results of Measurements

The north shore beach retreat measured between 1949 and 1955, is slightly less than 50 m in 6 years at the point of greatest change. An average retreat of about 40 m is indicated along the almost parallel 1949 and 1955 shorelines (Fig. 5). The measurements from the 1974 photo give an average

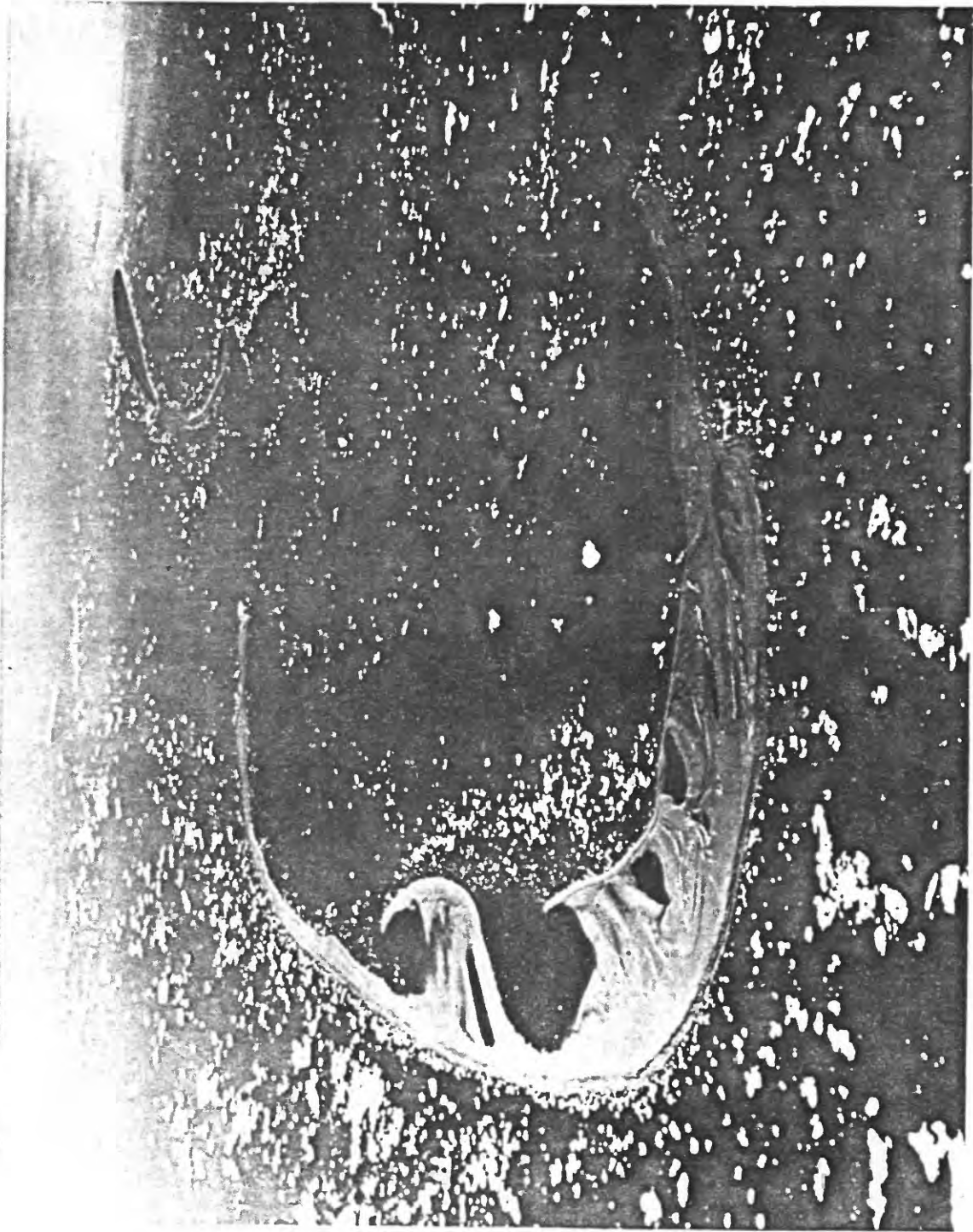


Figure 4. Aerial photograph looking southeast over Cross Island, taken in September, 1976. Note the ridges, lakes and vegetated areas; these morphologic features were used to register the photography of 1949, 1955, and 1974(Figs. 2 and 5).

retreat of 150 m from the 1949 position, with the largest value of 170 m near the point of maximum curvature of the north beach. This gives an average of 7 m a year from 1949 to 1955 and 6 m a year from 1949 to 1974. Extrapolating this back to 1914, the location for Cross Island should be about 245 m seaward of the 1949 position. On his map, Leffingwell (1919) puts the island 2000 m to the northeast. For this reason, we chose to disregard his location, and blame lack of adequate survey control for the error.

Figures 2 and 5 suggest that sediment eroded from the northern shore is transported to and deposited on both ends of the island, but movement of beach material seems to be mainly toward the west. On the west end of the island a recurved spit is being formed (Fig. 2), that eventually may become similar in shape and morphology to the spits that enclose the two shallow embayments on the landward side of the islands (Fig. 4). This would form a third embayment. The embayments enclosed by recurved spits record the migration of the island. The two existing embayments indicate northwesterly migration, the presently forming embayment seems to indicate a shift in migration direction to westerly. A westward migration of Cross Island is in agreement with the migration direction of other barrier islands along this section of the Beaufort Sea coast (Short, 1973; Burrell and others, 1974).

Discussion and Conclusion

From 1949 to 1974, Cross Island has lost 6 to 7 m a year on the seaward side. It is becoming narrower, because the landward side is not accreting at the same rate. Possibly most of the eroded material can be accounted for by spit accretion, mainly on the west end. Various types of evidence indicate that Cross Island presently is not receiving gravel from an outside source.

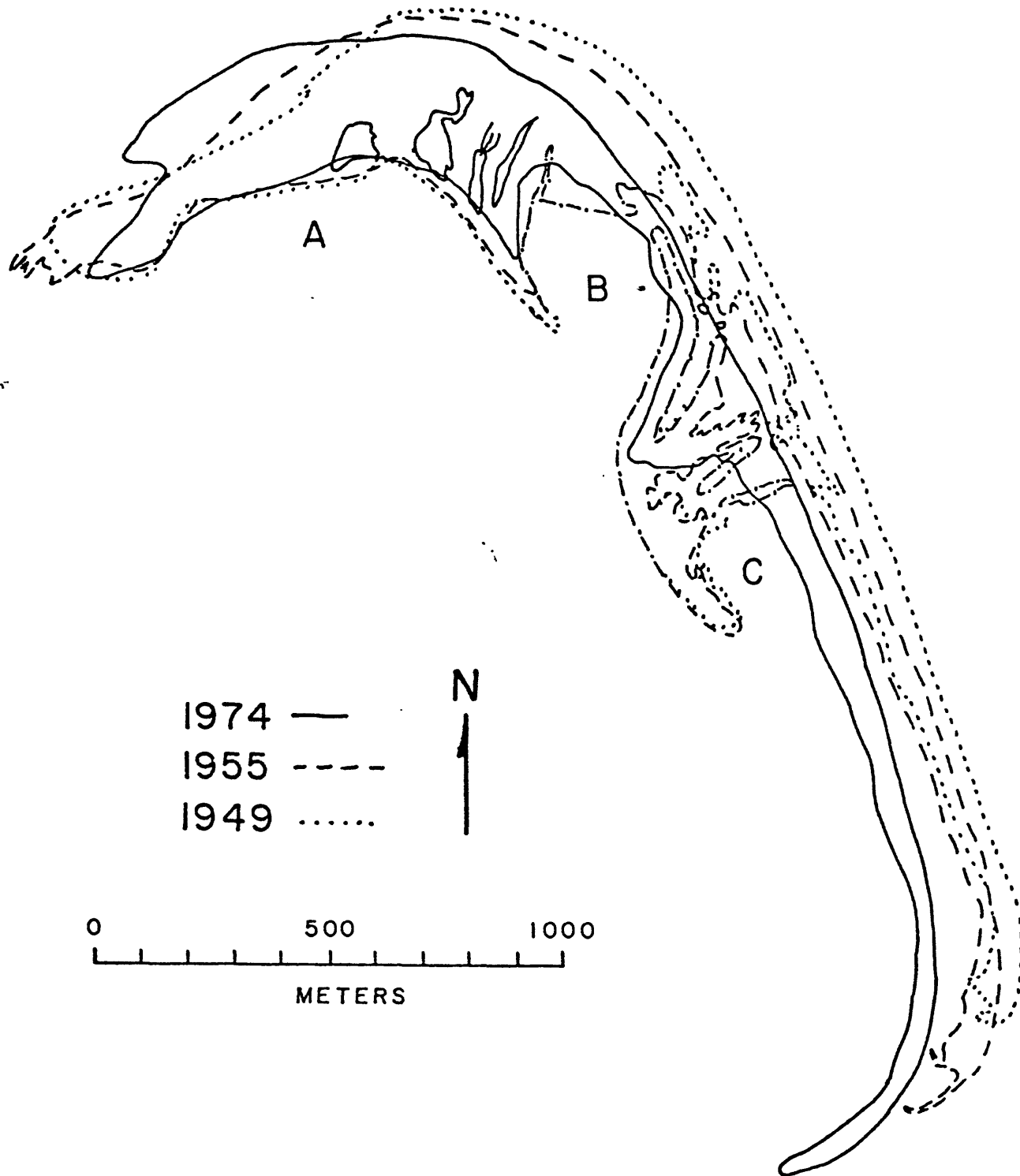


Figure 5. Comparative configuration and location of Cross Island, 1949 to 1974, showing the southwestward movement of the island since 1949.

Reimnitz and his co-workers (1976) show that Cross Island is the focal point for the early winter shear lines in the sea ice. Major ridges form close to the island, and ice shove commonly affects the beaches. Other islands in the area, protected from shear zone dynamics are little affected by ice shove. Ice shove brings cobbles and pebbles, found by diving near the beach at 5 - 7 m depth, up onto the beach face. This ice shove may be one of the reasons why Cross Island is a meter or more higher than the characteristic barrier islands along Simpson Lagoon. The bottom off Cross Island also slopes much steeper than off other islands that are protected from shear zone dynamics, as shown in the above report (Fig. 6). Grounded ridges off the island commonly remain stationary throughout the summer. Therefore, the north side is almost completely protected from wave action during the average year (Fig.4). Figure 3 was taken during an unusually ice-free summer.

Cross Island is located at the western terminus of an 80 km channel of barrier islands (Fig. 1). The morphology, size and orientation of this island are strikingly similar to Thetis Island which lies at the western end of the next island chain to the west (Figs. 1 and 7). This comparison is even more pronounced when one considers the unsketched appendage to the southeast of Cross Island (Fig. 4). This would suggest that the origin or the processes influencing the two islands are similar. As we postulate that Cross Island may not be presently supplied with sediment, perhaps both Cross and Thetis represent the dying phase of the barrier island system off northern Alaska. If a sediment supply were defined as is suggested by the accretion reported for Thetis Island (Dygas, 1972), both these islands may be the initial stages of barrier chain extension and stable or growing in size. This enigma remains.

A comparison of the geographic setting of the two islands with regard to the seasonal sea ice regime (Reimnitz and others, 1976), shows that Thetis

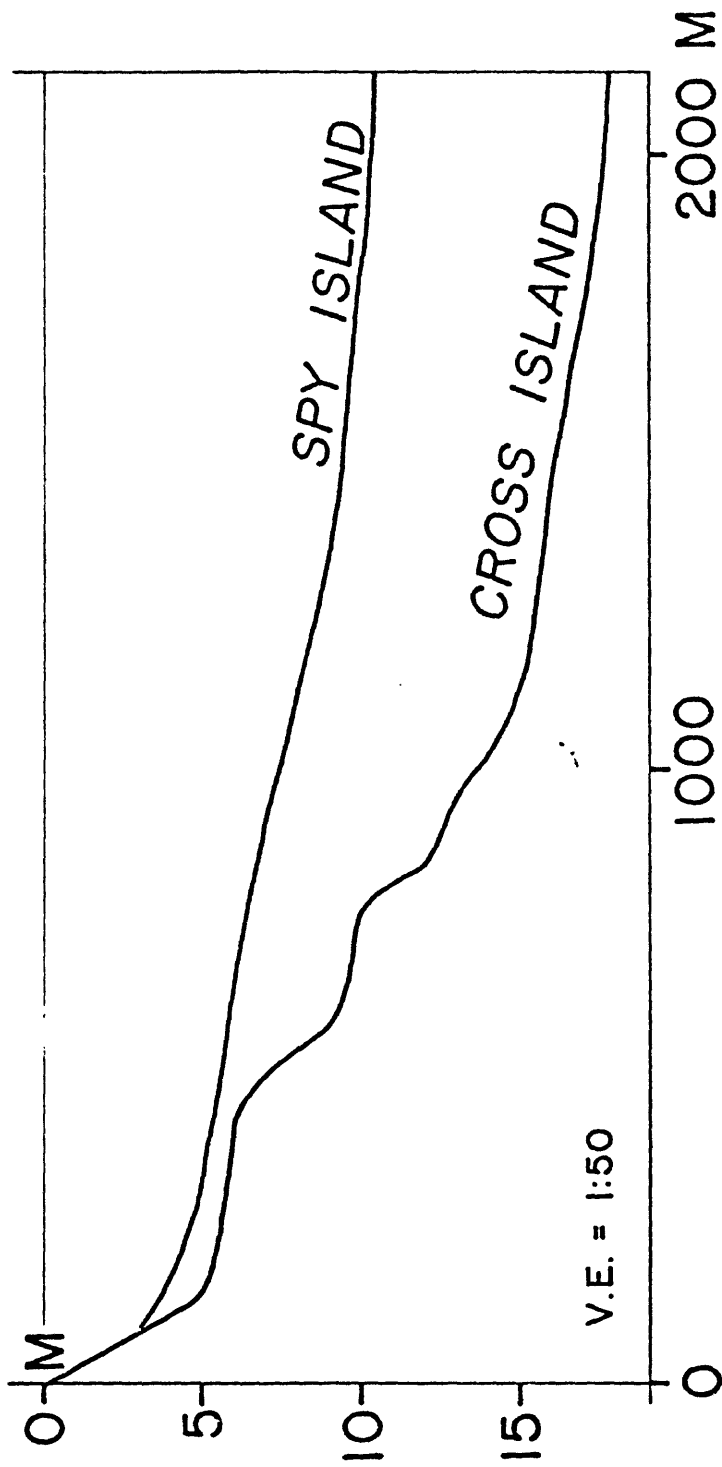


Figure 6. Comparison of bottom slope off an island with intense ice-bottom interaction (Cross) and an island protected from the direct forces of the pack ice.

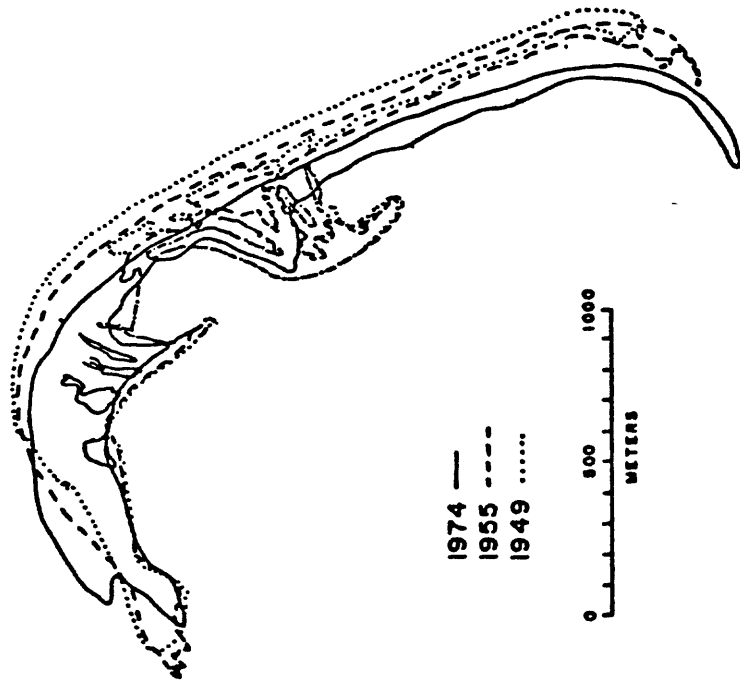
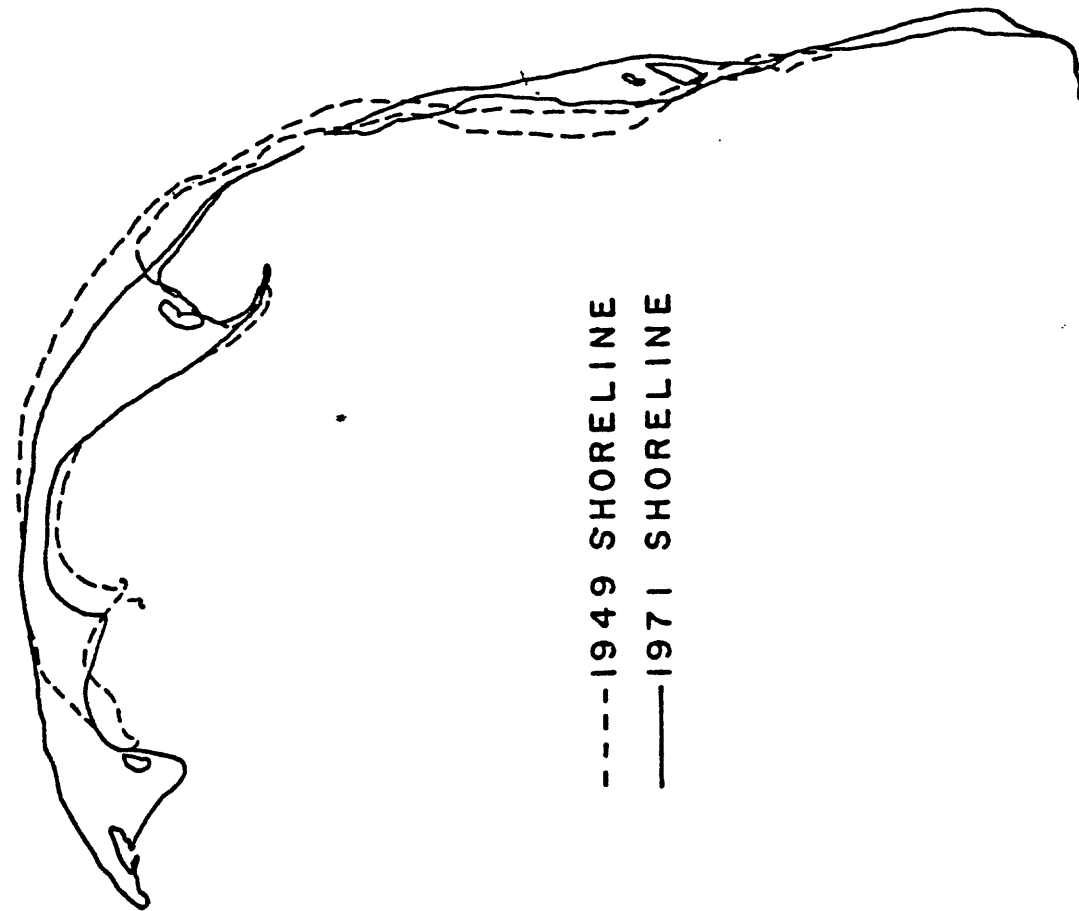


Figure 7. Thetis and Cross Islands compared, showing the similarities in shape and orientation. Location in Figure 1.

Island is not as important in controlling the ice zonation. This suggests that the major patterns of sea ice ridging are not influential on the planimetric shape of these two islands.

The above observations on Cross Island may have certain implications for offshore development and construction by man, because artificial drilling islands have been used in the Canadian Arctic. It lies further offshore, and in deeper water than those, and is exposed to pack ice drift. In fact, Cross Island controls the pack ice drift, and the extent of the relatively undeformed fast ice (Reimnitz and others 1976). Further studies of ice dynamics in relationship to the island may provide information on the feasibility of modifying the ice zonation off Prudhoe Bay to expand the area of stable ice available for development.

REFERENCES

- Burrell, D.C., J.A. Dygas, and R.W. Tucker, 1974, Beach morphology and sedimentology of Simpson Lagoon, in: V. Alexander, ed., "Environmental Studies of an Arctic Estuarine System," University of Alaska Institute of Marine Studies, IMS Report R74, p. 45-144.
- Dygas, J.A., R. Tucker, and D.C. Burrell, 1972, Geological report on the heavy minerals, sediment transport, and shoreline changes of the barrier islands and coast between Oliktok Point and Beechy Point, in: (P.J. Kinney et al., eds.) Baseline data study of the Alaskan Arctic aquatic environment. Univ. of Alaska, Inst. of Marine Sci., Rept. R-72-3, p. 61-121.
- Leffingwell, E. de K., 1919, The Canning River region, northern Alaska, U.S. Geol. Survey Prof. Paper 109, 251 p.
- Reimnitz, E., P.W. Barnes, L.J. Toimil, D. Harden, 1976, Studies of the inner shelf and coastal sedimentation environment of the Beaufort Sea from ERTS-A, Final Report to NASA, Nat. Tech. Infor. Service Document #7710043, 105 p.
- Short, A.D., 1973, "Beach dynamics and nearshore morphology of the Alaskan arctic coast," Unpublished Ph.D. dissertation, Louisiana State University, Baton Rouge, Louisiana, 140 p.

RECONNAISSANCE STUDY OF KOGRU RIVER,
HARRISON BAY, ALASKA

by

Erk Reimnitz, Douglas Maurer, and Larry J. Toimil

During the middle of September, 1976, the R/V KARLUK made a reconnaissance survey of the navigable parts of Kogru River in southwestern Harrison Bay (Fig. 1). During this survey the following systems were operated: a) Uniboom sub-bottom seismic profiler using 300 joules of power, b) Raytheon sub-bottom profiler, c) Raytheon and Simrad fathometer, d) E.G. & G. side-scanning sonar, e) salinity and temperature sensor, and f) transmissometer.

Navigational control is based on radar ranges to favorably located promontories along the embayment, giving sharp returns. Position inaccuracies may range to as much as 50 m, but generally are less.

The purpose of this survey was severalfold:

- 1) Not previously charted, Kogru River, if found deep enough may serve as a protected harbor for small craft and barges bringing supplies to the North Slope.
- 2) Kogru River extends for a considerable distance into the coastal plain. It therefore provides the opportunity to compare coastal plain geology, seen in seismic profiles, to continental shelf geology.
- 3) Offshore seismic profiles in southwestern Harrison Bay show a very pronounced change in character of the Quaternary Gubic Formation underlying the shelf. Kogru River seismic data would help in defining this boundary.
- 4) Previous workers have speculated that the irregular embayment of Kogru River represents a series of coastal plain lakes, breached by erosion and

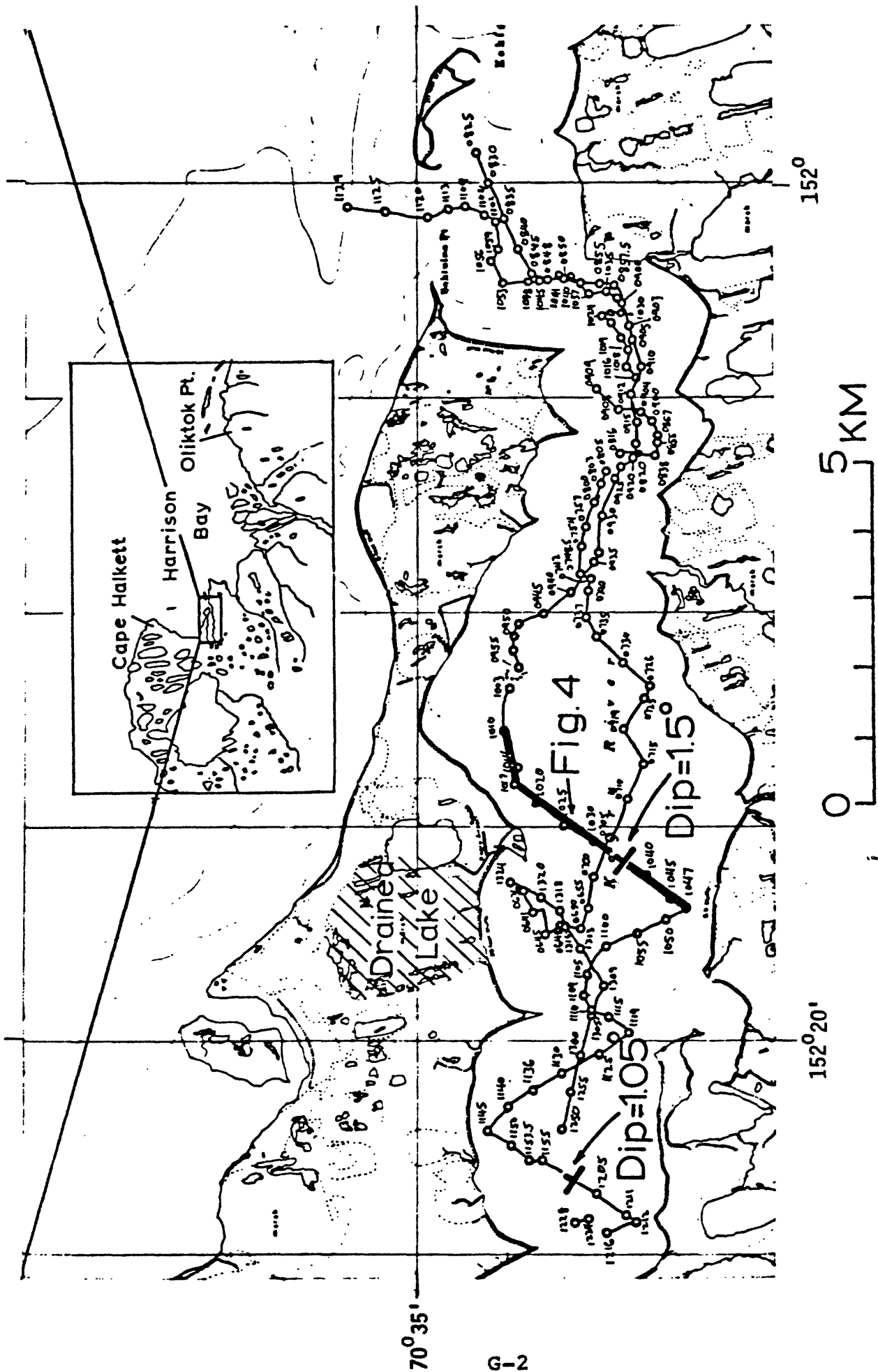


Figure 1.- Kogru River study area, showing tracklines, apparent dip of sub-bottom reflectors, and location for seismic profile in Figure 4.

Figure 2.- Bathymetry of Kogru River contoured from Ratheon record along 1976 trackline.

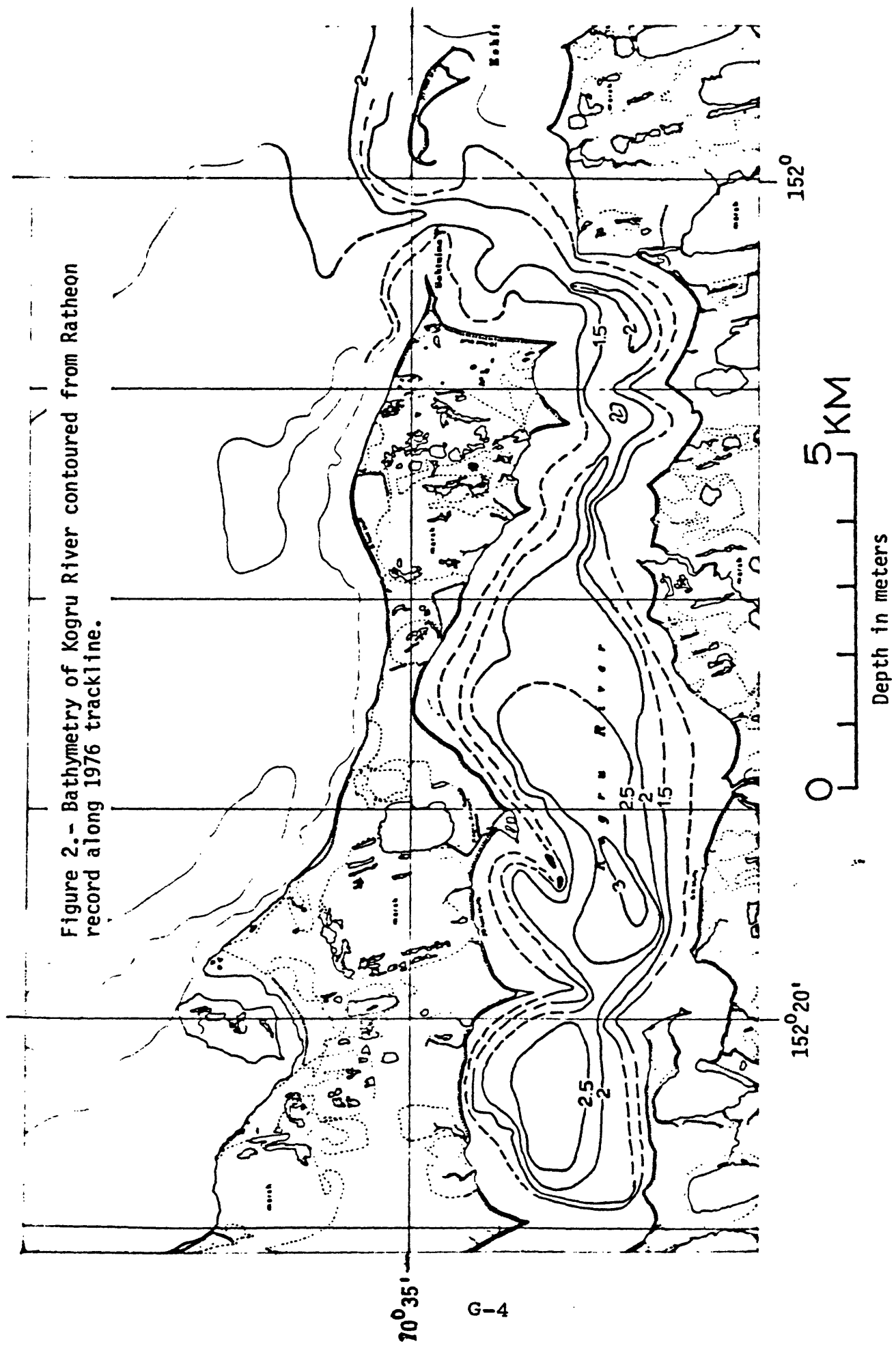
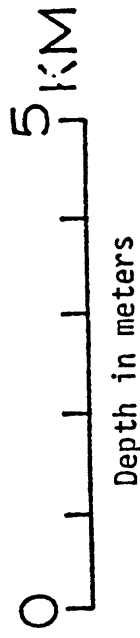
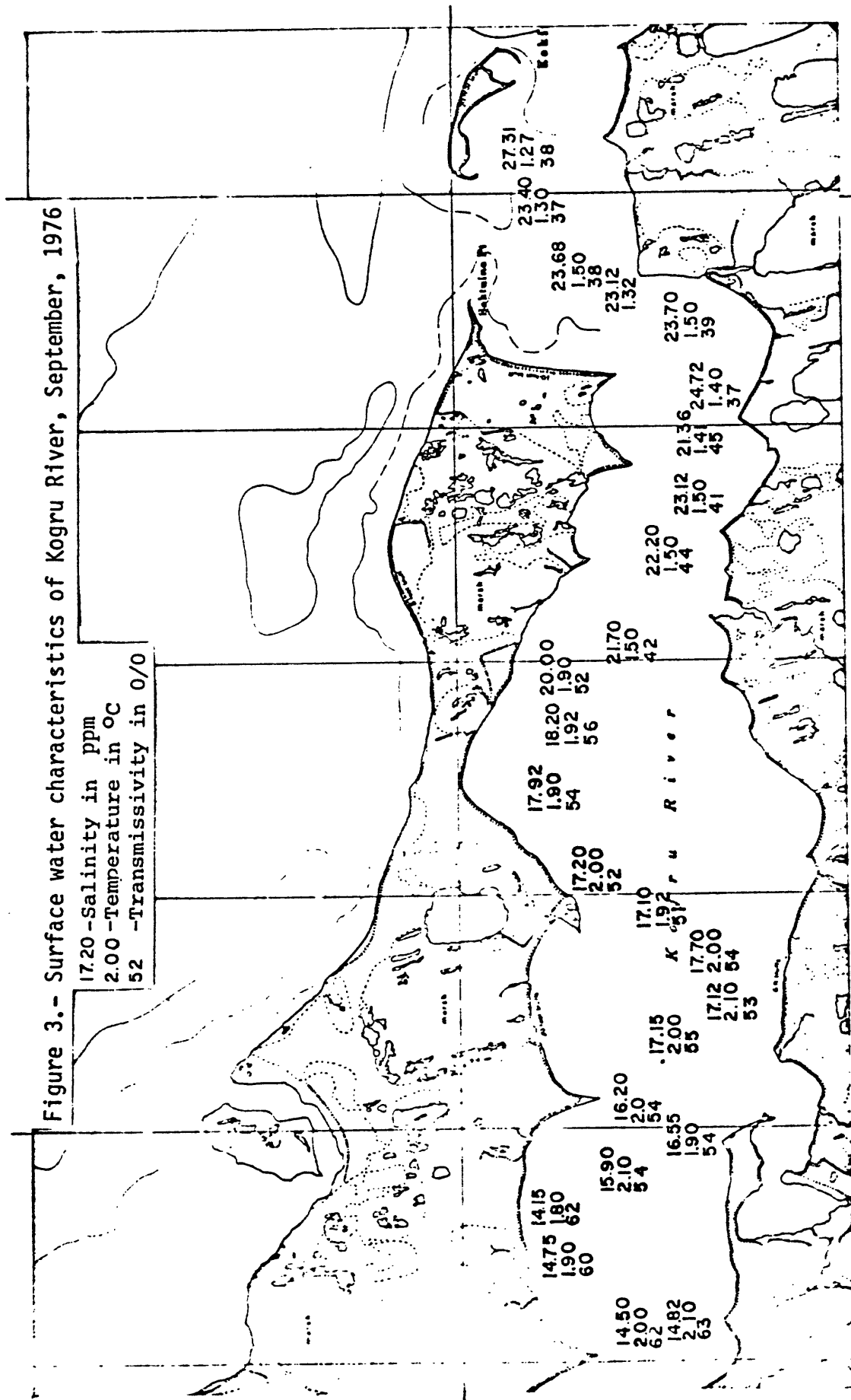


Figure 3.- Surface water characteristics of Kogru River, September, 1976

17.20 -Salinity in ppm
 2.00 -Temperature in °C
 52 -Transmissivity in O/O



Bay, and extending far up into the coastal plain along the Kogru River (Fig. 1), are very different from seismic records obtained with similar equipment on the arctic shelf in general. The records in this area exhibit strong, flat-lying, and continuous reflectors down to a sub-bottom depth of about 70 m (Fig. 4). The inner shelf sub-bottom seen in high resolution seismic reflection records elsewhere in general is characterized by irregular, ill-defined, discontinuous reflectors (Reimnitz, 1976). This difference leads us to believe that a geologic boundary separates Quaternary Gubic deposits underlying the coastal plain from Barrow to Cape Halkett from those underlying the coastal plain and shelf to the east. It is important to know the nature and configuration of this boundary.

Line drawings prepared from two intersecting track lines in Kogru River are shown in Figure 4, along with a sketch of surrounding bluffs and the coastal plain. About 5 m of modern sediments, labeled basin fill, covers the floor of this embayment. The rather flat-lying unit (about 10 m thick) below this rests on an unconformity, apparently an erosional surface, 15 to 20 m below the sea floor. The stratified section below this unconformity dips about 1.3° towards 30° T. This uniformly dipping section can be traced about 10 km farther northward into Harrison Bay.

The unit above the unconformity is exposed in the bluffs along the north side of Kogru River, in the vicinity of the drained lake shown in Figure 4. A brief study of the exposures here revealed that the unit is composed of eolian, lacustrine, beach, and shallow marine sediments. We feel these exposures belong to the Barrow Unit of the Gubic Formation (Black, 1964). Distinct facies changes over short horizontal distances within this unit account for the somewhat irregular reflectors seen in the seismic profiles. These deposits of the Barrow unit, underlying the coastal plain and

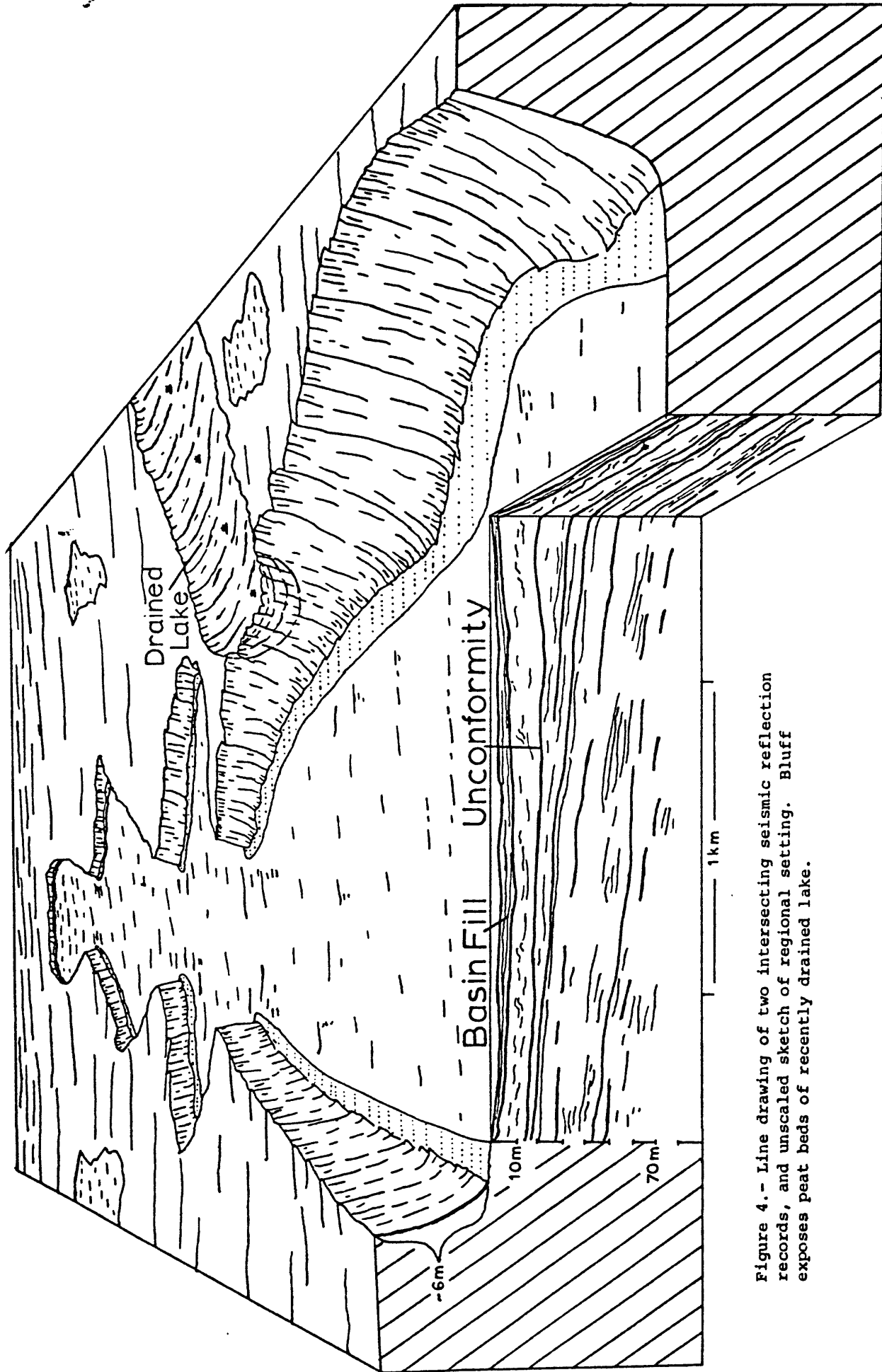


Figure 4.- Line drawing of two intersecting seismic reflection records, and unscaled sketch of regional setting. Bluff exposes peat beds of recently drained lake.

shallow shelf in western Harrison Bay indeed are very different from anything we have seen in coastal bluffs and seismic records to the east which lack easily identifiable units. If, and how far the Barrow unit in the Kogru River area extends to the south is unknown at this time.

Short and Wright (1974) show a pattern of primary and secondary "lineaments", as traced from map contour patterns and surficial geomorphic trends. One of their illustrations is reproduced here as Figure 5. These authors state that the lineaments have pronounced effect on the coastal configuration, including alignment of barrier island chains, and that major offsets in the coast occur at intersections of lineaments. Our seismic profiles from the continental shelf in general, and around Cape Halkett and Kogru River in particular, provide no evidence for a geologic basis of the lineaments of Short and Wright (1974) (Fig. 5). Kogru River, in fact, lies along and parallel to a pronounced boundary separating distinct physiographic provinces of the coastal plain. This boundary is clearly visible on Landsat images, and runs oblique to the lineaments of Figure 5. The landform north of the boundary is dominated by large, elongated, oriented lakes trending north-northwest to south-southeast. The landform south of Kogru River is marked by a pattern of distinct lineation oriented parallel to Kogru River, essentially east-west. Sellman, et al. (1975) in their classification of lake types draw a boundary along, and parallel to, Kogru River. In their classification the lakes south of this boundary are the same as lakes to the east on the coastal plain from Oliktok to Prudhoe Bay.

Based on landform analysis some workers have proposed that the Kogru River boundary represents the limit for the last transgression during mid- to late-Wisconsin time (Sellman, et al., 1975). Furthermore, Black (1964) draws the boundary between the Barrow unit and the Meade River unit of the Gubic Formation along the Kogru River, but from the location of the sites he

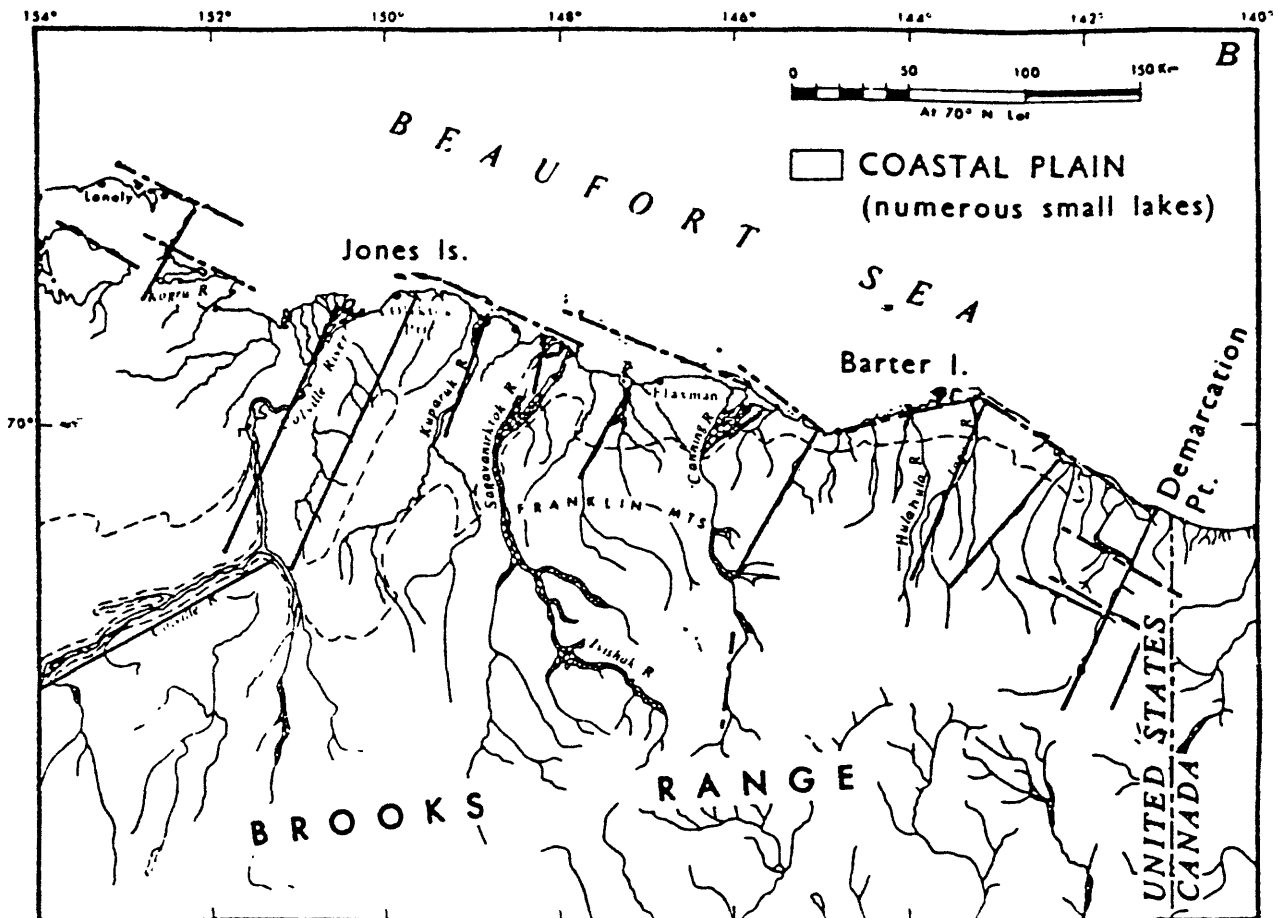


Figure 5.- Location of some of the most prominent and continuous lineaments on the north slope (From Short & Wright, 1974).

studied or described it appears that Black did not intend to position the boundary exactly along the Kogru River. Moreover he points out that the relation of one unit to the other is gradational or interfingering. Locally both units lie unconformably on the Skull Cliff unit of the Gubic Formation (Black, 1964). Based on available evidence we suggest that the surface of the Skull Cliff unit is the unconformity in the seismic reflection records of Kogru River (Fig. 4).

The nature of the Barrow unit in the seismic records of Kogru River does not change within the surveyed area, therefore the gradational boundary into the Meade River unit must lie slightly south of the embayment.

Permafrost

High resolution seismic reflection records in the arctic to date have given no clue on the depth to ice bonded sediments. The Kogru River setting is unique, and we therefore hoped that the high quality records might show the top of the ice bonded sediments as a recognizable reflector. The reasons are:

a) the geologic setting provides easily identifiable, dipping reflectors, which should allow us to trace a high velocity surface that is unrelated to geologic structure, b) the embayment was thought to consist of a series of recently breached lakes in which the narrow bottlenecks represent recently inundated terrain where the permafrost surface should rise, c) the seismic profiles in many places cross the 2 m depth contour which appears to be the place where the top of the ice bonded section drops off rapidly toward deeper water. Careful analysis of the seismic records provides no clues on the distribution of ice bonded sediments.

Origin of Kogru River and other North Slope embayments

Thermal erosion plays a strong role in shaping the coastline of the Beaufort Sea. A better knowledge of how a) thermal erosion, b) a low-relief coastal plain underlain by frozen deposits, c) numerous lake basins ranging from very small to very large, and d) thaw settlement of the upper section of the coastal plain after inundation, interact, is important for the development of the

arctic coastal region. The first thought which comes to mind when contemplating the effects of rapid coastal retreat into large lakes, their draining, filling with sea water, and subsequent thaw settlement, is to explain the large embayments of the North Coast as recently breached, coalesced thaw lakes. Prudhoe Bay may be a large breached lake, and a long core sample in the center of the bay would penetrate through marine sediments into lake sediments. Wiseman, et al., (1973) believe that even the lagoons backing the larger barrier chains originated through the erosion and coalescing of thaw lakes, as shown in Figure 6. We feel that this explanation is oversimplified, and acceptance of the hypothesis may prevent the search for the true answer. Some problems with this explanation are as follows:

In plan view, the lake pattern around Prudhoe Bay and around Kogru River is not coarse enough to permit the formation of another embayment similar in size by future breaching and coalescing. But more important, the surrounding lakes in these two areas are not deep enough. Most of them are about 2 m deep (for example, Sellman, et al., 1975). In Figure 7 the cross-sectional profiles of several lakes adjacent to Kogru River and Prudhoe Bay are compared to the profiles of these two embayments. Also, the bluff along the north side of Kogru River exposes the peaty lake beds of a recently drained large lake, as sketched in Figure 4. The base of the modern fill in Kogru River, determined from seismic profiles, is shown in Figure 7. The base of the fill in Prudhoe Bay is sketched from Hopkins, et al. (1976). Comparing the elevation of the embayment fill with the elevation of lake bottoms, (Sellman, et al., 1976). We find a discrepancy of 6 to 7 m in both cases. Thaw settlement of originally frozen deposits below lakes after encroachment of the sea is not sufficient to account for the discrepancy. To form a deep embayment like Prudhoe Bay, one would have to start from a deep lake, and such a lake would already be underlain by a thaw bulb. We must also

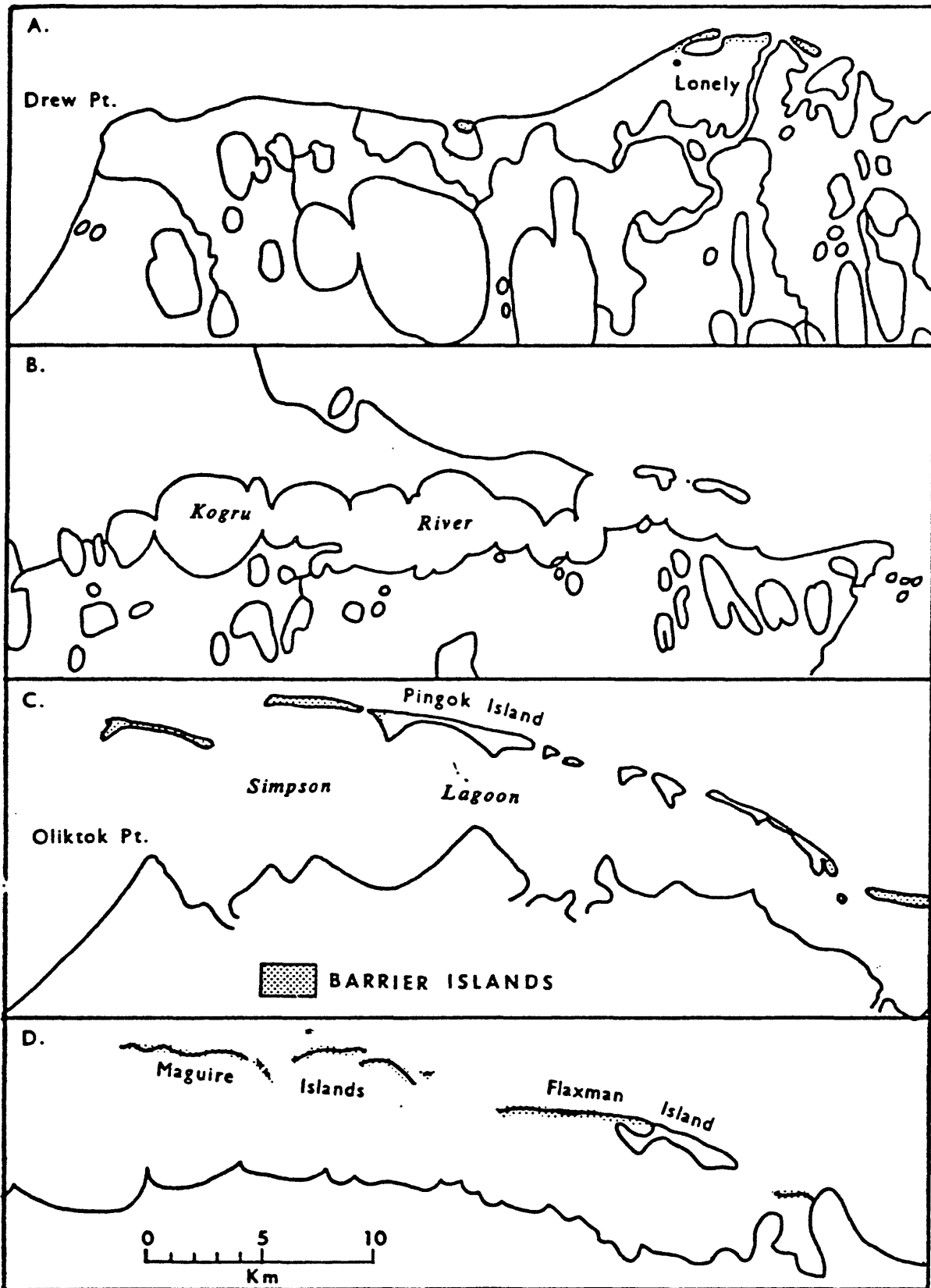


Figure 6. Sequence of lagoon formation and barrier island isolation by thaw-lake coalescence. A. Initial tapping, draining, and coalescing of lakes. B. Continued coalescing of lakes and thermal erosion of shoreline. C. Continuing thermal erosion and isolation of offshore tundra remnants. D. Erosion of tundra remnants and reworking of sand and gravel into offshore barriers.

(From Wiseman, et.al., 1973).

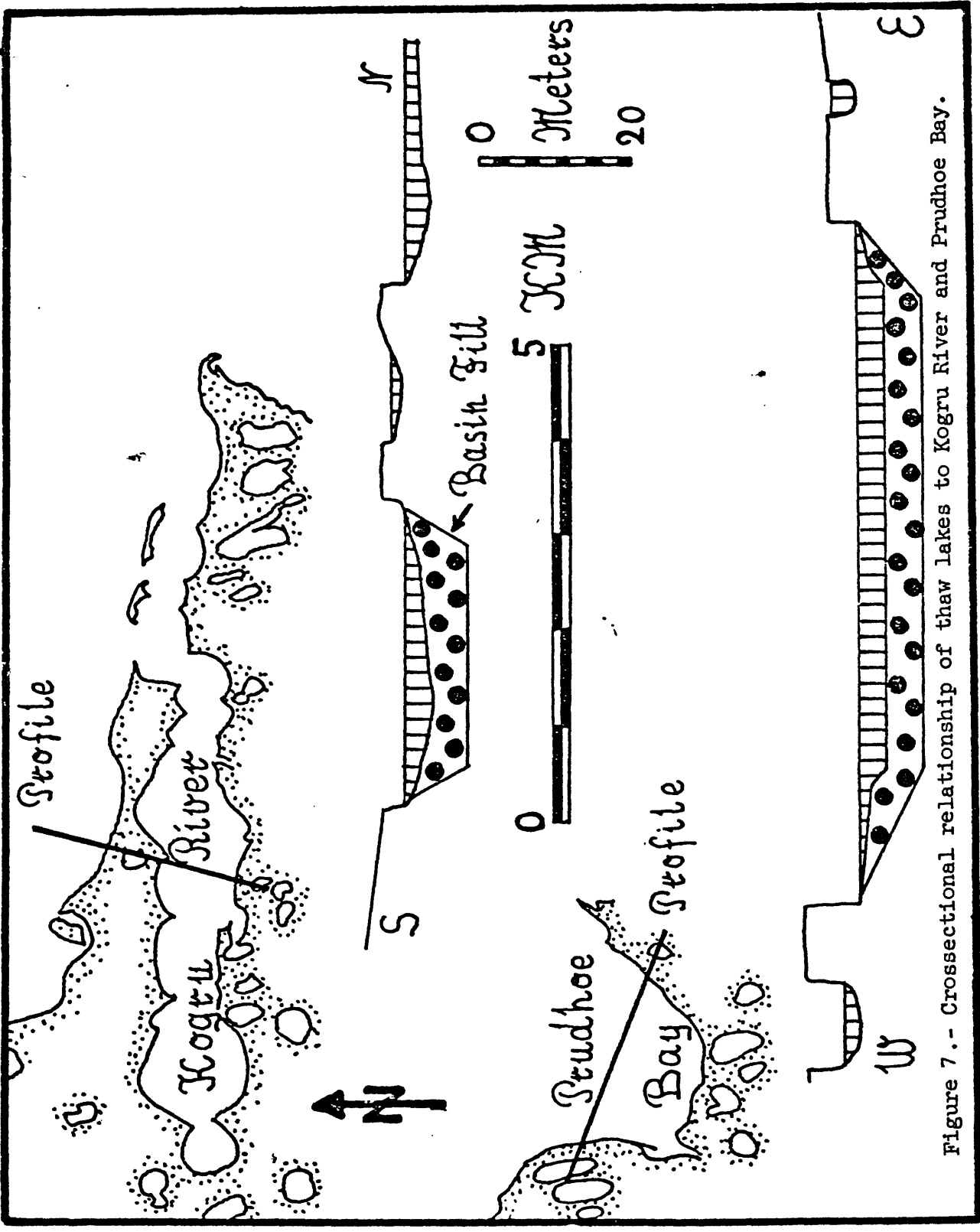


Figure 7.- Cross-sectional relationship of thaw lakes to Kogru River and Prudhoe Bay.

rule out erosion as an agent to make a thaw lake into a deep embayment or lagoon. Prudhoe Bay contains 6 m of marine sediments (Hopkins, 1976), and Kogru River has a similar thickness of fill, indicating that both embayments become shallower with time.

From the data at hand, therefore, the origin of the long narrow embayment called Kogru River remains unknown. Teschekpuk Lake, with the lake level 1.5 m above sea level, and a depth of up to 14 m (Charles Sloan personal commun.), if breached, would result in a large embayment. But this lake is not a thaw lake, but a topographic anomaly in the general surface of the coastal plain that is due to other causes.

References Cited

- Black, R.F., 1964, Gubic Formation of Quaternary age in Northern Alaska, U.S.G.S. Prof. Paper 302-C, 91 pp.
- Hopkins, D.M., et al., 1976, Offshore Permafrost Studies, Beaufort Sea, Research Unit 204, U.S.G.S. Quarterly Report, July-Aug.-Sept., 8 pp.
- Reimnitz, E., 1976, High Resolution Seismic Profiles, Beaufort Sea, U.S.G.S. Open File Report 76-848.
- Sellman, P.V., Brown, J., Lewellen, R.I., McKim, H., and Merry, C., 1976. The classification and geomorphic implication of thaw lakes on the arctic coastal plain, Alaska, CRREL Research Report #344.
- Short, A.D., Wright, L.D., 1974, Lineaments and Coastal geomorphic patterns in the Alaskan Arctic, GSA Bull., Vol. 85, p. 934-936.
- Wiseman, Wm. J., Jr., Coleman, J.M., Gregory, A., Hsu, S.A., Short, A.D., Suhayda, J.N., Walters, D.C., Jr., and Wright, L.D., 1973, Alaskan arctic coastal processes and morphology. Louisiana State University.